

# Global Carbon Budget 2015

Correspondence to: C. Le Quéré ([c.lequere@uea.ac.uk](mailto:c.lequere@uea.ac.uk))

Significant text differences from last year are shown in red

C Le Quéré[1], R Moriarty[1], RM Andrew[2], JG Canadell[3], S Sitch[4], JI Korsbakken[2], P Friedlingstein[5], GP Peters[2], RJ Andres[6], TA Boden[6], RA Houghton[7], JI House[8], RF Keeling[9], P Tans[10], A Arneth[11], DCE Bakker[12], L Barbero [13, 14], L Bopp[15], J Chang[15], F Chevallier[15], LP Chini[16], P Ciais[15], M Fader[17], R Feely[18], T Gkritzalis[19], I Harris[20], J Hauck[21], T Ilyina[22], AK Jain[23], E Kato[24], V Kitidis[25], K Klein Goldewijk[26], C Koven[27], P Landschützer[28], SK Lauvset[29], N Lefèvre[30], A Lenton[31], ID Lima[32], N Metzl[30], F Millero[33], DR Munro[34], A Murata[35], JEMS Nabel[22], S Nakaoka[36], Y Nojiri[36], K O'Brien[37], A Olsen[38, 39], T Ono[40], FF Pérez[41], B Pfeil[38, 39], D Pierrot[13, 14], B Poulter[42], G Rehder[43], C Rödenbeck[44], S Saito[45], U Schuster[4], J Schwinger[29], R Séférian[46], T Steinhoff[47], BD Stocker[48, 49], AJ Sutton[50, 18], T Takahashi[51], B Tilbrook[52], IT van der Laan-Luijkx[53, 54], GR van der Werf[55], S van Heuven[56], D Vandemark[57], N Viovy[15], A Wiltshire[58], S Zaehle[44], and N Zeng[59]

[1] Tyndall Centre for Climate Change Research, University of East Anglia, Norwich Research Park, Norwich NR4 7TJ, UK

[2] Center for International Climate and Environmental Research – Oslo (CICERO), Norway

[3] Global Carbon Project, CSIRO Oceans and Atmosphere Flagship, GPO Box 3023, Canberra, ACT 2601, Australia

[4] College of Life and Environmental Sciences, University of Exeter, Exeter EX4 4QE, UK

[5] College of Engineering, Mathematics and Physical Sciences, University of Exeter, Exeter EX4 4QF, UK

[6] Carbon Dioxide Information Analysis Center (CDIAC), Oak Ridge National Laboratory, Oak Ridge, TN, USA

[7] Woods Hole Research Centre (WHRC), Falmouth, MA 02540, USA

[8] Cabot Institute, Department of Geography, University of Bristol, Bristol BS8 1TH, UK

[9] University of California, San Diego, Scripps Institution of Oceanography, La Jolla, California 92093-0244, USA

[10] National Oceanic & Atmospheric Administration, Earth System Research Laboratory (NOAA/ESRL), Boulder, Colorado 80305, USA

[11] Institute of Meteorology and Climate Research – Atmospheric Environmental Research (IMK-IFU), Karlsruhe Institute of Technology (KIT), 82467 Garmisch-Partenkirchen, Germany

[12] Centre for Ocean and Atmospheric Sciences, School of Environmental Sciences, University of East Anglia, Norwich NR4 7TJ, United Kingdom

[13] Cooperative Institute for Marine and Atmospheric Studies, Rosenstiel School for Marine and Atmospheric Science, University of Miami, Miami FL 33149, USA

[14] National Oceanic & Atmospheric Administration/Atlantic Oceanographic & Meteorological Laboratory (NOAA/AOML), Miami, FL 33149, USA

[15] Laboratoire des Sciences du Climat et de l'Environnement, Institut Pierre-Simon Laplace, CEA-CNRS-UVSQ, CE Orme des Merisiers, 91191 Gif sur Yvette Cedex, France

[16] Department of Geographical Sciences, University of Maryland, College Park, Maryland 20742, USA

[17] Institut Méditerranéen de Biodiversité et d'Ecologie marine et continentale. Aix-Marseille Université, CNRS, IRD, Avignon Université, Technopôle Arbois-Méditerranée, Bâtiment Villemain, BP 80, F-13545 Aix-en-Provence cedex 04, France.

[18] National Oceanic & Atmospheric Administration/Pacific Marine Environmental Laboratory (NOAA/PMEL), 7600 Sand Point Way NE, Seattle, WA 98115, USA

- 1 [19]Flanders Marine Institute, InnovOcean, Wandelaarkaai 7, 8400 Ostend, Belgium
- 2 [20]Climatic Research Unit, University of East Anglia, Norwich Research Park, Norwich, NR4 7TJ, UK
- 3 [21]Alfred-Wegener-Institut, Helmholtz Zentrum für Polar- und Meeresforschung, Am Handelshafen 12,
- 4 27570 Bremerhaven, Germany
- 5 [22]Max Planck Institute for Meteorology, Bundesstr. 53, 20146 Hamburg, Germany
- 6 [23]Department of Atmospheric Sciences, University of Illinois, Urbana, IL 61821, USA
- 7 [24]Institute of Applied Energy (IAE), Minato-ku, Tokyo 105-0003, Japan
- 8 [25]Plymouth Marine Laboratory, Prospect Place, Plymouth, PL1 3DH, United Kingdom
- 9 [26]PBL Netherlands Environmental Assessment Agency, The Hague/Bilthoven and Utrecht University,
- 10 Utrecht, The Netherlands
- 11 [27]Earth Sciences Division, Lawrence Berkeley National Lab, 1 Cyclotron Road, Berkeley, California 94720,
- 12 USA
- 13 [28]Environmental Physics Group, Institute of Biogeochemistry and Pollutant Dynamics, ETH Zürich,
- 14 Universitätstrasse 16, 8092 Zürich, Switzerland
- 15 [29]Uni Research Climate, Bjerknes Centre for Climate Research, Allég. 55, 5007 Bergen, Norway
- 16 [30]Sorbonne Universités (UPMC, Univ Paris 06)-CNRS-IRD-MNHN, LOCEAN/IPSL Laboratory, 4 place
- 17 Jussieu, F-75005 Paris, France
- 18 [31]CSIRO Oceans and Atmosphere, PO BOX 1538 Hobart, Tasmania, Australia
- 19 [32]Woods Hole Oceanographic Institution (WHOI), Woods Hole, MA 02543, USA
- 20 [33]Department of Ocean Sciences, RSMAS/MAC, University of Miami, 4600 Rickenbacker Causeway,
- 21 Miami, FL 33149
- 22 [34]Department of Atmospheric and Oceanic Sciences and Institute of Arctic and Alpine Research,
- 23 University of Colorado Campus Box 450 Boulder, CO 80309-0450 US
- 24 [35]Japan Agency for Marine-Earth Science and Technology (JAMSTEC), 2-15 Natsushimacho, Yokosuka,
- 25 Kanagawa Prefecture 237-0061, Japan
- 26 [36]Center for Global Environmental Research, National Institute for Environmental Studies (NIES), 16-2
- 27 Onogawa, Tsukuba, Ibaraki 305-8506 Japan
- 28 [37]University of Washington, Joint Institute for the Study of the Atmosphere and Ocean, Seattle, WA,
- 29 98115 US
- 30 [38]Geophysical Institute, University of Bergen, Allégaten 70, 5007 Bergen, Norway
- 31 [39]Bjerknes Centre for Climate Research, Allégaten 70, 5007 Bergen, Norway
- 32 [40]National Research Institute for Fisheries Science, Fisheries Research Agency 2-12-4 Fukuura, Kanazawa-
- 33 Ku, Yokohama 236-8648, Japan
- 34 [41]Instituto de Investigaciones Marinas de Vigo, C/Eduardo Cabello, 6. Vigo. Pontevedra. E-36208 Spain.
- 35 [42]Department of Ecology, Montana State University, Bozeman, MT 59717, USA
- 36 [43]Leibniz Institute for Baltic Sea Research Warnemünde, Seestr 15, 18119 Rostock, Germany
- 37 [44]Max Planck Institut für Biogeochemie, P.O. Box 600164, Hans-Knöll-Str. 10, 07745 Jena, Germany
- 38 [45]Marine Division, Global Environment and Marine Department, Japan Meteorological Agency, 1-3-4
- 39 Otemachi, Chiyoda-ku, Tokyo 100-8122, Japan
- 40 [46]Centre National de Recherche Météorologique–Groupe d’Etude de l’Atmosphère Météorologique
- 41 (CNRM-GAME), Météo-France/CNRS, 42 Avenue Gaspard Coriolis, 31100 Toulouse, France
- 42 [47]GEOMAR Helmholtz Centre for Ocean Research Kiel, Düsternbrooker Weg 20, 24105, Kiel, Germany
- 43 [48]Climate and Environmental Physics, and Oeschger Centre for Climate Change Research, University of
- 44 Bern, Switzerland
- 45 [49]Imperial College London, Life Science Department, Silwood Park, Ascot, Berkshire SL5 7PY UK
- 46 [50]Joint Institute for the Study of the Atmosphere and Ocean, University of Washington, Seattle, WA, USA
- 47 [51]Lamont-Doherty Earth Observatory of Columbia University, Palisades, NY 10964 USA
- 48 [52]CSIRO Oceans and Atmosphere and Antarctic Climate and Ecosystems Co-operative Research Centre,
- 49 Hobart, Australia
- 50 [53]Department of Meteorology and Air Quality, Wageningen University, PO Box 47 6700AA
- 51 Wageningen, The Netherlands

- [54]ICOS-Carbon Portal, c/o Wageningen University, PO Box 47 6700AA Wageningen, The Netherlands  
 [55]Faculty of Earth and Life Sciences, VU University Amsterdam, Netherlands  
 [56]Royal Netherlands Institute for Sea Research, Landsdiep 4, 1797 SZ 't Horntje (Texel), The Netherlands  
 [57]University of New Hampshire, Ocean Process Analysis Laboratory, 161 Morse Hall, 8 College Road,  
 Durham, NH 03824, US  
 [58]Met Office Hadley Centre, FitzRoy Road, Exeter, EX1 3PB, UK  
 [59]Department of Atmospheric and Oceanic Science, University of Maryland, College Park, MD 20742, USA

## Abstract

Accurate assessment of anthropogenic carbon dioxide ( $\text{CO}_2$ ) emissions and their redistribution among the atmosphere, ocean, and terrestrial biosphere is important to better understand the global carbon cycle, support the development of climate policies, and project future climate change. Here we describe data sets and a methodology to quantify all major components of the global carbon budget, including their uncertainties, based on the combination of a range of data, algorithms, statistics and model estimates and their interpretation by a broad scientific community. We discuss changes compared to previous estimates, consistency within and among components, alongside methodology and data limitations.  $\text{CO}_2$  emissions from fossil fuel combustion and cement production ( $E_{\text{FF}}$ ) are based on energy statistics and cement production data, respectively, while emissions from land-use change ( $E_{\text{LUC}}$ ), mainly deforestation, are based on combined evidence from land-cover change data, fire activity associated with deforestation, and models. The global atmospheric  $\text{CO}_2$  concentration is measured directly and its rate of growth ( $G_{\text{ATM}}$ ) is computed from the annual changes in concentration. The mean ocean  $\text{CO}_2$  sink ( $S_{\text{OCEAN}}$ ) is based on observations from the 1990s, while the annual anomalies and trends are estimated with ocean models. The variability in  $S_{\text{OCEAN}}$  is evaluated with data products based on surveys of ocean  $\text{CO}_2$  measurements. The global residual terrestrial  $\text{CO}_2$  sink ( $S_{\text{LAND}}$ ) is estimated by the difference of the other terms of the global carbon budget and compared to results of independent Dynamic Global Vegetation Models forced by observed climate,  $\text{CO}_2$  and land-cover change (some including nitrogen-carbon interactions). We compare the mean land and ocean fluxes and their variability to estimates from three atmospheric inverse methods for three broad latitude bands. All uncertainties are reported as  $\pm 1\sigma$ , reflecting the current capacity to characterise the annual estimates of each component of the global carbon budget. For the last decade available (2005–2014),  $E_{\text{FF}}$  was  $9.0 \pm 0.5 \text{ GtC yr}^{-1}$ ,  $E_{\text{LUC}}$   $0.9 \pm 0.5 \text{ GtC yr}^{-1}$ ,  $G_{\text{ATM}}$   $4.4 \pm 0.1 \text{ GtC yr}^{-1}$ ,  $S_{\text{OCEAN}}$   $2.6 \pm 0.5 \text{ GtC yr}^{-1}$ , and  $S_{\text{LAND}}$   $3.0 \pm 0.8 \text{ GtC yr}^{-1}$ . For year 2014 alone,  $E_{\text{FF}}$  grew to  $9.8 \pm 0.5 \text{ GtC yr}^{-1}$ , 0.6 % above 2013, continuing the growth trend in these emissions albeit at a slower rate compared to the average growth of 2.2 %  $\text{yr}^{-1}$  that took place during 2005–2014. Also for 2014,  $E_{\text{LUC}}$  was  $1.1 \pm 0.5$

GtC yr<sup>-1</sup>,  $G_{\text{ATM}}$  was  $3.9 \pm 0.2$  GtC yr<sup>-1</sup>,  $S_{\text{OCEAN}}$  was  $2.9 \pm 0.5$  GtC yr<sup>-1</sup> and  $S_{\text{LAND}}$  was  $4.1 \pm 0.9$  GtC yr<sup>-1</sup>.  $G_{\text{ATM}}$  was lower in 2014 compared to the past decade (2005-2014), reflecting a larger  $S_{\text{LAND}}$  for that year. The global atmospheric CO<sub>2</sub> concentration reached  $397.15 \pm 0.10$  ppm averaged over 2014. For 2015, preliminary data indicate that the growth in  $E_{\text{FF}}$  will be near of slightly below zero, with a projection of  $-0.6$  [range of  $-1.6$  to  $+0.5$ ]%, based on national emissions projections for China and USA, and projections of Gross Domestic Product corrected for recent changes in the carbon intensity of the global economy for the rest of the world. From this projection of  $E_{\text{FF}}$  and assumed constant  $E_{\text{LUC}}$  for 2015, cumulative emissions of CO<sub>2</sub> will reach about  $555 \pm 55$  GtC ( $2035 \pm 205$  GtCO<sub>2</sub>) for 1870-2015, about 75% from  $E_{\text{FF}}$  and 25% from  $E_{\text{LUC}}$ . This living data update documents changes in the methods and data sets used in this new carbon budget compared with previous publications of this data set (Le Quéré et al., 2015; 2014; 2013). All observations presented here can be downloaded from the Carbon Dioxide Information Analysis Center (doi: 10.3334/CDIAC/GCP\_2015).

## 1 Introduction

The concentration of carbon dioxide (CO<sub>2</sub>) in the atmosphere has increased from approximately 277 parts per million (ppm) in 1750 (Joos and Spahni, 2008), the beginning of the Industrial Era, to 397.15 ppm in 2014 (Dlugokencky and Tans, 2015). Daily averages went above 400 ppm for the first time at Mauna Loa station in May 2013 (Scripps, 2013). This station holds the longest running record of direct measurements of atmospheric CO<sub>2</sub> concentration (Tans and Keeling, 2014). The global monthly average concentration was above 400 ppm in March through May 2015 for the first time (Dlugokencky and Tans, 2015; Fig. 1), while at Mauna Loa the seasonally-corrected monthly average concentration reached 400 ppm in March 2015 and continued to rise. The atmospheric CO<sub>2</sub> increase above preindustrial levels was, initially, primarily caused by the release of carbon to the atmosphere from deforestation and other land-use change activities (Ciais et al., 2013). While emissions from fossil fuel combustion started before the Industrial Era, they only became the dominant source of anthropogenic emissions to the atmosphere from around 1920 and their relative share has continued to increase until present. Anthropogenic emissions occur on top of an active natural carbon cycle that circulates carbon between the atmosphere, ocean, and terrestrial biosphere reservoirs on time scales from days to millennia, while exchanges with geologic reservoirs occur at longer timescales (Archer et al., 2009).

The global carbon budget presented here refers to the mean, variations, and trends in the perturbation of CO<sub>2</sub> in the atmosphere, referenced to the beginning of the Industrial Era. It quantifies the input of CO<sub>2</sub> to the atmosphere by emissions from human activities, the growth of CO<sub>2</sub> in the atmosphere, and the resulting changes in the storage of carbon in the land and ocean reservoirs in response to increasing atmospheric CO<sub>2</sub> levels, climate and variability, and other anthropogenic and natural changes (Fig. 2). An understanding of this perturbation budget over time and the underlying variability and trends of the natural carbon cycle are necessary to understand the response of natural sinks to changes in climate, CO<sub>2</sub> and land-use change drivers, and the permissible emissions for a given climate stabilization target.

The components of the CO<sub>2</sub> budget that are reported annually in this paper include separate estimates for (1) the CO<sub>2</sub> emissions from fossil fuel combustion and oxidation and cement production ( $E_{FF}$ ; GtC yr<sup>-1</sup>), (2) the CO<sub>2</sub> emissions resulting from deliberate human activities on land leading to land-use change ( $E_{LUC}$ ; GtC yr<sup>-1</sup>), (3) the growth rate of CO<sub>2</sub> in the atmosphere ( $G_{ATM}$ ; GtC yr<sup>-1</sup>), and the uptake of CO<sub>2</sub> by the 'CO<sub>2</sub> sinks' in (4) the ocean ( $S_{OCEAN}$ ; GtC yr<sup>-1</sup>) and (5) on land ( $S_{LAND}$ ; GtC yr<sup>-1</sup>). The CO<sub>2</sub> sinks as defined here include the response of the land and ocean to elevated CO<sub>2</sub> and changes in climate and other environmental conditions. The global emissions and their partitioning among the atmosphere, ocean and land are in balance:

$$E_{FF} + E_{LUC} = G_{ATM} + S_{OCEAN} + S_{LAND}. \quad (1)$$

$G_{ATM}$  is usually reported in ppm yr<sup>-1</sup>, which we convert to units of carbon mass, GtC yr<sup>-1</sup>, using 1 ppm = 2.12 GtC (Ballantyne et al., 2012; Prather et al., 2012; Table 1). We also include a quantification of  $E_{FF}$  by country, computed with both territorial and consumption based accounting (see Methods).

Equation (1) partly omits two kinds of processes. The first is the net input of CO<sub>2</sub> to the atmosphere from the chemical oxidation of reactive carbon-containing gases from sources other than fossil fuels (e.g. fugitive anthropogenic CH<sub>4</sub> emissions, industrial processes, and changes of biogenic emissions from changes in vegetation, fires, wetlands, etc.), primarily methane (CH<sub>4</sub>), carbon monoxide (CO), and volatile organic compounds such as isoprene and terpene. CO emissions are currently implicit in  $E_{FF}$  while anthropogenic CH<sub>4</sub> emissions are not and thus their inclusion would result in a small increase in  $E_{FF}$ . The second is the anthropogenic perturbation to carbon cycling in terrestrial freshwaters, estuaries, and coastal areas, that modifies lateral fluxes from land ecosystems to the open ocean, the evasion CO<sub>2</sub> flux from rivers, lakes and estuaries to

the atmosphere, and the net air-sea anthropogenic CO<sub>2</sub> flux of coastal areas (Regnier et al., 2013). The inclusion of freshwater fluxes of anthropogenic CO<sub>2</sub> would affect the estimates of, and partitioning between,  $S_{\text{LAND}}$  and  $S_{\text{OCEAN}}$  in Eq. (1) in complementary ways, but would not affect the other terms. These flows are omitted in absence of annual information on the natural versus anthropogenic perturbation terms of these loops of the carbon cycle, and they are discussed in Section 2.7.

The CO<sub>2</sub> budget has been assessed by the Intergovernmental Panel on Climate Change (IPCC) in all assessment reports (Ciais et al., 2013; Denman et al., 2007; Prentice et al., 2001; Schimel et al., 1995; Watson et al., 1990), and by others (e.g. Ballantyne et al., 2012). These assessments included budget estimates for the decades of the 1980s, 1990s (Denman et al., 2007) and, most recently, the period 2002-2011 (Ciais et al., 2013). The IPCC methodology has been adapted and used by the Global Carbon Project (GCP, [www.globalcarbonproject.org](http://www.globalcarbonproject.org)), which has coordinated a cooperative community effort for the annual publication of global carbon budgets up to year 2005 (Raupach et al., 2007; including fossil emissions only), year 2006 (Canadell et al., 2007), year 2007 (published online; GCP, 2007), year 2008 (Le Quéré et al., 2009), year 2009 (Friedlingstein et al., 2010), year 2010 (Peters et al., 2012b), year 2012 (Le Quéré et al., 2013; Peters et al., 2013), year 2013 (Le Quéré et al., 2014), and most recently year 2014 (Friedlingstein et al., 2014; Le Quéré et al., 2015), where the carbon budget year refers to the initial year of publication. Each of these papers updated previous estimates with the latest available information for the entire time series. From 2008, these publications projected fossil fuel emissions for one additional year using the projected World Gross Domestic Product and estimated improvements in the carbon intensity of the global economy.

We adopt a range of  $\pm 1$  standard deviation ( $\sigma$ ) to report the uncertainties in our estimates, representing a likelihood of 68% that the true value will be within the provided range if the errors have a Gaussian distribution. This choice reflects the difficulty of characterising the uncertainty in the CO<sub>2</sub> fluxes between the atmosphere and the ocean and land reservoirs individually, particularly on an annual basis, as well as the difficulty of updating the CO<sub>2</sub> emissions from land-use change. A likelihood of 68% provides an indication of our current capability to quantify each term and its uncertainty given the available information. For comparison, the Fifth Assessment Report of the IPCC (AR5) generally reported a likelihood of 90% for large data sets whose uncertainty is well characterised, or for long time intervals less affected by year-to-year variability.

Our 68% uncertainty value is near the 66% which the IPCC characterises as ‘likely’ for values falling into the  $\pm 1\sigma$  interval. The uncertainties reported here combine statistical analysis of the underlying data and expert judgement of the likelihood of results lying outside this range. The limitations of current information are discussed in the paper and have been examined in detail elsewhere (Ballantyne et al., 2015).

All quantities are presented in units of gigatonnes of carbon (GtC,  $10^{15}$  gC), which is the same as petagrams of carbon (PgC; Table 1). Units of gigatonnes of CO<sub>2</sub> (or billion tonnes of CO<sub>2</sub>) used in policy are equal to 3.664 multiplied by the value in units of GtC.

This paper provides a detailed description of the data sets and methodology used to compute the global carbon budget estimates for the period preindustrial (1750) to 2014 and in more detail for the period 1959 to 2014. We also provide decadal averages starting in 1960 including the last decade (2005-2014), results for the year 2014, and a projection of  $E_{FF}$  for year 2015. Finally we provide the total or cumulative emissions from fossil fuels and land-use change since year 1750, the preindustrial period, and since year 1870, the reference year for the cumulative carbon estimate used by the IPCC (AR5) based on the availability of global temperature data (Stocker et al., 2013). This paper will be updated every year using the format of ‘living data’ to keep a record of budget versions and the changes in new data, revision of data, and changes in methodology that lead to changes in estimates of the carbon budget. Additional materials associated with the release of each new version will be posted at the Global Carbon Project (GCP) website (<http://www.globalcarbonproject.org/carbonbudget>). Data associated with this release are also available through the Global Carbon Atlas (<http://www.globalcarbonatlas.org>). With this approach, we aim to provide the highest transparency and traceability in the reporting of CO<sub>2</sub>, the key driver of climate change.

## 2 Methods

Multiple organizations and research groups around the world generated the original measurements and data used to complete the global carbon budget. The effort presented here is thus mainly one of synthesis, where results from individual groups are collated, analysed and evaluated for consistency. We facilitate access to original data with the understanding that primary data sets will be referenced in future work (See Table 2 for ‘How to cite’ the data sets). Descriptions of the measurements, models, and methodologies follow below and in depth

descriptions of each component are described elsewhere (e.g. Andres et al., 2012; Houghton et al., 2012).

This is the tenth version of the ‘global carbon budget’ (see Introduction for details) and the fourth revised version of the ‘global carbon budget living data update’. It is an update of Le Quéré et al. (2015), including data to year 2014 (inclusive) and a projection for fossil fuel emissions for year 2015. The main changes from Le Quéré et al. (2015) are: (1) the use of national emissions for  $E_{FF}$  from the United Nations Framework Convention on Climate Change (UNFCCC) where available and (2) the projection of  $E_{FF}$  for 2015 is based on national emissions projections for China and USA, and Gross Domestic Product corrected for recent changes in the carbon intensity of the global economy for the rest of the world. The main methodological differences between annual carbon budgets are summarised in Table 3.

## **2.1 CO<sub>2</sub> emissions from fossil fuel combustion and cement production ( $E_{FF}$ )**

### **2.1.1 Fossil fuel and cement emissions and their uncertainty**

The calculation of global and national CO<sub>2</sub> emissions from fossil fuel combustion, including gas flaring and cement production ( $E_{FF}$ ), relies primarily on energy consumption data, specifically data on hydrocarbon fuels, collated and archived by several organisations (Andres et al., 2012). These include the Carbon Dioxide Information Analysis Center (CDIAC), the International Energy Agency (IEA), the United Nations (UN), the United States Department of Energy (DoE) Energy Information Administration (EIA), and more recently also the Planbureau voor de Leefomgeving (PBL) Netherlands Environmental Assessment Agency. Where available, we use national emissions estimated by the countries themselves and reported to the UNFCCC for the period 1990-2012 (42 countries). We assume that national emissions reported to the UNFCCC are the most accurate because national experts have access to additional and country-specific information, and because these emission estimates are verified by the UNFCCC. We also use global and national emissions estimated by CDIAC (Boden et al., 2013). The CDIAC emission estimates are the only data set that extends back in time to 1751 with consistent and well-documented emissions from fossil fuel combustion, cement production, and gas flaring for all countries and their uncertainty (Andres et al., 2014; Andres et al., 2012; Andres et al., 1999); this makes the data set a unique resource for research of the carbon cycle during the fossil fuel era. The global emissions presented here are



from the CDIAC analysis, which provides an internally-consistent global estimate including bunker fuels.

During the period 1959-2011, the emissions from fossil fuels estimated by CDIAC are based primarily on energy data provided by the UN Statistics Division (UN, 2014a; b; Table 4). When necessary, fuel masses/volumes are converted to fuel energy content using coefficients provided by the UN and then to CO<sub>2</sub> emissions using conversion factors that take into account the relationship between carbon content and energy (heat) content of the different fuel types (coal, oil, gas, gas flaring) and the combustion efficiency (to account, for example, for soot left in the combustor or fuel otherwise lost or discharged without oxidation). Most data on energy consumption and fuel quality (carbon content and heat content) are available at the country level (UN, 2014a). In general, CO<sub>2</sub> emissions for equivalent primary energy consumption are about 30% higher for coal compared to oil, and 70% higher for coal compared to natural gas (Marland et al., 2007). All estimated fossil fuel emissions are based on the mass flows of carbon and assume that the fossil carbon emitted as CO or CH<sub>4</sub> will soon be oxidized to CO<sub>2</sub> in the atmosphere and can be accounted for with CO<sub>2</sub> emissions (see Section 2.7).

For the most recent 2-3 years when the UNFCCC estimates and UN statistics used by CDIAC are not yet available (or there was insufficient time to process and verify them), we generated preliminary estimates based on the BP annual energy review by applying the growth rates of energy consumption (coal, oil, gas) for 2013-2014 to the UNFCCC national emissions in 2012, and for 2012-2014 for the CDIAC national and global emissions in 2011 (BP, 2015). BP's sources for energy statistics overlap with those of the UN data, but are compiled more rapidly from about 70 countries covering about 96% of global emissions. We use the BP values only for the year-to-year rate of change, because the rates of change are less uncertain than the absolute values and to avoid discontinuities in the time-series when linking the UN-based data with the BP data. These preliminary estimates are replaced by the more complete UNFCCC or CDIAC data based on UN statistics when they become available. Past experience and work by others (Andres et al., 2014; Myhre et al., 2009) shows that projections based on the BP rate of change are within the uncertainty provided (see Sect. 3.2 and Supplementary Information from Peters et al., 2013).

Estimates of emissions from cement production by CDIAC are based on cement production data from the US Geological Survey up to year 2013 (van Oss, 2013), and up to 2014 for the top 18 countries (representing 85% of global production; USGS, 2015). For countries without data in 2014

we use the 2013 values (zero growth). Some fraction of the CaO and MgO in cement is returned to the carbonate form during cement weathering but this is generally regarded to be small and is ignored here.

Estimates of emissions from gas flaring by CDIAC are calculated in a similar manner as those from solid, liquid, and gaseous fuels, and rely on the UN Energy Statistics to supply the amount of flared or vented fuel. For emission years 2012-2014, flaring is assumed constant from 2011 (emission year) UN-based data. The basic data on gas flaring report atmospheric losses during petroleum production and processing that have large uncertainty and do not distinguish between gas that is flared as CO<sub>2</sub> or vented as CH<sub>4</sub>. Fugitive emissions of CH<sub>4</sub> from the so-called upstream sector (e.g., coal mining and natural gas distribution) are not included in the accounts of CO<sub>2</sub> emissions except to the extent that they are captured in the UN energy data and counted as gas 'flared or lost'.

The published CDIAC data set includes 250 countries and regions. This expanded list includes countries that no longer exist, such as the USSR or East Pakistan. For the carbon budget, we reduce the list to 216 countries by reallocating emissions to the currently defined territories. This involved both aggregation and disaggregation, and does not change global emissions. Examples of aggregation include merging East and West Germany to the currently defined Germany. Examples of disaggregation include reallocating the emissions from former USSR to the resulting independent countries. For disaggregation, we use the emission shares when the current territory first appeared. For the most recent years, 2012-2014, the BP statistics are more aggregated, but we retain the detail of CDIAC by applying the growth rates of each aggregated region in the BP data set to its constituent individual countries in CDIAC.

Estimates of CO<sub>2</sub> emissions show that the global total of emissions is not equal to the sum of emissions from all countries. This is largely attributable to emissions that occur in international territory, in particular the combustion of fuels used in international shipping and aviation (bunker fuels), where the emissions are included in the global totals but are not attributed to individual countries. In practice, the emissions from international bunker fuels are calculated based on where the fuels were loaded, but they are not included with national emissions estimates. Other differences occur because globally the sum of imports in all countries is not equal to the sum of exports and because of differing treatment of oxidation of non-fuel uses of hydrocarbons (e.g. as solvents, lubricants, feedstocks, etc.), and changes in stock (Andres et al., 2012).

The uncertainty of the annual fossil fuel and cement emissions for the globe has been estimated at  $\pm 5\%$  (scaled down from the published  $\pm 10\%$  at  $\pm 2\sigma$  to the use of  $\pm 1\sigma$  bounds reported here; Andres et al., 2012). This is consistent with a more detailed recent analysis of uncertainty of  $\pm 8.4\%$  at  $\pm 2\sigma$  (Andres et al., 2014) and at the high-end of the range of  $\pm 5\text{--}10\%$  at  $\pm 2\sigma$  reported by Ballantyne et al. (2015). This includes an assessment of uncertainties in the amounts of fuel consumed, the carbon and heat contents of fuels, and the combustion efficiency. While in the budget we consider a fixed uncertainty of  $\pm 5\%$  for all years, in reality the uncertainty, as a percentage of the emissions, is growing with time because of the larger share of global emissions from non-Annex B countries (emerging economies and developing countries) with less precise statistical systems (Marland et al., 2009). For example, the uncertainty in Chinese emissions has been estimated at around  $\pm 10\%$  (for  $\pm 1\sigma$ ; Gregg et al., 2008), and important potential biases have been identified suggesting China's emissions could be overestimated in published studies (Liu et al. 2015). Generally, emissions from mature economies with good statistical bases have an uncertainty of only a few per cent (Marland, 2008). Further research is needed before we can quantify the time evolution of the uncertainty, and its temporal error correlation structure. We note that even if they are presented as  $1\sigma$  estimates, uncertainties of emissions are likely to be mainly country-specific systematic errors related to underlying biases of energy statistics and to the accounting method used by each country. We assign a medium confidence to the results presented here because they are based on indirect estimates of emissions using energy data (Durant et al., 2010). There is only limited and indirect evidence for emissions, although there is a high agreement among the available estimates within the given uncertainty (Andres et al., 2014; Andres et al., 2012), and emission estimates are consistent with a range of other observations (Ciais et al., 2013), even though their regional and national partitioning is more uncertain (Francey et al., 2013).

### 2.1.2 Emissions embodied in goods and services

National emission inventories take a territorial (production) perspective and 'include greenhouse gas emissions and removals taking place within national territory and offshore areas over which the country has jurisdiction' (Rypdal et al., 2006). That is, emissions are allocated to the country where and when the emissions actually occur. The territorial emission inventory of an individual country does not include the emissions from the production of goods and services produced in other countries (e.g. food and clothes) that are used for consumption. Consumption-based

emission inventories for an individual country is another attribution point of view that allocates global emissions to products that are consumed within a country, and are conceptually calculated as the territorial emissions minus the ‘embedded’ territorial emissions to produce exported products plus the emissions in other countries to produce imported products (Consumption = Territorial – Exports + Imports). The difference between the territorial- and consumption-based emission inventories is the net transfer (exports minus imports) of emissions from the production of internationally traded products. Consumption-based emission attribution results (e.g. Davis and Caldeira, 2010) provide additional information to territorial-based emissions that can be used to understand emission drivers (Hertwich and Peters, 2009), quantify emission (virtual) transfers by the trade of products between countries (Peters et al., 2011b) and potentially design more effective and efficient climate policy (Peters and Hertwich, 2008).

We estimate consumption-based emissions by enumerating the global supply chain using a global model of the economic relationships between economic sectors within and between every country (Andrew and Peters, 2013; Peters et al., 2011a). Due to availability of the input data, detailed estimates are made for the years 1997, 2001, 2004, 2007, and 2011 (using the methodology of Peters et al., 2011b) using economic and trade data from the Global Trade and Analysis Project version 9 (GTAP; Narayanan et al., 2015). The results cover 57 sectors and 140 countries and regions. The results are extended into an annual time-series from 1990 to the latest year of the fossil fuel emissions or GDP data (2013 in this budget), using Gross Domestic Product (GDP) data by expenditure in current exchange rate of US dollars (USD; from the UN National Accounts main Aggregates database; UN, 2014c) and time series of trade data from GTAP (based on the methodology in Peters et al., 2011b ).

The consumption-based emission inventories in this carbon budget incorporate several improvements over previous versions (Le Quéré et al., 2013; Peters et al., 2012b; Peters et al., 2011b). The detailed estimates for 2004, 2007 and 2011 and time series approximation from 1990-2013 are based on an updated version of the GTAP database (Narayanan et al., 2015). We estimate the sector level CO<sub>2</sub> emissions using our own calculations based on the GTAP data and methodology, include flaring and cement emissions from CDIAC, and then scale the national totals (excluding bunker fuels) to match the CDIAC estimates from the most recent carbon budget. We do not include international transportation in our estimates of national totals, but include them in the global total. The time-series of trade data provided by GTAP covers the period 1995-2011 and

our methodology uses the trade shares as this data set. For the period 1990-1994 we assume the trade shares of 1995, while for 2012 and 2013 we assume the trade shares of 2011.

We do not provide an uncertainty estimate for these emissions, but based on model comparisons and sensitivity analysis, they are unlikely to be larger than for the territorial emission estimates (Peters et al., 2012a). Uncertainty is expected to increase for more detailed results, and to decrease with aggregation (Peters et al., 2011b; e.g. the results for Annex B countries will be more accurate than the sector results for an individual country).

The consumption-based emissions attribution method considers the CO<sub>2</sub> emitted to the atmosphere in the production of products, but not the trade in fossil fuels (coal, oil, gas). It is also possible to account for the carbon trade in fossil fuels (Davis et al., 2011), but we do not present those data here. Peters et al. (2012a) additionally considered trade in biomass.

The consumption data do not modify the global average terms in Eq. (1), but are relevant to the anthropogenic carbon cycle as they reflect the trade-driven movement of emissions across the Earth's surface in response to human activities. Furthermore, if national and international climate policies continue to develop in an un-harmonised way, then the trends reflected in these data will need to be accommodated by those developing policies.

### 2.1.3 Growth rate in emissions

We report the annual growth rate in emissions for adjacent years (in percent per year) by calculating the difference between the two years and then comparing to the emissions in the first year:  $\left[ \frac{E_{FF(t_0+1)} - E_{FF(t_0)}}{E_{FF(t_0)}} \right] \times 100 \text{ yr}^{-1}$ . This is the simplest method to characterise a one-year growth compared to the previous year and is widely used. We apply a leap-year adjustment to ensure valid interpretations of annual growth rates. This affects the growth rate by about 0.3% yr<sup>-1</sup> ( $\frac{1}{365}$ ) and causes growth rates to go up approximately 0.3% if the first year is a leap year and down 0.3% if the second year is a leap year.

The relative growth rate of  $E_{FF}$  over time periods of greater than one year can be re-written using its logarithm equivalent as follows:

$$\frac{1}{E_{FF}} \frac{dE_{FF}}{dt} = \frac{d(\ln E_{FF})}{dt} \quad (2)$$

Here we calculate relative growth rates in emissions for multi-year periods (e.g. a decade) by fitting a linear trend to  $\ln(E_{FF})$  in Eq. (2), reported in percent per year. We fit the logarithm of  $E_{FF}$  rather than  $E_{FF}$  directly because this method ensures that computed growth rates satisfy Eq. (6). This method differs from previous papers (Canadell et al., 2007; Le Quéré et al., 2009; Raupach et al., 2007) that computed the fit to  $E_{FF}$  and divided by average  $E_{FF}$  directly, but the difference is very small ( $<0.05\%$ ) in the case of  $E_{FF}$ .

#### 2.1.4 Emissions projections

Energy statistics from BP are normally available around June for the previous year. To gain insight on emission trends for the current year (2015), we provide an assessment of global emissions for  $E_{FF}$  by combining individual assessments of emissions for China and the USA (the two biggest emitting countries), and the rest of the world.

We specifically estimate emissions in China as the evidence suggests a departure from the long-term trends in the carbon intensity of the economy used in emissions projections in previous global carbon budgets (e.g. Le Quéré et al. 2015), resulting from significant drops in industrial production against continued growth in economic output. This departure could be temporary (Jackson et al., submitted). Our 2015 estimate for China uses: (1) apparent consumption of coal for January to August estimated using production data from the National Bureau of Statistics (2015), imports and exports of coal from China Customs Statistics (General Administration of Customs of the People's Republic of China, 2015a, b), and from partial data on stock changes from industry sources (China Coal Industry Association, 2015; China Coal Resource, 2015), (2) apparent consumption of oil and gas for January to June from the National Energy Administration (2015), and (3) production of cement reported for January to August (National Bureau of Statistics of China, 2015). Using these data, we estimate the change in emissions for the corresponding months in 2015 compared to 2014 assuming constant emission factors. We then assume that the changes during the first 6-8 months will persist throughout the year. The main sources of uncertainty are from the incomplete data on stock changes, the carbon content of coal and the assumption of persistent behaviour for the rest of 2015. These are discussed further in section 3.2.1. We tested our new method using data available in October 2014 to make a 2014 projection of coal consumption and cement production, both of which changed substantially in 2014. For the apparent consumption of coal we would have projected a change of  $-3.2\%$  in coal use for 2014, compared to  $-2.9\%$  reported by NBS in February 2015, while for the production of cement we

would have projected a change of +3.5%, compared to a realised change of +2.3%. In both cases, the projection of a decrease is consistent with the realised change.

For the USA, we use the forecast of the U.S. Energy Information Administration (EIA) 'Short-term energy outlook' (October 2015) for emissions from fossil fuel combustion. This is based on an energy forecasting model which is revised monthly, and takes into account heating-degree days, household expenditures by fuel type, energy markets, policies, and other effects. We combine this with our estimate of emissions from cement production using the monthly U.S. cement data from USGS for January-July, assuming changes in cement production over the first seven months apply throughout the year. We estimate an uncertainty range using the revisions of the October forecasts made by the EIA one year later. These were less than 2% during 2009-2014 (when a forecast was done), except for 2011 when it was -4.0%. We thus use a conservative uncertainty range of -4.0% to +1.8% around the central forecast.

For the rest of the world, we use the close relationship between the growth in GDP and the growth in emissions (Raupach et al., 2007) to project emissions for the current year. This is based on the so-called Kaya identity (also called IPAT identity, the acronym standing for human impact (I) on the environment, which is equal to the product of P= population, A= affluence, T= technology), whereby  $E_{FF}$  (GtC yr<sup>-1</sup>) is decomposed by the product of GDP (USD yr<sup>-1</sup>) and the fossil fuel carbon intensity of the economy ( $I_{FF}$ ; GtC USD<sup>-1</sup>) as follows:

$$E_{FF} = GDP \times I_{FF} \quad (3)$$

Such product-rule decomposition identities imply that the relative growth rates of the multiplied quantities are additive. Taking a time derivative of Equation (3) gives:

$$\frac{dE_{FF}}{dt} = \frac{d(GDP \times I_{FF})}{dt} \quad (4)$$

and applying the rules of calculus:

$$\frac{dE_{FF}}{dt} = \frac{dGDP}{dt} \times I_{FF} + GDP \times \frac{dI_{FF}}{dt} \quad (5)$$

finally, dividing (5) by (3) gives :

$$\frac{1}{E_{FF}} \frac{dE_{FF}}{dt} = \frac{1}{GDP} \frac{dGDP}{dt} + \frac{1}{I_{FF}} \frac{dI_{FF}}{dt} \quad (6)$$

where the left hand term is the relative growth rate of  $E_{FF}$ , and the right hand terms are the relative growth rates of GDP and  $I_{FF}$ , respectively, which can simply be added linearly to give overall growth rate. The growth rates are reported in percent by multiplying each term by 100. As preliminary estimates of annual change in GDP are made well before the end of a calendar year, making assumptions on the growth rate of  $I_{FF}$  allows us to make projections of the annual change in  $CO_2$  emissions well before the end of a calendar year. The  $I_{FF}$  is based on GDP in constant PPP (purchasing power parity) from the IEA (2014) up to 2012 (IEA/OECD, 2014) and extended using the IMF growth rates for 2013 and 2014. Experience of the past year has highlighted that the interannual variability in  $I_{FF}$  is the largest source of uncertainty in the GDP-based emissions projections. We thus use the standard deviation of the annual  $I_{FF}$  for the period 2005-2014 as a measure of uncertainty, reflecting a  $\pm 1\sigma$  as in the rest of the carbon budget. This is  $\pm 1.4\% \text{ yr}^{-1}$  for the rest of the world (global emissions minus China and USA).

The 2015 projection for the world is made of the sum of the projections for China, USA, and the rest. The uncertainty is added quadratically among the three regions because they are unrelated. The uncertainty here reflects the best of our expert opinion.

## 2.2 $CO_2$ emissions from land use, land-use change and forestry ( $E_{LUC}$ )

Land-use change emissions reported here ( $E_{LUC}$ ) include  $CO_2$  fluxes from deforestation, afforestation, logging (forest degradation and harvest activity), shifting cultivation (cycle of cutting forest for agriculture, then abandoning), and regrowth of forests following wood harvest or abandonment of agriculture. Only some land management activities (Table 5) are included in our land-use change emissions estimates (e.g. emissions or sinks related to management and management changes of established pasture and croplands are not included). Some of these activities lead to emissions of  $CO_2$  to the atmosphere, while others lead to  $CO_2$  sinks.  $E_{LUC}$  is the net sum of all anthropogenic activities considered. Our annual estimate for 1959-2010 is from a bookkeeping method (Sect. 2.2.1) primarily based on net forest area change and biomass data from the Forest Resource Assessment (FRA) of the Food and Agriculture Organisation (FAO) which is only available at intervals of five years. We use the FAO FRA 2010 here (Houghton et al., 2012). Inter-annual variability in emissions due to deforestation and degradation have been coarsely estimated from satellite-based fire activity in tropical forest areas (Section 2.2.2; Giglio et al., 2013; van der Werf et al., 2010). The bookkeeping method is used to quantify the  $E_{LUC}$  over the



time period of the available data, and the satellite-based deforestation fire information to incorporate interannual variability ( $E_{LUC}$  flux annual anomalies) from tropical deforestation fires. The satellite-based deforestation and degradation fire emissions estimates are available for years 1997-2014. We calculate the global annual anomaly in deforestation and degradation fire emissions in tropical forest regions for each year, compared to the 1997-2010 period, and add this annual flux anomaly to the  $E_{LUC}$  estimated using the bookkeeping method that is available up to 2010 only and assumed constant at the 2010 value during the period 2011-2014. We thus assume that all land management activities apart from deforestation and degradation do not vary significantly on a year-to-year basis. Other sources of interannual variability (e.g. the impact of climate variability on regrowth fluxes) are accounted for in  $S_{LAND}$ . In addition, we use results from Dynamic Global Vegetation Models (see Section 2.2.3 and Table 6) that calculate net land-use change  $CO_2$  emissions in response to land-cover change reconstructions prescribed to each model, to help quantify the uncertainty in  $E_{LUC}$ , and to explore the consistency of our understanding. The three methods are described below, and differences are discussed in Section 3.2.

### 2.2.1 Bookkeeping method

Land-use change  $CO_2$  emissions are calculated by a bookkeeping method approach (Houghton, 2003) that keeps track of the carbon stored in vegetation and soils before deforestation or other land-use change, and the changes in forest age classes, or cohorts, of disturbed lands after land-use change including possible forest regrowth after deforestation. It tracks the  $CO_2$  emitted to the atmosphere immediately during deforestation, and over time due to the follow-up decay of soil and vegetation carbon in different pools, including wood products pools after logging and deforestation. It also tracks the regrowth of vegetation and associated build-up of soil carbon pools after land-use change. It considers transitions between forests, pastures and cropland; shifting cultivation; degradation of forests where a fraction of the trees is removed; abandonment of agricultural land; and forest management such as wood harvest and, in the USA, fire management. In addition to tracking logging debris on the forest floor, the bookkeeping method tracks the fate of carbon contained in harvested wood products that is eventually emitted back to the atmosphere as  $CO_2$ , although a detailed treatment of the lifetime in each product pool is not performed (Earles et al., 2012). Harvested wood products are partitioned into three pools with different turnover times. All fuel-wood is assumed burnt in the year of harvest ( $1.0 \text{ yr}^{-1}$ ). Pulp and paper products are oxidized at a rate of  $0.1 \text{ yr}^{-1}$ , timber is assumed to be oxidized at a rate of  $0.01$

yr<sup>-1</sup>, and elemental carbon decays at 0.001 yr<sup>-1</sup>. The general assumptions about partitioning wood products among these pools are based on national harvest data (Houghton, 2003).

The primary land-cover change and biomass data for the bookkeeping method analysis is the Forest Resource Assessment of the FAO which provides statistics on forest-cover change and management at intervals of five years (FAO, 2010). The data is based on countries' self-reporting some of which include satellite data in more recent assessments (Table 4). Changes in land cover other than forest are based on annual, national changes in cropland and pasture areas reported by the FAO Statistics Division (FAOSTAT, 2010). Land-use change country data are aggregated by regions. The carbon stocks on land (biomass and soils), and their response functions subsequent to land-use change, are based on FAO data averages per land cover type, per biome and per region. Similar results were obtained using forest biomass carbon density based on satellite data (Baccini et al., 2012). The bookkeeping method does not include land ecosystems' transient response to changes in climate, atmospheric CO<sub>2</sub> and other environmental factors, but the growth/decay curves are based on contemporary data that will implicitly reflect the effects of CO<sub>2</sub> and climate at that time. Results from the bookkeeping method are available from 1850 to 2010.

### 2.2.2 Fire-based interannual variability in E<sub>LUC</sub>

Land-use change associated CO<sub>2</sub> emissions calculated from satellite-based fire activity in tropical forest areas (van der Werf et al., 2010) provide information on emissions due to tropical deforestation and degradation that are complementary to the bookkeeping approach. They do not provide a direct estimate of E<sub>LUC</sub> as they do not include non-combustion processes such as respiration, wood harvest, wood products or forest regrowth. Legacy emissions such as decomposition from on-ground debris and soils are not included in this method either. However, fire estimates provide some insight in the year-to-year variations in the sub-component of the total E<sub>LUC</sub> flux that result from immediate CO<sub>2</sub> emissions during deforestation caused, for example, by the interactions between climate and human activity (e.g. there is more burning and clearing of forests in dry years) that are not represented by other methods. The 'deforestation fire emissions' assume an important role of fire in removing biomass in the deforestation process, and thus can be used to infer gross instantaneous CO<sub>2</sub> emissions from deforestation using satellite-derived data on fire activity in regions with active deforestation. The method requires information on the fraction of total area burned associated with deforestation versus other types of fires, and this information can be merged with information on biomass stocks and the fraction of the biomass

lost in a deforestation fire to estimate CO<sub>2</sub> emissions. The satellite-based deforestation fire emissions are limited to the tropics, where fires result mainly from human activities. Tropical deforestation is the largest and most variable single contributor to E<sub>LUC</sub>. Fire emissions associated with deforestation and tropical peat burning are based on the Global Fire Emissions Database (GFED4; accessed October 2015) described in van der Werf et al. (2010) but with updated burned area (Giglio et al., 2013) as well as burned area from relatively small fires that are detected by satellite as thermal anomalies but not mapped by the burned area approach (Randerson, 2012). The burned area information is used as input data in a modified version of the satellite-driven Carnegie Ames Stanford Approach (CASA) biogeochemical model to estimate carbon emissions associated with fires, keeping track of what fraction of fire emissions was due to deforestation (see van der Werf et al., 2010). The CASA model uses different assumptions to compute decay functions compared to the bookkeeping method, and does not include historical emissions or regrowth from land-use change prior to the availability of satellite data. Comparing coincident CO emissions and their atmospheric fate with satellite-derived CO concentrations allows for some validation of this approach (e.g. van der Werf et al., 2008). Results from the fire-based method to estimate land-use change emissions anomalies added to the bookkeeping mean E<sub>LUC</sub> estimate are available from 1997 to 2014. Our combination of land-use change CO<sub>2</sub> emissions where the variability of annual CO<sub>2</sub> deforestation emissions is diagnosed from fires assumes that year-to-year variability is dominated by variability in deforestation.

### 2.2.3 Dynamic Global Vegetation Models (DGVMs)

Land-use change CO<sub>2</sub> emissions have been estimated using an ensemble of ten DGVMs. New model experiments up to year 2014 have been coordinated by the project 'Trends and drivers of the regional-scale sources and sinks of carbon dioxide (TRENDY; Sitch et al., 2015)'. We use only models that have estimated land-use change CO<sub>2</sub> emissions and the terrestrial residual sink following the TRENDY protocol (see Section 2.5.2), thus providing better consistency in the assessment of the causes of carbon fluxes on land. Models use their latest configurations, summarised in Tables 5 and 6.

The DGVMs were forced with historical changes in land cover distribution, climate, atmospheric CO<sub>2</sub> concentration, and N deposition. As further described below, each historical DGVM simulation was repeated with a time-invariant pre-industrial land cover distribution, allowing to estimate, by difference with the first simulation, the dynamic evolution of biomass and soil carbon

1 pools in response to prescribed land-cover change. All DGVMs represent deforestation and (to  
 2 some extent) regrowth, the most important components of  $E_{LUC}$ , but they do not represent all  
 3 processes resulting directly from human activities on land (Table 5). DGVMs represent processes  
 4 of vegetation growth and mortality, as well as decomposition of dead organic matter associated  
 5 with natural cycles, and include the vegetation and soil carbon response to increasing atmospheric  
 6  $CO_2$  levels and to climate variability and change. In addition, three models explicitly simulate the  
 7 coupling of C and N cycles and account for atmospheric N deposition (Table 5). The DGVMs are  
 8 independent from the other budget terms except for their use of atmospheric  $CO_2$  concentration  
 9 to calculate the fertilization effect of  $CO_2$  on primary production.

10 The DGVMs used a consistent land-use change data set (Hurtt et al., 2011), which provided  
 11 annual, half-degree, fractional data on cropland, pasture, primary vegetation and secondary  
 12 vegetation, as well as all underlying transitions between land-use states, including wood harvest  
 13 and shifting cultivation. This data set used the HYDE (Klein Goldewijk et al., 2011) spatially gridded  
 14 maps of cropland, pasture, and ice/water fractions of each grid cell as an input. The HYDE data are  
 15 based on annual FAO statistics of change in agricultural area available to 2012 (FAOSTAT, 2010)  
 16 For the years 2013 and 2014, the HYDE data were extrapolated by country for pastures and  
 17 cropland separately based on the trend in agricultural area over the previous 5 years. The HYDE  
 18 data are independent from the data set used in the bookkeeping method (Houghton, 2003 and  
 19 updates), which is based primarily on forest area change statistics (FAO, 2010). Although the HYDE  
 20 land-use change data set indicates whether land-use changes occur on forested or non-forested  
 21 land, typically only the changes in agricultural areas are used by the models and are implemented  
 22 differently within each model (e.g. an increased cropland fraction in a grid cell can either be at the  
 23 expense of grassland, or forest, the latter resulting in deforestation; land cover fractions of the  
 24 non-agricultural land differ between models). Thus the DGVM forest area and forest area change  
 25 over time is not consistent with the Forest Resource Assessment of the FAO forest area data used  
 26 for the bookkeeping model to calculate  $E_{LUC}$ . Similarly, model-specific assumptions are applied to  
 27 convert deforested biomass or deforested area, and other forest product pools, into carbon in  
 28 some models (Table 5).

29 The DGVM model runs were forced by either 6 hourly CRU-NCEP or by monthly CRU temperature,  
 30 precipitation, and cloud cover fields (transformed into incoming surface radiation) based on  
 31 observations and provided on a  $0.5^\circ \times 0.5^\circ$  grid and updated to 2014 (CRU TS3.23; Harris et al.,

2015). The forcing data include both gridded observations of climate and global atmospheric CO<sub>2</sub>, which change over time (Dlugokencky and Tans, 2015), and N deposition (as used in 3 models, Table 5; Lamarque et al., 2010). E<sub>LUC</sub> is diagnosed in each model by the difference between a model simulation with prescribed historical land cover change and a simulation with constant, preindustrial land cover distribution. Both simulations were driven by changing atmospheric CO<sub>2</sub>, climate, and in some models N deposition over the period 1860-2014. Using the difference between these two DGVM simulations to diagnose E<sub>LUC</sub> is not fully consistent with the definition of E<sub>LUC</sub> in the bookkeeping method (Gasser and Ciais, 2013; Pongratz et al., 2014; Pongratz et al., 2013). The DGVM approach to diagnose land-use change CO<sub>2</sub> emissions would be expected to produce systematically higher E<sub>LUC</sub> emissions than the bookkeeping approach if all the parameters of the two approaches were the same, which is not the case (see Section 2.5.2).

#### 2.2.4 Commentary on other published E<sub>LUC</sub> methods

Other methods have been used to estimate CO<sub>2</sub> emissions from land-use change. We describe some of the most important methodological differences between the approach used here and other published methods, and for completion, we explain why they are not used in the budget.

Different definitions and boundary conditions for E<sub>LUC</sub> can lead to significantly different estimates within models (Gasser and Ciais, 2013; Hansis et al., 2015; Pongratz et al., 2014) as well as between models and other approaches (Houghton et al., 2012; Smith et al., 2014b). An IPCC Tier 1-type approach (e.g. Tubiello et al., 2015) is used by the FAO to produce a 'Land use – forest land' estimate from FRA data updated from the one used in the bookkeeping method described in Section 2.2.1 (MacDicken, 2015). This method applies a nationally reported mean forest carbon stock change (above and below ground living biomass) to nationally reported net forest area change, across all forest land combined (planted and natural forests). The methods implicitly assumes instantaneous loss or gain of mean forest. Thus the IPCC Tier 1-type approach provides an estimate of attributable emissions from the process of land-cover change, but it does not distribute these emissions through time. It also captures some of what the global modelling approach considers residual carbon flux (S<sub>LAND</sub>), it does not consider loss of soil carbon, and there are no legacy fluxes. Land use fluxes estimated with this method were 0.47 GtC yr<sup>-1</sup> in 2001-2010 and 0.22 GtC yr<sup>-1</sup> in 2011-2015 (Federici et al., 2015). This estimate is not directly comparable with E<sub>LUC</sub> used here because of the different boundary conditions.

Recent advances in satellite data leading to higher resolution area change data (e.g. Hansen et al., 2013) and estimates of biomass in live vegetation (e.g. Baccini et al., 2012; Saatchi, 2011), have led to several satellite-based estimates of CO<sub>2</sub> emissions due to tropical deforestation (typically gross loss of forest area; Achard and House, in press). These include estimates of 1.0 GtC yr<sup>-1</sup> for 2000 to 2010 (Baccini et al., 2012), 0.8 GtC yr<sup>-1</sup> for 2000 to 2005 (Harris, 2012), 0.9 GtC yr<sup>-1</sup> for 2000 to 2010 for net area change (Achard et al., 2014), and 1.3 GtC yr<sup>-1</sup> 2000 to 2010 (Tyukavina et al., 2015). These estimates include belowground carbon biomass using a scaling factor. Some estimate soil carbon loss, some assume instantaneous emissions, some do not account for regrowth fluxes, and none account for legacy fluxes from land-use change prior to the availability of satellite data. They are mostly estimates of tropical deforestation only, and do not capture regrowth flux after abandonment, or planting (Achard and House, in press). These estimate are also difficult to compare with E<sub>LUC</sub> used here because they do not fully include legacy fluxes and forest regrowth.

#### 2.2.5 Uncertainty assessment for E<sub>LUC</sub>

Differences between the bookkeeping, the addition of fire-based interannual variability to the bookkeeping, and DGVM methods originate from three main sources: the land cover change data set, the different approaches used in models, and the different processes represented (Table 5). We examine the results from the ten DGVM models and of the bookkeeping method to assess the uncertainty in E<sub>LUC</sub>.

The uncertainties in annual E<sub>LUC</sub> estimates are examined using the standard deviation across models, which averages 0.4 GtC yr<sup>-1</sup> from 1959 to 2014 (Table 7). The mean of the multi-model E<sub>LUC</sub> estimates is consistent with a combination of the bookkeeping method and fire-based emissions (Le Quéré et al. 2014), with the multi-model mean and bookkeeping method differing by less than 0.5 GtC yr<sup>-1</sup> over 85% of the time. Based on this comparison, we assess that an uncertainty of ±0.5 GtC yr<sup>-1</sup> provides a semi-quantitative measure of uncertainty for annual emissions, and reflects our best value judgment that there is at least 68% chance (±1σ) that the true land-use change emission lies within the given range, for the range of processes considered here. This is consistent with the uncertainty analysis of Houghton et al. (2012), which partly reflects improvements in data on forest area change using data, and partly more complete understanding and representation of processes in models.

The uncertainties in the decadal  $E_{LUC}$  estimates are also examined using the DGVM ensemble, although they are likely correlated between decades. The correlations between decades come from (1) common biases in system boundaries (e.g. not counting forest degradation in some models); (2) common definition for the calculation of  $E_{LUC}$  from the difference of simulations with and without land-use change (a source of bias vs. the unknown truth); (3) common and uncertain land-cover change input data which also cause a bias, though if a different input data set is used each decade, decadal fluxes from DGVMs may be partly decorrelated; (4) model structural errors (e.g. systematic errors in biomass stocks). In addition, errors arising from uncertain DGVM parameter values would be random but they are not accounted for in this study, since no DGVM provided an ensemble of runs with perturbed parameters.

Prior to 1959, the uncertainty in  $E_{LUC}$  is taken as  $\pm 33\%$ , which is the ratio of uncertainty to mean from the 1960s (Table 7), the first decade available. This ratio is consistent with the mean standard deviation of DGVMs land-use change emissions over 1870-1958 (0.38 GtC) over the multi-model mean (1.1 GtC).

## 2.3 Atmospheric CO<sub>2</sub> growth rate ( $G_{ATM}$ )

### 2.3.1 Global atmospheric CO<sub>2</sub> growth rate estimates

The atmospheric CO<sub>2</sub> growth rate is provided by the US National Oceanic and Atmospheric Administration Earth System Research Laboratory (NOAA/ESRL; Dlugokencky and Tans, 2015), which is updated from Ballantyne et al. (2012). For the 1959-1980 period, the global growth rate is based on measurements of atmospheric CO<sub>2</sub> concentration averaged from the Mauna Loa and South Pole stations, as observed by the CO<sub>2</sub> Program at Scripps Institution of Oceanography (Keeling et al., 1976). For the 1980-2014 time period, the global growth rate is based on the average of multiple stations selected from the marine boundary layer sites with well-mixed background air (Ballantyne et al., 2012), after fitting each station with a smoothed curve as a function of time, and averaging by latitude band (Masarie and Tans, 1995). The annual growth rate is estimated by Dlugokencky and Tans (2015) from atmospheric CO<sub>2</sub> concentration by taking the average of the most recent December-January months corrected for the average seasonal cycle and subtracting this same average one year earlier. The growth rate in units of ppm yr<sup>-1</sup> is converted to units of GtC yr<sup>-1</sup> by multiplying by a factor of 2.12 GtC per ppm (Ballantyne et al., 2012) for consistency with the other components.

The uncertainty around the annual growth rate based on the multiple stations data set ranges between 0.11 and 0.72 GtC yr<sup>-1</sup>, with a mean of 0.61 GtC yr<sup>-1</sup> for 1959-1979 and 0.19 GtC yr<sup>-1</sup> for 1980-2014, when a larger set of stations were available (Dlugokencky and Tans, 2015). It is based on the number of available stations, and thus takes into account both the measurement errors and data gaps at each station. This uncertainty is larger than the uncertainty of  $\pm 0.1$  GtC yr<sup>-1</sup> reported for decadal mean growth rate by the IPCC because errors in annual growth rate are strongly anti-correlated in consecutive years leading to smaller errors for longer time scales. The decadal change is computed from the difference in concentration ten years apart based on a measurement error of 0.35 ppm. This error is based on offsets between NOAA/ESRL measurements and those of the World Meteorological Organization World Data Center for Greenhouse Gases (NOAA/ESRL, 2015a) for the start and end points (the decadal change uncertainty is the  $\sqrt{(2(0.35\text{ppm})^2)}(10\text{ yr})^{-1}$  assuming that each yearly measurement error is independent). This uncertainty is also used in Table 8.

The contribution of anthropogenic CO and CH<sub>4</sub> is neglected from the global carbon budget (see Sect. 2.7.1). We assign a high confidence to the annual estimates of G<sub>ATM</sub> because they are based on direct measurements from multiple and consistent instruments and stations distributed around the world (Ballantyne et al., 2012).

In order to estimate the total carbon accumulated in the atmosphere since 1750 or 1870, we use an atmospheric CO<sub>2</sub> concentration of  $277 \pm 3$  ppm or  $288 \pm 3$  ppm, respectively, based on a cubic spline fit to ice core data (Joos and Spahni, 2008). The uncertainty of  $\pm 3$  ppm (converted to  $\pm 1\sigma$ ) is taken directly from the IPCC's assessment (Ciais et al., 2013). Typical uncertainties in the atmospheric growth rate from ice core data are  $\pm 1$ -1.5 GtC per decade as evaluated from the Law Dome data (Etheridge et al., 1996) for individual 20-year intervals over the period from 1870 to 1960 (Bruno and Joos, 1997).

## 2.4 Ocean CO<sub>2</sub> sink

Estimates of the global ocean CO<sub>2</sub> sink are based on a combination of a mean CO<sub>2</sub> sink estimate for the 1990s from observations, and a trend and variability in the ocean CO<sub>2</sub> sink for 1959-2014 from eight global ocean biogeochemistry models. We use two observation-based estimates of S<sub>OCEAN</sub> available for recent decades to provide a qualitative assessment of confidence in the reported results.



#### 2.4.1 Observation-based estimates

A mean ocean CO<sub>2</sub> sink of  $2.2 \pm 0.4$  GtC yr<sup>-1</sup> for the 1990s was estimated by the IPCC (Denman et al., 2007) based on indirect observations and their spread: ocean/land CO<sub>2</sub> sink partitioning from observed atmospheric O<sub>2</sub>/N<sub>2</sub> concentration trends (Keeling et al., 2011; Manning and Keeling, 2006), an oceanic inversion method constrained by ocean biogeochemistry data (Mikaloff Fletcher et al., 2006), and a method based on penetration time scale for CFCs (McNeil et al., 2003). This is comparable with the sink of  $2.0 \pm 0.5$  GtC yr<sup>-1</sup> estimated by Khatiwala et al. (2013) for the 1990s, and with the sink of 1.9 to 2.5 GtC yr<sup>-1</sup> estimated from a range of methods for the period 1990–2009 (Wanninkhof et al., 2013), with uncertainties ranging from  $\pm 0.3$  GtC yr<sup>-1</sup> to  $\pm 0.7$  GtC yr<sup>-1</sup>. The most direct way for estimating the observation-based ocean sink is from the product of (sea-air pCO<sub>2</sub> difference) x (gas transfer coefficient). Estimates based on sea-air pCO<sub>2</sub> are fully consistent with indirect observations (Zeng et al., 2005), but their uncertainty is larger mainly due to difficulty in capturing complex turbulent processes in the gas transfer coefficient (Sweeney et al., 2007) and because of uncertainties in the pre-industrial river outgas of CO<sub>2</sub> (Jacobson et al., 2007).

Both observation-based estimates compute the ocean CO<sub>2</sub> sink and its variability using interpolated measurements of surface ocean fugacity of CO<sub>2</sub> (pCO<sub>2</sub> corrected for the non-ideal behaviour of the gas; Pfeil et al., 2013). The measurements were from the Surface Ocean CO<sub>2</sub> Atlas (SOCAT v3; Bakker et al., 2014; Bakker et al., in prep) that contains 14.5 million data to the end of 2014. This was extended with 1.4 million additional measurements over years 2013–2014 (see data attribution Table 1A), submitted to SOCAT but not yet fully quality controlled following standard SOCAT procedures. Revisions and corrections to previously reported measurements were also included where they were available. All new data were subjected to an automated quality control system to detect and remove the most obvious errors (e.g. incorrect reporting of metadata such as position, wrong units, clearly unrealistic data etc.). The combined SOCAT v3 and preliminary new 2013–2014 measurements were mapped using a data-driven diagnostic method (Rödenbeck et al., 2013) and a combined self-organising map and feed-forward neural network (Landschützer et al., 2014). The global observation-based estimates were corrected to remove a background (not part of the anthropogenic ocean flux) ocean source of CO<sub>2</sub> to the atmosphere of 0.45 GtC yr<sup>-1</sup> from river input to the ocean (Jacobson et al., 2007), to make them comparable to S<sub>OCEAN</sub> which only represents the annual uptake of anthropogenic CO<sub>2</sub> by the ocean. Several other

data-based products are in preparation, but they show large discrepancies that need to be resolved (e.g. Rödenbeck et al., 2015).

We use the data-based product of Khatiwala et al. (2009) updated by Khatiwala et al. (2013) to estimate the anthropogenic carbon accumulated in the ocean during 1765-1958 (60.2 GtC) and 1870-1958 (47.5 GtC), and assume an oceanic uptake of 0.4 GtC for 1750-1765 (for which time no data are available) based on the mean uptake during 1765-1770. The estimate of Khatiwala et al. (2009) is based on regional disequilibrium between surface  $p\text{CO}_2$  and atmospheric  $\text{CO}_2$ , and a Green's function utilizing transient ocean tracers like CFCs and  $^{14}\text{C}$  to ascribe changes through time. It does not include changes associated with changes in ocean circulation, temperature and climate, but these are thought to be small over the time period considered here (Ciais et al., 2013). The uncertainty in cumulative uptake of  $\pm 20$  GtC (converted to  $\pm 1\sigma$ ) is taken directly from the IPCC's review of the literature (Rhein et al., 2013), or about  $\pm 30\%$  for the annual values (Khatiwala et al., 2009).

#### 2.4.2 Global Ocean Biogeochemistry models

The trend in the ocean  $\text{CO}_2$  sink for 1959-2014 is computed using a combination of eight global ocean biogeochemistry models (Table 6). The models represent the physical, chemical and biological processes that influence the surface ocean concentration of  $\text{CO}_2$  and thus the air-sea  $\text{CO}_2$  flux. The models are forced by meteorological reanalysis and atmospheric  $\text{CO}_2$  concentration data available for the entire time period. Models do not include the effects of anthropogenic changes in nutrient supply. They compute the air-sea flux of  $\text{CO}_2$  over grid boxes of  $1^\circ$  to  $4^\circ$  in latitude and longitude. The ocean  $\text{CO}_2$  sink for each model is normalised to the observations, by dividing the annual model values by their observed average over 1990-1999 and multiplying this with the observation-based estimate of  $2.2 \text{ GtC yr}^{-1}$  (obtained from Keeling et al., 2011; Manning and Keeling, 2006; McNeil et al., 2003; Mikaloff Fletcher et al., 2006). The ocean  $\text{CO}_2$  sink for each year ( $t$ ) in  $\text{GtC yr}^{-1}$  is therefore:

$$S_{OCEAN}(t) = \frac{1}{n} \sum_{m=1}^{m=n} \frac{S_{OCEAN}^m(t)}{S_{OCEAN}^m(1990 - 1999)} \times 2.2 \quad (7)$$

where  $n$  is the number of models. This normalisation ensures that the ocean  $\text{CO}_2$  sink for the global carbon budget is based on observations, whereas the trends and annual values in  $\text{CO}_2$  sinks are from model estimates. The normalisation based on a ratio assumes that if models over or

underestimate the sink in the 1990s, it is primarily due to the process of diffusion, which depends on the gradient of CO<sub>2</sub>. Thus a ratio is more appropriate than an offset as it takes into account the time-dependence of CO<sub>2</sub> gradients in the ocean. The mean uncorrected ocean CO<sub>2</sub> sink from the eight models for 1990-1999 ranges between 1.6 and 2.4 GtC yr<sup>-1</sup>, with a multi model mean of 1.9 GtC yr<sup>-1</sup>.

#### 2.4.3 Uncertainty assessment for S<sub>OCEAN</sub>

The uncertainty around the mean ocean sink of anthropogenic CO<sub>2</sub> was quantified by Denman et al. (2007) for the 1990s (see Section 2.4.1). To quantify the uncertainty around annual values, we examine the standard deviation of the normalised model ensemble. We use further information from the two data-based products to assess the confidence level. The average standard deviation of the normalised ocean model ensemble is 0.13 GtC yr<sup>-1</sup> during 1980-2010 (with a maximum of 0.27), but it increases as the model ensemble goes back in time, with a standard deviation of 0.22 GtC yr<sup>-1</sup> across models in the 1960s. We estimate that the uncertainty in the annual ocean CO<sub>2</sub> sink is about  $\pm 0.5$  GtC yr<sup>-1</sup> from the fractional uncertainty of the data uncertainty of  $\pm 0.4$  GtC yr<sup>-1</sup> and standard deviation across models of up to  $\pm 0.27$  GtC yr<sup>-1</sup>, reflecting both the uncertainty in the mean sink from observations during the 1990's (Denman et al., 2007; Section 2.4.1) and in the interannual variability as assessed by models.

We examine the consistency between the variability of the model-based and the data-based products to assess confidence in S<sub>OCEAN</sub>. The interannual variability of the ocean fluxes (quantified as the standard deviation) of the two data-based estimates for 1986-2014 (where they overlap) is  $\pm 0.38$  GtC yr<sup>-1</sup> (Rödenbeck et al., 2014) and  $\pm 0.40$  GtC yr<sup>-1</sup> (Landschützer et al., 2015), compared to  $\pm 0.27$  GtC yr<sup>-1</sup> for the normalised model ensemble. The standard deviation includes a component of trend and decadal variability in addition to interannual variability, and their relative influence differs across estimates. The phase is generally consistent between estimates, with a higher ocean CO<sub>2</sub> sink during El Niño events. The annual data-based estimates correlate with the ocean CO<sub>2</sub> sink estimated here with a correlation of  $r = 0.51$  (0.34 to 0.58 for individual models), and  $r = 0.71$  (0.54 to 0.72) for the data-based estimates of Rödenbeck et al. (2014) and Landschützer et al. (2015), respectively (simple linear regression), but their mutual correlation is only 0.55. The use of annual data for the correlation may reduce the strength of the relationship because the dominant source of variability associated with El Niño events is less than one year. We assess a medium confidence level to the annual ocean CO<sub>2</sub> sink and its uncertainty because

they are based on multiple lines of evidence, and the results are consistent in that the interannual variability in the model and data-based estimates are all generally small compared to the variability in atmospheric CO<sub>2</sub> growth rate. Nevertheless the various results do not show agreement in interannual variability on the global scale or for the relative roles of the annual and decadal variability compared to the trend.

## 2.5 Terrestrial CO<sub>2</sub> sink

The difference between, on the one hand fossil fuel ( $E_{FF}$ ) and land-use change emissions ( $E_{LUC}$ ), and on the other hand the growth rate in atmospheric CO<sub>2</sub> concentration ( $G_{ATM}$ ) and the ocean CO<sub>2</sub> sink ( $S_{OCEAN}$ ), is attributable to the net sink of CO<sub>2</sub> in terrestrial vegetation and soils ( $S_{LAND}$ ), within the given uncertainties (Eq. 1). Thus, this sink can be estimated as the residual of the other terms in the mass balance budget, as well as directly calculated using DGVMs. The residual land sink ( $S_{LAND}$ ) is thought to be in part because of the fertilising effect of rising atmospheric CO<sub>2</sub> on plant growth, N deposition and effects of climate change such as the lengthening of the growing season in northern temperate and boreal areas.  $S_{LAND}$  does not include gross land sinks directly resulting from land-use change (e.g. regrowth of vegetation) as these are estimated as part of the net land use flux ( $E_{LUC}$ ). System boundaries make it difficult to attribute exactly CO<sub>2</sub> fluxes on land between  $S_{LAND}$  and  $E_{LUC}$  (Erb et al., 2013), and by design most of the uncertainties in our method are allocated to  $S_{LAND}$  for those processes that are poorly known or represented in models.

### 2.5.1 Residual of the budget

For 1959-2014, the terrestrial carbon sink was estimated from the residual of the other budget terms by rearranging Eq. (1):

$$S_{LAND} = E_{FF} + E_{LUC} - (G_{ATM} + S_{OCEAN}) \quad (8)$$

The uncertainty in  $S_{LAND}$  is estimated annually from the root sum of squares of the uncertainty in the right-hand terms assuming the errors are not correlated. The uncertainty averages to  $\pm 0.8$  GtC yr<sup>-1</sup> over 1959-2014 (Table 7).  $S_{LAND}$  estimated from the residual of the budget includes, by definition, all the missing processes and potential biases in the other components of Eq. (8).

### 2.5.2 DGVMs

A comparison of the residual calculation of  $S_{LAND}$  in Eq. (8) with estimates from DGVMs as used to estimate  $E_{LUC}$  in Sect. 2.2.3, but here excluding the effects of changes in land cover (using a

constant pre-industrial land cover distribution), provides an independent estimate of the consistency of  $S_{\text{LAND}}$  with our understanding of the functioning of the terrestrial vegetation in response to  $\text{CO}_2$  and climate variability (Table 7). As described in Sect. 2.2.3, the DGVM runs that exclude the effects of changes in land cover include all climate variability and  $\text{CO}_2$  effects over land, but do not include reductions in  $\text{CO}_2$  sink capacity associated with human activity directly affecting changes in vegetation cover and management, which by design is allocated to  $E_{\text{LUC}}$ . This effect has been estimated to have led to a reduction in the terrestrial sink by  $0.5 \text{ GtC yr}^{-1}$  since 1750 (Gitz and Ciais, 2003). The models in this configuration estimate the mean and variability of  $S_{\text{LAND}}$  based on atmospheric  $\text{CO}_2$  and climate, and thus both terms can be compared to the budget residual.

The annual standard deviation of the  $\text{CO}_2$  sink across the ten DGVMs averages to  $\pm 0.7 \text{ GtC yr}^{-1}$  for the period 1959 to 2014. The model mean, over different decades, correlates with the budget residual with  $r = 0.71$  ( $0.52$  to  $r = 0.71$  for individual models). The standard deviation is similar to that of the five model ensembles presented in Le Quéré et al. (2009), but the correlation is improved compared to  $r = 0.54$  obtained in the earlier study. The DGVM results suggest that the sum of our knowledge on annual  $\text{CO}_2$  emissions and their partitioning is plausible (see Discussion), and provide insight on the underlying processes and regional breakdown. However as the standard deviation across the DGVMs (e.g.  $\pm 0.9 \text{ GtC yr}^{-1}$  for year 2014) is of the same magnitude as the combined uncertainty due to the other components ( $E_{\text{FF}}$ ,  $E_{\text{LUC}}$ ,  $G_{\text{ATM}}$ ,  $S_{\text{OCEAN}}$ ; Table 7), the DGVMs do not provide further reduction of uncertainty on the annual terrestrial  $\text{CO}_2$  sink compared to the residual of the budget (Eq. 8). Yet, DGVM results are largely independent from the residual of the budget, and it is worth noting that the residual method and ensemble mean DGVM results are consistent within their respective uncertainties. We attach a medium confidence level to the annual land  $\text{CO}_2$  sink and its uncertainty because the estimates from the residual budget and averaged DGVMs match well within their respective uncertainties, and the estimates based on the residual budget are primarily dependent on  $E_{\text{FF}}$  and  $G_{\text{ATM}}$ , both of which are well constrained.

## 2.6 The atmospheric perspective

The world-wide network of atmospheric measurements can be used with atmospheric inversion methods to constrain the location of the combined total surface  $\text{CO}_2$  fluxes from all sources, including fossil and land-use change emissions and land and ocean  $\text{CO}_2$  fluxes. The inversions

assume  $E_{FF}$  to be well known, and they solve for the spatial and temporal distribution of land and ocean fluxes from the residual gradients of  $CO_2$  between stations that are not explained by emissions. Inversions used atmospheric  $CO_2$  data to the end of 2014 (including preliminary values in some cases), and three atmospheric  $CO_2$  inversions (Table 6) to infer the total  $CO_2$  flux over land regions, and the distribution of the total land and ocean  $CO_2$  fluxes for the mid-high latitude northern hemisphere ( $30^\circ N$ - $90^\circ N$ ), Tropics ( $30^\circ S$ - $30^\circ N$ ) and mid-high latitude region of the southern hemisphere ( $30^\circ S$ - $90^\circ S$ ). We focus here on the largest and most consistent sources of information, and use these estimates to comment on the consistency across various data streams and process-based estimates.

### 2.6.1 Atmospheric inversions

The three inversion systems used in this release (Chevallier et al., 2005; Peters et al., 2010; Rödenbeck, 2005) are based on the same Bayesian inversion principles that interpret the same, for the most part, observed time series (or subsets thereof), but use different methodologies that represent some of the many approaches used in the field. This mainly concerns the time resolution of the estimates (i.e. weekly or monthly), spatial breakdown (i.e. grid size), assumed correlation structures, and mathematical approach. The details of these approaches are documented extensively in the references provided. Each system uses a different transport model, which was demonstrated to be a driving factor behind differences in atmospheric-based flux estimates, and specifically their global distribution (Stephens et al., 2007). The three inversions use atmospheric  $CO_2$  observations from various flask and in situ networks. They prescribe spatial and global  $E_{FF}$  that can vary from that presented here. Most inverse models use estimates for the ocean and land-biosphere, which can be very similar to those described in Section 2.4.1 and 2.5.1 to assign prior fluxes. Finally, results from atmospheric inversions include the natural  $CO_2$  fluxes from rivers (which need to be taken into account to allow comparison to other sources), and chemical oxidation of reactive carbon-containing gases (which are neglected here). These inverse estimates are not truly independent of the other estimates presented here as the atmospheric observations include a set of observations used to estimate the global atmospheric growth rate (Section 2.3). However they provide new information on the regional distribution of fluxes.

We focus the analysis on two known strengths of the inverse approach: the derivation of the year-to-year changes in total land fluxes ( $E_{\text{LUC}} + S_{\text{LAND}}$ ) consistent with the whole network of atmospheric observations, and the spatial breakdown of land and ocean fluxes ( $E_{\text{LUC}} + S_{\text{LAND}} + S_{\text{OCEAN}}$ ) across large regions of the globe. The total land flux correlates well with those estimated from the budget residual (Eq. 1) with correlations for the annual time series ranging from  $r = 0.89$  to  $0.93$ , and with the DGVM multi-model mean with correlations for the annual time series ranging from  $r = 0.71$  to  $0.80$  ( $r = 0.49$  to  $0.81$  for individual DGVMs and inversions). The spatial breakdown is discussed in Section 3.1.3.

## **2.7 Processes not included in the global carbon budget**

### **2.7.1 Contribution of anthropogenic CO and CH<sub>4</sub> to the global carbon budget**

Anthropogenic emissions of CO and CH<sub>4</sub> to the atmosphere are eventually oxidized to CO<sub>2</sub> and thus are part of the global carbon budget. These contributions are omitted in Eq. (1), but an attempt is made in this section to estimate their magnitude, and identify the sources of uncertainty. Anthropogenic CO emissions are from incomplete fossil fuel and biofuel burning and deforestation fires. The main anthropogenic emissions of fossil CH<sub>4</sub> that matter for the global carbon budget are the fugitive emissions of coal, oil and gas upstream sectors (see below). These emissions of CO and CH<sub>4</sub> contribute a net addition of fossil carbon to the atmosphere.

In our estimate of  $E_{\text{FF}}$  we assumed (Section 2.1.1) that all the fuel burned is emitted as CO<sub>2</sub>, thus CO anthropogenic emissions and their atmospheric oxidation into CO<sub>2</sub> within a few months are already counted implicitly in  $E_{\text{FF}}$  and should not be counted twice (same for  $E_{\text{LUC}}$  and anthropogenic CO emissions by deforestation fires). Anthropogenic emissions of fossil CH<sub>4</sub> are not included in  $E_{\text{FF}}$ , because these fugitive emissions are not included in the fuel inventories. Yet they contribute to the annual CO<sub>2</sub> growth rate after CH<sub>4</sub> gets oxidized into CO<sub>2</sub>. Anthropogenic emissions of fossil CH<sub>4</sub> represent 15% of total CH<sub>4</sub> emissions (Kirschke et al., 2013) that is  $0.061 \text{ GtC yr}^{-1}$  for the past decade. Assuming steady state, these emissions are all converted to CO<sub>2</sub> by OH oxidation, and thus explain  $0.06 \text{ GtC yr}^{-1}$  of the global CO<sub>2</sub> growth rate in the past decade.

Other anthropogenic changes in the sources of CO and CH<sub>4</sub> from wildfires, biomass, wetlands, ruminants or permafrost changes are similarly assumed to have a small effect on the CO<sub>2</sub> growth rate.

## 2.7.2 Anthropogenic carbon fluxes in the land to ocean aquatic continuum

The approach used to determine the global carbon budget considers only anthropogenic CO<sub>2</sub> emissions and their partitioning among the atmosphere, ocean and land. In this analysis, the land and ocean reservoirs that take up anthropogenic CO<sub>2</sub> from the atmosphere are conceived as independent carbon storage repositories. This approach thus omits that carbon is continuously displaced along the land-ocean aquatic continuum (LOAC) comprising freshwaters, estuaries and coastal areas (Bauer et al., 2013; Regnier et al., 2013). A significant fraction of this lateral carbon flux is entirely 'natural' and is thus a steady state component of the pre-industrial carbon cycle. The remaining fraction is anthropogenic carbon entrained into the lateral transport loop of the LOAC, a perturbation that is relevant for the global carbon budget presented here.

The results of the analysis of Regnier et al. (2013) can be summarized in three points of relevance to the anthropogenic CO<sub>2</sub> budget. First, the anthropogenic carbon input from land to hydrosphere,  $F_{LH}$ , estimated at  $1 \pm 0.5 \text{ GtC yr}^{-1}$  is significant compared to the other terms of Eq. (1) (Table 8), and implies that only a portion of the anthropogenic CO<sub>2</sub> taken up by land ecosystems remains sequestered in soil and biomass pools. Second, some of the exported anthropogenic carbon is stored in the LOAC ( $\Delta C_{LOAC}$ ,  $0.55 \pm 0.3 \text{ GtC yr}^{-1}$ ) and some is released back to the atmosphere as CO<sub>2</sub> ( $E_{LOAC}$ ,  $0.35 \pm 0.2 \text{ GtC yr}^{-1}$ ), the magnitude of these fluxes resulting from the combined effects of freshwaters, estuaries and coastal seas. Third, a small fraction of anthropogenic carbon displaced by the LOAC is transferred to the open ocean where it accumulates ( $F_{HO}$ ,  $0.1 \pm > 0.05 \text{ GtC yr}^{-1}$ ). The anthropogenic perturbation of the carbon fluxes from land to ocean does not contradict the method used in Section 2.5 to define the ocean sink and residual terrestrial sink. However, it does point to the need to account for the fate of anthropogenic carbon once it is removed from the atmosphere by land ecosystems (summarized in Fig 2). In theory, direct estimates of changes of the ocean inorganic carbon inventory over time would see the land flux of anthropogenic carbon and would thus have a bias relative to air-sea flux estimates and tracer based reconstructions. However, currently the value is small enough to be not noticeable relative to the errors in the individual techniques.

The residual terrestrial sink in a budget that accounts for the LOAC will be larger than  $S_{LAND}$ , as the flux is partially offset by the net source of CO<sub>2</sub> to the atmosphere, i.e.  $E_{LOAC}$ , of  $0.35 \pm 0.3 \text{ GtC yr}^{-1}$  from rivers, estuaries and coastal seas:



$$S_{LAND+LOAC} = E_{FF} + E_{LUC} - (G_{ATM} + S_{OCEAN}) + E_{LOAC} \quad (9)$$

The residual terrestrial sink ( $S_{LAND}$ ) is  $3.0 \pm 0.8 \text{ GtC yr}^{-1}$  for 2005-2014 as calculated according to Eq. (8; Table 7) while  $S_{LAND+LOAC}$  is  $3.3 \pm 0.9 \text{ GtC yr}^{-1}$  over the same time period. A fraction of anthropogenic  $\text{CO}_2$  taken up by land ecosystems is exported to the LOAC ( $F_{LH}$ ). With the LOAC included, we now have:

$$\Delta C_{TE} = S_{LAND+LOAC} - E_{LUC} - F_{LH} \quad (10)$$

where  $\Delta C_{TE}$  is the change in annual terrestrial ecosystems carbon storage, including land vegetation, litter and soil,  $\Delta C_{TE}$  is  $1.4 \text{ GtC yr}^{-1}$  for the period 2005-2014. It is notably smaller than what would be calculated in a traditional budget that ignores the LOAC. In this case, the change in carbon storage is estimated as  $2.1 \text{ Gt C yr}^{-1}$  from the difference between  $S_{LAND}$  ( $3.0 \text{ Gt C yr}^{-1}$ ) and  $E_{LUC}$  ( $0.9 \text{ Gt C yr}^{-1}$ ; Table 8). All estimates of LOAC are given with low confidence, because they originate from a single source. The carbon budget presented here implicitly incorporates the fluxes from the LOAC with  $S_{LAND}$ . We do not attempt to separate these fluxes because the uncertainties in either estimate are too large, and there is insufficient information available to estimate the LOAC fluxes on an annual basis.

### 3 Results

#### 3.1 Global carbon budget averaged over decades and its variability

The global carbon budget averaged over the last decade (2005-2014) is shown in Fig. 2. For this time period, 91% of the total emissions ( $E_{FF} + E_{LUC}$ ) were caused by fossil fuel combustion and cement production, and 9% by land-use change. The total emissions were partitioned among the atmosphere (44%), ocean (26%) and land (30%). All components except land-use change emissions have grown since 1959 (Figs. 3 and 4), with important interannual variability in the atmospheric growth rate and in the land  $\text{CO}_2$  sink (Fig. 4), and some decadal variability in all terms (Table 8).

##### 3.1.1 $\text{CO}_2$ emissions

Global  $\text{CO}_2$  emissions from fossil fuel combustion and cement production have increased every decade from an average of  $3.1 \pm 0.2 \text{ GtC yr}^{-1}$  in the 1960s to an average of  $9.0 \pm 0.5 \text{ GtC yr}^{-1}$  during 2005-2014 (Table 8 and Fig. 5). The growth rate in these emissions decreased between the 1960s and the 1990s, from  $4.5\% \text{ yr}^{-1}$  in the 1960s (1960-1969),  $2.9\% \text{ yr}^{-1}$  in the 1970s (1970-1979),  $1.9\%$

yr<sup>-1</sup> in the 1980s (1980-1989), and finally to 1.0 % yr<sup>-1</sup> in the 1990s (1990-1999), before it began increasing again in the 2000s at an average growth rate of 3.2 % yr<sup>-1</sup>, decreasing to 2.2 % yr<sup>-1</sup> for the last decade (2005-2014). In contrast, CO<sub>2</sub> emissions from land-use change have remained constant, in our analysis at around  $1.5 \pm 0.5$  GtC yr<sup>-1</sup> between 1960-1999 and  $1.0 \pm 0.5$  GtC yr<sup>-1</sup> during 2000-2014. The decrease in emissions from land-use change between the 1990s and 2000s is highly uncertain. It is not found in the current ensemble of the DGVMs (Fig. 6), which are otherwise consistent with the bookkeeping method within their respective uncertainty (Table 7). It is also not found in the study of tropical deforestation of Achard et al. (2014) where the fluxes in the 1990s were similar to those of the 2000s and outside our uncertainty range. A new study based on FAO data to 2015 (Federici et al., 2015) suggests that E<sub>LUC</sub> decreased during 2011-2015 compared to 2001-2010.

### 3.1.2 Partitioning

The growth rate in atmospheric CO<sub>2</sub> increased from  $1.7 \pm 0.1$  GtC yr<sup>-1</sup> in the 1960s to  $4.4 \pm 0.1$  GtC yr<sup>-1</sup> during 2005-2014 with important decadal variations (Table 8). Both ocean and land CO<sub>2</sub> sinks increased roughly in line with the atmospheric increase, but with significant decadal variability on land (Table 8). The ocean CO<sub>2</sub> sink increased from  $1.1 \pm 0.5$  GtC yr<sup>-1</sup> in the 1960s to  $2.6 \pm 0.5$  GtC yr<sup>-1</sup> during 2005-2014, with interannual variations of the order of a few tenths of GtC yr<sup>-1</sup> generally showing an increased ocean sink during El Niño (i.e. 1982-1983, 1991-1993, 1997-1998) events (Fig. 7; Rödenbeck et al., 2014). Although there is some coherence between the ocean models and data products and among data products, their mutual correlation is weak and highlights disagreement on the exact amplitude of the interannual variability, and on the relative importance of the trend versus the variability (Section 2.4.3 and Fig. 7). As shown in Fig. 7, the two data products and most model estimates produce a mean CO<sub>2</sub> sink for the 1990s that is below the mean assessed by the IPCC from indirect (but arguably more reliable) observations (Denman et al., 2007; Section 2.4.1). This discrepancy suggests we may need to reassess estimates of the mean ocean carbon sinks.

The land CO<sub>2</sub> sink increased from  $1.7 \pm 0.7$  GtC yr<sup>-1</sup> in the 1960s to  $3.0 \pm 0.8$  GtC yr<sup>-1</sup> during 2005-2014, with important interannual variations of up to 2 GtC yr<sup>-1</sup> generally showing a decreased land sink during El Niño events, overcompensating the increase in ocean sink and accounting for the enhanced atmospheric growth rate during El Niño events. The high uptake anomaly around year 1991 is thought to be caused by the effect of the volcanic eruption of Mount Pinatubo on climate

and is not generally reproduced by the DGVMs, but it is assigned to the land by the two inverse systems that include this period (Fig. 6). The larger land CO<sub>2</sub> sink during 2005-2014 compared to the 1960s is reproduced by all the DGVMs in response to combined atmospheric CO<sub>2</sub> increase, climate and variability ( $3.0 \pm 0.5$  GtC yr<sup>-1</sup> for the period 2005-2014 and average change of 1.9 GtC yr<sup>-1</sup> relative to the 1960s), consistent with the budget residual and reflecting a common knowledge of the processes (Table 7). The DGVM ensemble mean of  $3.0 \pm 0.5$  GtC yr<sup>-1</sup> also reproduce the observed mean for the period 2005-2014 calculated from the budget residual (Table 7).

The total CO<sub>2</sub> fluxes on land ( $E_{LUC} + S_{LAND}$ ) constrained by the atmospheric inversions show in general very good agreement with the global budget estimate, as expected given the strong constraints of  $G_{ATM}$  and the small relative uncertainty typically assumed on  $S_{OCEAN}$  and  $E_{FF}$  by inversions. The total land flux is of similar magnitude for the decadal average, with estimates for 2005-2014 from the three inversions of 2.0, 2.0 and 3.3 GtC yr<sup>-1</sup> compared to  $2.1 \pm 0.7$  GtC yr<sup>-1</sup> for the total flux computed with the carbon budget from other terms in Eq. 1 (Table 7). The three inversions' total land sink would be 1.6, 1.6 and 2.9 GtC yr<sup>-1</sup> when including a mean river flux correction of 0.45 GtC yr<sup>-1</sup>, though the exact correction would be smaller when taking into account the anthropogenic contribution to river fluxes (Section 2.7.2). The interannual variability of the inversions also matched the residual-based  $S_{LAND}$  closely (Fig. 6). The total land flux from the DGVM multi-model mean also compares well with the estimate from the carbon budget and atmospheric inversions, with a decadal mean of  $1.6 \pm 0.4$  GtC yr<sup>-1</sup> (Table 7; 2005-2014), although individual models differ by several GtC for some years (Fig. 6).

### 3.1.3 Distribution

The total surface CO<sub>2</sub> fluxes on land and ocean including land-use change ( $S_{LAND} + S_{OCEAN} - E_{LUC}$ ) is estimated from process models and atmospheric inversions can provide information on the regional distribution of those fluxes by latitude band (Fig. 8). The global mean CO<sub>2</sub> fluxes from process models for 2005-2014 is  $4.2 \pm 0.5$  GtC yr<sup>-1</sup>. This is comparable to the fluxes of  $4.7 \pm 0.5$  GtC yr<sup>-1</sup> inferred from the remainder of the carbon budget ( $E_{FF} - G_{ATM}$  in Equation 1; Table 8) within their respective uncertainties. The total CO<sub>2</sub> fluxes from the three inversions range between 4.4 and 4.9 GtC yr<sup>-1</sup>, consistent with the carbon budget as expected from the constraints on the inversions.

In the South (south of 30°S), the atmospheric inversions and combined models all suggest a CO<sub>2</sub> sink for 2005-2014 of between 1.2 and 1.5 GtC yr<sup>-1</sup> (Fig. 8), although the details of the interannual variability are not fully consistent across methods. The interannual variability in the South is low because of the dominance of ocean area with low variability compared to land areas. In the Tropics (30°S-30°N), both the atmospheric inversions and combined models suggest the carbon balance in this region is close to neutral over the past decade, with fluxes for 2005-2014 ranging between -0.6 and +0.6 GtC yr<sup>-1</sup>. This region also shows the largest variability, both on interannual and decadal time scales.

In the North (north of 30°N), the inversions and combined models are not in full agreement on the magnitude of the CO<sub>2</sub> sink with the ensemble mean of the process models suggesting a total northern hemisphere sink for 2005-2014 of  $2.3 \pm 0.4$  GtC yr<sup>-1</sup> while the three inversions estimate a sink of 2.5, 3.4 and 3.6 GtC yr<sup>-1</sup>. The mean difference can only partly be explained by the influence of river fluxes, as this flux in the Northern Hemisphere would be less than 0.45 GtC yr<sup>-1</sup>, particularly when the anthropogenic contribution to river fluxes are accounted for.

### 3.2 Global carbon budget for year 2014 and emissions projection for 2015

#### 3.2.1 CO<sub>2</sub> emissions

Global CO<sub>2</sub> emissions from fossil fuel combustion and cement production reached  $9.8 \pm 0.5$  GtC in 2014 (Fig. 5), distributed among coal (42%), oil (33%), gas (19%), cement (5.7%) and gas flaring (0.6%). The first four categories increased by 0.4%, 0.8%, 0.4% and 2.5% respectively over the previous year. Due to lack of data, gas flaring in 2012-2014 are assumed the same as 2011.

Emissions in 2014 were 0.6% higher than the emissions in 2013, an increase well below the decadal average of 2.2% yr<sup>-1</sup> (2005-2014). Growth in 2014 is lower than our projection of 2.5% yr<sup>-1</sup> made last year (Le Quéré et al., 2015) based on an estimated GDP growth of 3.3% yr<sup>-1</sup> and improvement in I<sub>FF</sub> of 0.7% yr<sup>-1</sup> (Table 9), and also outside the provided likely range of 1.3-3.5%. The latest estimate of GDP growth for 2014 was still 3.3% yr<sup>-1</sup> (IMF, 2015) and hence I<sub>FF</sub> improved by 2.7% yr<sup>-1</sup>. This I<sub>FF</sub> is low compared to recent years (Table 9), but not outside the range of variability observed in recent decades, suggesting that our uncertainty range may have been underestimated. Almost half of the lower growth compared to expectations can be attributed to a lower growth in emissions than anticipated in China (1.1% compared to 4.5% in our projection; Friedlingstein et al. 2014), which primarily reflects structural changes in China's economy (Green

and Stern, 2015). Similar structural change occurred following the Global Financial Crisis of 2008-2009 that particularly affected western economies, which also made the emissions projections based on GDP temporarily problematic and outside of the steady behaviour assumed by the GDP/intensity approach (Peters et al. 2012). For this reason we provide an emissions projection with explicit projection for China based on energy and cement data during January – August 2015 (see Section 2.1.4). Climatic variability could also have contributed to the lower emissions in China (from reported high rainfall possibly leading to higher hydropower capacity utilisation), and in Europe and the USA where the combined emissions change account for 37% of the lower growth compared to expectations (Friedlingstein et al. 2014).

Using separate projections for China, the USA, and the rest of the world as described in Section 2.1.4, we project that the growth in global CO<sub>2</sub> emissions from fossil fuels and cement production will be near or slightly below zero in 2015, with a change of -0.6% (range of -1.6% to +0.5%) from 2014 levels. Our method is imprecise and contains several assumptions that could influence the results beyond the given range, and as such is indicative only. Within the given assumptions, global emissions decrease to  $9.7 \pm 0.5$  GtC ( $35.7 \pm 1.8$  GtCO<sub>2</sub>) in 2015, but are still 59% above emissions in 1990.

For China, the expected change based largely on available data during January to August (see Section 2.1.4) is for a decrease in emissions of -3.9% (range of -4.6% to -1.1%) in 2015 compared to 2014. This uncertainty includes a range of -4.6% to -3.2% considering different adjustments for stocks and no changes in the carbon content of coal, and is based on estimated decreases in apparent coal consumption (-5.3%) and cement production (-5.0%) and estimated growth in apparent oil (+3.2%) and natural gas (+1.4%) consumption. However, there are additional uncertainties from the carbon content of coal. While China's Energy Statistical Yearbooks indicate declining carbon content over recent years, preliminary data suggest an increase of up to 3% in 2014. The Chinese government has introduced measures expressly to address the declining quality of coal (which also leads to lower carbon content) by closing lower-quality mines and placing restrictions on the quality of imported coal. Allowing for a similar increase in 2015 (0% to 3%), we expand the uncertainty range of emissions growth to -4.6% to -1.1%.

For the USA, the EIA emissions projection for 2015 combined with cement data from USGS gives a decrease of -1.5% (range of -5.5% to +0.3%) compared to 2014. For the rest of the world, the expected growth for 2015 of +1.2% (range of -0.2 to +2.6%) is computed using the GDP projection

for the world excluding China and the USA of 2.3% made by the IMF (2015) and a growth rate for  $I_{FF}$  of  $-1.1\% \text{ yr}^{-1}$  which is the average from 2005-2014. The uncertainty range is based on the standard deviation of the interannual variability in  $I_{FF}$  during 2005-2014 of  $\pm 1.4\%$ .

In 2014, the largest contributions to global  $\text{CO}_2$  emissions were from China (27%; Liu et al., 2015), the USA (15%), the EU (28 member states; 10%), and India (7%), with the percentages compared to the global total including bunker fuels (3.0%). These four regions account for 59% of global emissions. Growth rates for these countries from 2013 to 2014 were 1.2% (China), 0.8% (USA),  $-5.8\%$  (EU28), and 8.6% (India). The per-capita  $\text{CO}_2$  emissions in 2014 were  $1.3 \text{ tC person}^{-1} \text{ yr}^{-1}$  for the globe, and were 4.8 (USA), 1.9 (China), 1.8 (EU28) and 0.5 (India)  $\text{tC person}^{-1} \text{ yr}^{-1}$  for the four highest emitting countries (Fig. 5e).

Territorial emissions in Annex B countries have decreased slightly by 0.1% per year on average from 1990-2013, while consumption emissions grew at  $0.4\% \text{ yr}^{-1}$  (Fig. 5c). In non-Annex B countries, territorial emissions have grown at  $4.4\% \text{ yr}^{-1}$ , while consumption emissions have grown at  $4.1\% \text{ yr}^{-1}$ . In 1990, 66% of global territorial emissions were emitted in Annex B countries (34% in non-Annex B, and 2% in bunker fuels used for international shipping and aviation), while in 2013 this had reduced to 38% (58% in non-Annex B, and 3% in bunker fuels). In terms of consumption emissions this split was 64% in 1990 and 39% in 2013 (34% to 55% in non-Annex B). The difference between territorial and consumption emissions (the net emission transfer via international trade) from non-Annex B to Annex B countries has increased from near zero in 1990 to  $0.3 \text{ GtC yr}^{-1}$  around 2005 and remained relatively stable between 2006 and 2013 (Fig. 5). The increase in net emission transfers of  $0.30 \text{ GtC yr}^{-1}$  between 1990 and 2013 compares with the emission reduction of  $0.37 \text{ GtC yr}^{-1}$  in Annex B countries. These results show the importance of net emission transfer via international trade from non-Annex B to Annex B countries, and the stabilisation of emissions transfer when averaged over Annex B countries during the past decade. In 2013, the biggest emitters from a consumption perspective were China (23% of the global total), USA (16%), EU28 (12%), and India (6%).

Based on fire activity, the global  $\text{CO}_2$  emissions from land-use change are estimated as  $1.1 \pm 0.5 \text{ GtC}$  in 2014, similar to the 2005-2014 average of  $0.9 \pm 0.5 \text{ GtC yr}^{-1}$  and the DGVM estimate for 2014 of  $1.4 \pm 0.5 \text{ GtC yr}^{-1}$ . However, the estimated annual variability is not generally consistent between methods, except that all methods estimate that variability in  $E_{LUC}$  is small relative to the variability from  $S_{LAND}$  (Fig. 6a). This could be partly due to the design of the DGVM experiments,

which use flux differences between simulations with and without land-cover change, and thus may overestimate variability e.g. due to fires in forest regions where the contemporary forest cover is smaller than pre-industrial cover used in the 'without land cover change' runs. The extrapolated land cover input data for 2013-2014 in the DGVM may also explain part of the discrepancy.

### 3.2.2 Partitioning

The atmospheric CO<sub>2</sub> growth rate was  $3.9 \pm 0.2$  GtC in 2014 ( $1.83 \pm 0.09$  ppm; Fig. 4; Dlugokencky and Tans, 2015). This is below the 2005-2014 average of  $4.4 \pm 0.1$  GtC yr<sup>-1</sup>, though the interannual variability in atmospheric growth rate is large.

The ocean CO<sub>2</sub> sink was  $2.9 \pm 0.5$  GtC yr<sup>-1</sup> in 2014, an increase of 0.1 GtC yr<sup>-1</sup> over 2013 according to ocean models. Seven of the eight ocean models produce an increase in the ocean CO<sub>2</sub> sink in 2014 compared to 2013, with the last model producing a very small reduction. However, of the two data products available over that period, Rödenbeck et al. (2014) produce a decrease of -0.1 GtC yr<sup>-1</sup> while Landschützer et al. (2015) produce an increase of 0.2 GtC yr<sup>-1</sup>. Thus there is no overall consistency in the annual change in the ocean CO<sub>2</sub> sink, although there is an indication of increasing convergence among products for the assessment of multi-year changes, as suggested by the time-series correlations reported in Section 2.4.3 (see also Landschützer et al., 2015). A small increase in the ocean CO<sub>2</sub> in 2014 sink would be consistent with the observed El Niño neutral conditions and continued rising atmospheric CO<sub>2</sub>. All estimates suggest an ocean CO<sub>2</sub> sink for 2014 that is larger than the 2005-2014 average of  $2.6 \pm 0.5$  GtC yr<sup>-1</sup>.

The terrestrial CO<sub>2</sub> sink calculated as the residual from the carbon budget was  $4.1 \pm 0.9$  GtC in 2014, 1.1 GtC higher than the  $3.0 \pm 0.8$  GtC yr<sup>-1</sup> averaged over 2005-2014 (Fig. 4). This is the largest S<sub>LAND</sub> calculated since 1959, equal to year 2011 (Poulter et al. 2014). In contrast to 2011 where La Niña conditions prevailed, the large S<sub>LAND</sub> in 2014 occurred in neutral El Niño condition. The DGVM model mean produce a sink of  $3.6 \pm 0.9$  GtC in 2014, 0.7 GtC yr<sup>-1</sup> over the 2005-2014 average (Table 7), smaller but still consistent with observations (Poulter et al., 2014). In the DGVM ensemble, 2014 is the fifth largest S<sub>LAND</sub>, after 1974, 2011, 2004 and 2000. There is no agreement between models and inversions on the regional origin on the 2014 flux anomaly (Fig. 8).

Cumulative emissions for 1870-2014 were  $400 \pm 20$  GtC for E<sub>FF</sub>, and  $145 \pm 50$  GtC for E<sub>LUC</sub> based on the bookkeeping method of Houghton et al. (2012) for 1870-1996 and a combination with fire-

based emissions for 1997-2014 as described in Section 2.2 (Table 10). The cumulative emissions are rounded to the nearest 5 GtC. The total cumulative emissions for 1870-2014 are  $545 \pm 55$  GtC. These emissions were partitioned among the atmosphere ( $230 \pm 5$  GtC based on atmospheric measurements in ice cores of 288 ppm (Section 2.3.1; Joos and Spahni, 2008) and recent direct measurements of 397.2 ppm (Dlugokencky and Tans, 2014)), ocean ( $155 \pm 20$  GtC using Khatiwala et al. (2013) prior to 1959 and Table 8 otherwise), and the land ( $160 \pm 60$  GtC by the difference).

Cumulative emissions for the early period 1750-1869 were 3 GtC for  $E_{FF}$ , and about 45 GtC for  $E_{LUC}$  (rounded to nearest 5) of which 10 GtC were emitted in the period 1850-1870 (Houghton et al. 2012) and 30 GtC were emitted in the period 1750-1850 based on the average of four publications (22 GtC by Pongratz et al. (2009); 15 GtC by van Minnen et al. (2009); 64 GtC by Shevliakova et al. (2009) and 24 GtC by Zaehle et al. (2011)). The growth in atmospheric  $CO_2$  during that time was about 25 GtC, and the ocean uptake about 20 GtC, implying a land uptake of 5 GtC. These numbers have large relative uncertainties but balance within the limits of our understanding.

Cumulative emissions for 1750-2014 based on the sum of the two periods above (before rounding to the nearest five GtC) were  $405 \pm 20$  GtC for  $E_{FF}$ , and  $190 \pm 65$  GtC for  $E_{LUC}$ , for a total of  $590 \pm 70$  GtC, partitioned among the atmosphere ( $255 \pm 5$  GtC), ocean ( $170 \pm 20$  GtC), and the land ( $165 \pm 70$  GtC).

Cumulative emissions through to year 2015 can be estimated based on the 2015 projections of  $E_{FF}$  (Section 3.2), the largest contributor, and assuming a constant  $E_{LUC}$  of 0.9 GtC. For 1870–2015, these are  $555 \pm 55$  GtC ( $2040 \pm 200$  Gt $CO_2$ ) for total emissions, with about 75% contribution from  $E_{FF}$  ( $410 \pm 20$  GtC) and about 25% contribution from  $E_{LUC}$  ( $145 \pm 50$  GtC). Cumulative emissions since year 1870 are higher than the emissions of 515 [445 to 585] GtC reported in the IPCC (Stocker et al., 2013) because they include an additional 43 GtC from emissions in 2012-2015 (mostly from  $E_{FF}$ ). The uncertainty presented here ( $\pm 1\sigma$ ) is smaller than the range of 90% used by IPCC, but both estimates overlap within their uncertainty ranges.

## 4 Discussion

Each year when the global carbon budget is published, each component for all previous years is updated to take into account corrections that are the result of further scrutiny and verification of the underlying data in the primary input data sets. The updates have generally been relatively small and focused on the most recent years, except for land-use change, where they are more



significant but still generally within the provided uncertainty range (Fig. 9). The difficulty in accessing land-cover change data to estimate  $E_{LUC}$  is the key problem to providing continuous records of emissions in this sector. Current FAO estimates are based on statistics reported at the country level and are not spatially-explicit. Advances in satellite recovery of land-cover change could help to keep track of land-use change through time (Achard et al., 2014; Harris, 2012). Revisions in  $E_{LUC}$  for the 2008/2009 budget were the result of the release of FAO 2010, which contained a major update to forest cover change for the period 2000-2005 and provided the data for the following 5 years to 2010 (Fig. 9b). The differences this year could be attributable to both the different data and the different methods. Updates to values for any given year in each component of the global carbon budget were highest at  $0.82 \text{ GtC yr}^{-1}$  for the atmospheric growth rate (from a one-off correction to year 1979),  $0.24 \text{ GtC yr}^{-1}$  for the fossil fuel and cement emissions, and  $0.52 \text{ GtC yr}^{-1}$  for the ocean  $\text{CO}_2$  sink (from a change from one to multiple models; Fig. 9). The update for the residual land  $\text{CO}_2$  sink was also large (Fig. 9e), with a maximum value of  $0.83 \text{ GtC yr}^{-1}$ , directly reflecting revisions in other terms of the budget.

Our capacity to separate the carbon budget components can be evaluated by comparing the land  $\text{CO}_2$  sink estimated through two approaches: (1) the budget residual ( $S_{LAND}$ ), which includes errors and biases from all components, and (2) the land  $\text{CO}_2$  sink estimate by the DGVM ensemble, which are based on our understanding of processes of how the land responds to increasing  $\text{CO}_2$ , climate and variability. Furthermore, the inverse model estimates which formally merge observational constraints with process-based models to close the global budget can provide constraints on the total land flux. These estimates are generally close (Fig. 6), both for the mean and for the interannual variability. The annual estimates from the DGVM over 1959 to 2014 correlate with the annual budget residual with  $r = 0.71$  (Section 2.5.2; Fig. 6). The DGVMs produce a decadal mean and standard deviation across models of  $3.0 \pm 0.4 \text{ GtC yr}^{-1}$  for the period 2005-2014, fully consistent with the estimate of  $3.0 \pm 0.8 \text{ GtC yr}^{-1}$  produced with the budget residual (Table 7). New insights into total surface fluxes arise from the comparison with the atmospheric inversions and their regional breakdown already provide a semi-independent way to validate the results. The comparison shows a first-order consistency between inversions and process models but with a lot of discrepancies, particularly for the allocation of the mean land sink between the tropics and the Northern hemisphere. Understanding these discrepancies and further analysis of regional carbon budgets would provide additional information to quantify and improve our estimates, as has been

undertaken by the project REgional Carbon Cycle Assessment and Processes (RECAPP; Canadell et al., 2012-2013).

Annual estimates of each component of the global carbon budgets have their limitations, some of which could be improved with better data and/or better understanding of carbon dynamics. The primary limitations involve resolving fluxes on annual time scales and providing updated estimates for recent years for which data-based estimates are not yet available or only beginning to emerge. Of the various terms in the global budget, only the burning of fossil fuels and atmospheric growth rate terms are based primarily on empirical inputs supporting annual estimates in this carbon budget. The data on fossil fuel consumption and cement production are based on survey data in all countries. The other terms can be provided on an annual basis only through the use of models. While these models represent the current state of the art, they provide only simulated changes in primary carbon budget components. For example, the decadal trends in global ocean uptake and the interannual variations associated with El Niño-Southern Ocean Oscillation (e.g. ENSO) are not directly constrained by observations, although many of the processes controlling these trends are sufficiently well known that the model-based trends still have value as benchmarks for further validation. Data-based products for the ocean CO<sub>2</sub> sink provide new ways to evaluate the model results, and could be used directly as data become more rapidly available and methods for creating such products improve. However, there are still large discrepancies among data-based estimates, in large part due to the lack of routine data sampling, that preclude their direct use for now (see Rödenbeck et al., 2015). Estimates of land-use emissions and their year-to-year variability have even larger uncertainty, and much of the underlying data are not available as an annual update. Efforts are underway to work with annually available satellite area change data or FAO reported data in combination with fire data and modelling to provide annual updates for future budgets. The best resolved changes are in atmospheric growth ( $G_{ATM}$ ), fossil fuel emissions ( $E_{FF}$ ), and by difference, the change in the sum of the remaining terms ( $S_{OCEAN} + S_{LAND} - E_{LUC}$ ). The variations from year-to-year in these remaining terms are largely model-based at this time. Further efforts to increase the availability and use of annual data for estimating the remaining terms with annual to decadal resolution are especially needed.

Our approach also depends on the reliability of the energy and land-cover change statistics provided at the country level, and are thus potentially subject to biases. Thus it is critical to develop multiple ways to estimate the carbon balance at the global and regional level, including

estimates from the inversion of atmospheric CO<sub>2</sub> concentration, the use of other oceanic and atmospheric tracers, and the compilation of emissions using alternative statistics (e.g. sectors). It is also important to challenge the consistency of information across observational streams, for example to contrast the coherence of temperature trends with those of CO<sub>2</sub> sink trends. Multiple approaches ranging from global to regional scale would greatly help increase confidence and reduce uncertainty in CO<sub>2</sub> emissions and their fate.

## **5 Conclusions**

The estimation of global CO<sub>2</sub> emissions and sinks is a major effort by the carbon cycle research community that requires a combination of measurements and compilation of statistical estimates and results from models. The delivery of an annual carbon budget serves two purposes. First, there is a large demand for up-to-date information on the state of the anthropogenic perturbation of the climate system and its underpinning causes. A broad stakeholder community relies on the data sets associated with the annual carbon budget including scientists, policy makers, businesses, journalists, and the broader society increasingly engaged in adapting to and mitigating human-driven climate change. Second, over the last decade we have seen unprecedented changes in the human and biophysical environments (e.g. increase in the growth of fossil fuel emissions, ocean temperatures, and strength of the land sink), which call for more frequent assessments of the state of the Planet, and by implications a better understanding of the future evolution of the carbon cycle, and the requirements for climate change mitigation and adaptation. Both the ocean and the land surface presently remove a large fraction of anthropogenic emissions. Any significant change in the function of carbon sinks is of great importance to climate policymaking, as they affect the excess carbon dioxide remaining in the atmosphere and therefore the compatible emissions for any climate stabilization target. Better constraints of carbon cycle models against contemporary data sets raises the capacity for the models to become more accurate at future projections.

This all requires more frequent, robust, and transparent data sets and methods that can be scrutinized and replicated. After ten annual releases from the GCP, the effort is growing and the traceability of the methods has become increasingly complex. Here, we have documented in detail the data sets and methods used to compile the annual updates of the global carbon budget, explained the rationale for the choices made, the limitations of the information, and finally highlighted need for additional information where gaps exist.

This paper via 'living data' will help to keep track of new budget updates. The evolution over time of the carbon budget is now a key indicator of the anthropogenic perturbation of the climate system, and its annual delivery joins a set of other climate indicators to monitor the evolution of human-induced climate change, such as the annual updates on the global surface temperature, sea level rise, minimum Arctic sea ice extent among others.

#### **Data access**

The data presented here are made available in the belief that their wide dissemination will lead to greater understanding and new scientific insights of how the carbon cycle works, how humans are altering it, and how we can mitigate the resulting human-driven climate change. The free availability of these data does not constitute permission for publication of the data. For research projects, if the data are essential to the work, or if an important result or conclusion depends on the data, co-authorship may need to be considered. Full contact details and information on how to cite the data are given at the top of each page in the accompanying database, and summarised in Table 2.

The accompanying database includes two Excel files organised in the following spreadsheets (accessible with the free viewer <http://www.microsoft.com/en-us/download/details.aspx?id=10>):

File Global\_Carbon\_Budget\_2015.xlsx includes:

1. Summary
2. The global carbon budget (1959-2014);
3. Global CO<sub>2</sub> emissions from fossil fuels and cement production by fuel type, and the per-capita emissions (1959-2014);
4. CO<sub>2</sub> emissions from land-use change from the individual methods and models (1959-2014);
5. Ocean CO<sub>2</sub> sink from the individual ocean models and data products (1959-2014);
6. Terrestrial residual CO<sub>2</sub> sink from the DGVMs (1959-2014);
7. Additional information on the carbon balance prior to 1959 (1750-2014).

File National\_Carbon\_Emissions\_2015.xlsx includes:

1. Summary
2. Territorial country CO<sub>2</sub> emissions from fossil fuel combustion and cement production (1959-2014) from CDIAC, extended to 2014 using BP data;

3. Territorial country CO<sub>2</sub> emissions from fossil fuel combustion and cement production (1959-2014) from CDIAC with UNFCCC data overwritten where available, extended to 2014 using BP data;
4. Consumption country CO<sub>2</sub> emissions from fossil fuel combustion and cement production and emissions transfer from the international trade of goods and services (1990-2013) using CDIAC/UNFCCC data (worksheet 3 above) as reference;
5. Emissions transfers (Consumption minus territorial emissions; 1990-2013);
6. Country definitions.

National emissions data are also available on the Global Carbon Atlas ([globalcarbonatlas.org](http://globalcarbonatlas.org)).

**Acknowledgments** We thank all people and institutions who provided the data used in this carbon budget, P Cadule, C Enright, J Ghattas, G Hurtt, L. Mercado, S Shu, and S Jones for support to the model simulations and data analysis, and F Joos and S Khatiwala for providing historical data. We thank E. Dlugokencky who provided the atmospheric and oceanographic CO<sub>2</sub> measurements used here, and all those involved in collecting and providing oceanographic data CO<sub>2</sub> measurements used here, in particular for the ocean data for years 2013-2014 that are not included in SOCAT v3: M Becker, A Körtzinger, S Alin, G Lebon, D Diverrès, R Wanninkhof, M Glockzin, I Skjelvan, I Brown, C Sweeney, C Lo Monaco, A Omar, T Johannessen, M Hoppema, XA Padin, T Ichikawa, A Kuwata, and K Tadokoro. We thank the institutions and funding agencies responsible for the collection and quality control of the data included in SOCAT, and the support of the International Ocean Carbon Coordination Project (IOCCP), the Surface Ocean Lower Atmosphere Study (SOLAS), and the Integrated Marine Biogeochemistry, Ecosystem Research program (IMBER) and UK Natural Environment Research Council (NERC) projects including National Capability, Ocean Acidification, Greenhouse Gases and Shelf Seas Biogeochemistry. We thank W Peters for CTE2015 model simulations, and all data providers to ObsPack GLOBALVIEWplus v1.0 for atmospheric CO<sub>2</sub> observations.

NERC provided funding to C Le Quéré, R Moriarty and the GCP through their International Opportunities Fund specifically to support this publication (NE/103002X/1). C Le Quéré was also supported by the EU FP7 for funding through projects GEOCarbon (283080). GP Peters and RM Andrew were supported by the Norwegian Research Council (236296). JG Canadell was supported by the Australian Climate Change Science Program. S Sitch was supported by EU FP7 for funding through projects LUC4C (GA603542). RJ Andres was supported by US Department of Energy, Office of Science, Biological and Environmental Research (BER) programs under US Department of Energy contract DE-AC05-00OR22725. TA Boden was supported by US Department of Energy, Office of Science, Biological and Environmental Research (BER) programs under US Department of Energy contract DE-AC05-00OR22725. JI House was supported by the Leverhulme foundation and the EU FP7 through project LUC4C (GA603542). P Friedlingstein was supported by the EU FP7 for funding through projects LUC4C (GA603542) and EMBRACE (GA282672). A Arneeth was supported by the EU FP7 for funding through LUC4C (603542), and the Helmholtz foundation and its ATMO programme. DCE Bakker was supported by the EU FP7 for funding through project CARBOCHANGE (284879), the UK Ocean Acidification Research Programme (NE/H017046/1; funded by the Natural Environment Research Council, the Department for Energy and Climate Change and the Department for Environment, Food and Rural Affairs). L Barbero was supported by NOAA's Ocean Acidification Program

and acknowledges support for this work from the National Aeronautics and Space Administration (NASA) ROSES Carbon Cycle Science under NASA grant 13-CARBON13\_2-0080. P Ciais acknowledges support from the European Research Council through Synergy grant ERC-2013-SyG-610028 'IMBALANCE-P'. M. Fader was supported by the EU FP7 for funding through project LUC4C (GA603542). J Hauck was supported by the Helmholtz PostDoc Programme (Initiative and Networking Fund of the Helmholtz Association). RA Feely and AJ Sutton were supported by the Climate Observation Division, Climate Program Office, NOAA, U.S. Department of Commerce. AK Jain was supported by the US National Science Foundation (NSF AGS 12-43071) the US Department of Energy, Office of Science and BER programs (DOE DE-SC0006706) and NASA LCLUC program (NASA NNX14AD94G). E Kato was supported by the ERTDF (S-10) from the Ministry of Environment, Japan. K Klein Goldewijk was supported by the Dutch NWO VENI grant no. 863.14.022. Siv K. Lauvset was supported by the project 'Monitoring ocean acidification in Norwegian waters' from the Norwegian Ministry of Climate and Environment. V Kitidis was supported by the EU FP7 for funding through project CARBOCHANGE (264879). C Koven was supported by the Director, Office of Science, Office of Biological and Environmental Research of the US Department of Energy under Contract No. DE-AC02-05CH11231 as part of their Regional and Global Climate Modelling Program. P Landschützer was supported by GEOCarbon. IT van der Lann-Luijkx received financial support from OCW/NWO for ICOS-NL and computing time from NWO (SH-060-13). SK Lauvset was supported by the project 'Monitoring ocean acidification in Norwegian waters' from the Norwegian Ministry of Climate and Environment. ID Lima was supported by the U.S. National Science Foundation (NSF AGS-1048827). N Metzl was supported by Institut National des Sciences de l'Univers (INSU) and Institut Paul Emile Victor (IPEV) for OISO cruises. DR Munro was supported by the U.S. National Science Foundation (NSF PLR-1341647 and NSF AOAS-0944761). JEMS Nabel was supported by the German Research Foundation's Emmy Noether Program (PO1751/1-1) and acknowledges Julia Pongratz and Kim Naudts for their contributions. Y Nojiri and S Nakaoka were supported by the Global Environment Research Account for National Institutes (1432) by the Ministry of Environment of Japan. A Olsen appreciates support from the Norwegian Research Council (SNACS, 229752). F.F. Pérez were supported by BOCATS (CTM2013-41048-P) project co-founded by the Spanish Government and the Fondo Europeo de Desarrollo Regional (FEDER). D Pierrot was supported by NOAA through the Climate Observation Division of the Climate Program Office. B Poulter was supported by the EU FP7 for funding through GEOCarbon. G Rehder was supported by BMBF (Bundesministerium für Bildung und Forschung) through project ICOS, Grant No 01LK1224D. U Schuster was supported by NERC UKOARP (NE/H017046/1), NERC RAGANRoCC (NE/K002473/1), European Space Agency (ESA) OceanFlux Evolution project and EU FP7 CARBOCHANGE (264879). T Steinhoff was supported by ICOS-D (BMBF FK 01LK1101C) and EU FP7 for funding through project CARBOCHANGE (264879). J Schwiger was supported by the Research Council of Norway through project EVA (229771), and acknowledges the Norwegian metacenter for computational science (NOTUR, project nn2980k), and the Norwegian Storage Infrastructure (NorStore, project ns2980k) for supercomputer time and storage resources. T Takahashi was supported by grants from NOAA and the Comer Education and Science Foundation. B Tilbrook was supported by the Australian Department of Environment and the Integrated Marine Observing System. BD Stocker was supported by the Swiss National Science Foundation and FP7 funding through project EMBRACE (282672). S van Heuven was supported by the EU FP7 for funding through project CARBOCHANGE (264879). GR van der Werf was supported by the European Research Council (280061). A Wiltshire was supported by the Joint UK DECC/Defra Met Office Hadley Centre Climate Programme (GA01101) and EU FP7 Funding through project LUC4C (603542). S Zaehle was supported by the European Research Council (ERC) under the European Union's Horizon 2020 research and innovation programme (QUINCY; grant agreement No 647204). ISAM (PI: Atul K Jain) simulations were carried out at the National Energy Research Scientific Computing Center

(NERSC), which is supported by the U.S. DOE under contract DE-AC02-05CH11231. Contributions from the Scripps Institution of Oceanography were supported under DoE grant DE-SC0012167 and by Schmidt Philanthropies. This is NOAA-PMEL contribution number 4400.

## References

- Achard, F., Beuchle, R., Mayaux, P., Stibig, H. J., Bodart, C., Brink, A., Carboni, S., Desclée, B., Donnay, F., and Eva, H.: Determination of tropical deforestation rates and related carbon losses from 1990 to 2010, *Global change biology*, 20, 2540-2554, 2014.
- Achard, F. and House, J. I.: Reporting Carbon losses from tropical deforestation with Pan-tropical biomass maps, *Environmental Research Letters*, in press. in press.
- Andres, R., Boden, T., and Higdon, D.: A new evaluation of the uncertainty associated with CDIAC estimates of fossil fuel carbon dioxide emission, *Tellus B*, 2014. 2014.
- Andres, R. J., Boden, T. A., Bréon, F.-M., Ciais, P., Davis, S., Erickson, D., Gregg, J. S., Jacobson, A., Marland, G., Miller, J., Oda, T., Olivier, J. G. J., Raupach, M. R., Rayner, P., and Treanton, K.: A synthesis of carbon dioxide emissions from fossil-fuel combustion, *Biogeosciences*, 9, 1845-1871, 2012.
- Andres, R. J., Fielding, D. J., Marland, G., Boden, T. A., Kumar, N., and Kearney, A. T.: Carbon dioxide emissions from fossil fuel use, 1751–1950, *Tellus*, 51, 759-765, 1999.
- Andrew, R. M. and Peters, G. P.: A multi-region input-output table based on the Global Trade Analysis Project Database (GTAP-MRIO), *Economic Systems Research*, 25, 99-121, 2013.
- Archer, D., Eby, M., Brovkin, V., Ridgwell, A., Cao, L., Mikolajewicz, U., Caldeira, K. M., K., Munhoven, G., Montenegro, A., and Tokos, K.: Atmospheric Lifetime of Fossil Fuel Carbon Dioxide, *Annual Review of Earth and Planetary Sciences*, 37, 117-134, 2009.
- Arora, V. and Boer, G.: A parameterization of leaf phenology for the terrestrialecosystem component of climate models, *Global Change Biology*, 11, 39–59, 2005.
- Assmann, K. M., Bentsen, M., Segschneider, J., and Heinze, C.: An isopycnic ocean carbon cycle model, *Geoscientific Model Development*, 3, 143-167, 2010.
- Atlas, R., Hoffman, R. N., Ardizzone, J., Leidner, S. M., Jusem, J. C., Smith, D. K., and Gombos, D.: A cross-calibrated, multiplatform ocean surface wind velocity product for meteorological and oceanographic applications, *Bull. Amer. Meteor. Soc.*, 92, 157-174, 2011.
- Aumont, O. and Bopp, L.: Globalizing results from ocean in situ iron fertilization studies, *Global Biogeochemical Cycles*, 20, 2006.
- Baccini, A., Goetz, S. J., Walker, W. S., Laporte, N. T., Sun, M., Sulla-Menashe, D., Hackler, J., Beck, P. S. A., Dubayah, R., Friedl, M. A., Samanta, S., and Houghton, R. A.: Estimated carbon dioxide emissions from tropical deforestation improved by carbon-density maps, *Nature Clim. Change*, 2, 182-186, 2012.
- Bakker, D. C. E., Pfeil, B., Smith, K., Hankin, S., Olsen, A., Alin, S. R., Cosca, C., Harasawa, S., Kozyr, A., Nojiri, Y., O'Brien, K. M., Schuster, U., Telszewski, M., Tilbrook, B., Wada, C., Akl, J., Barbero, L., Bates, N. R., Boutin, J., Bozec, Y., Cai, W.-J., Castle, R. D., Chavez, F. P., Chen, L., Chierici, M., Currie, K., de Baar, H. J. W., Evans, W., Feely, R. A., Fransson, A., Gao, Z., Hales, B., Hardman-Mountford, N. J., Hoppema, M., Huang, W.-J., Hunt, C. W., Huss, B., Ichikawa, T., Johannessen, T., Jones, E. M., Jones, S. D., Jutterström, S., Kitidis, V., Körtzinger, A., Landschützer, P., Lauvset, S. K., Lefèvre, N., Manke, A. B., Mathis, J. T., Merlivat, L., Metzl, N., Murata, A., Newberger, T., Omar, A. M., Ono, T., Park, G.-H., Paterson, K., Pierrot, D., Ríos, A. F., Sabine, C. L., Saito, S., Salisbury, J., Sarma, V. V. S. S., Schlitzer, R., Sieger, R., Skjelvan, I., Steinhoff, T., Sullivan, K. F., Sun, H., Sutton, A. J., Suzuki, T., Sweeney, C., Takahashi, T., Tjiputra, J., Tsurushima, N., van Heuven, S. M. A. C., Vandemark, D., Vlahos, P., Wallace, D. W. R., Wanninkhof, R., and Watson, A. J.: An update to the Surface Ocean CO<sub>2</sub> Atlas (SOCAT version 2), *Earth Syst. Sci. Data*, doi: 10.5194/essd-6-69-2014, 2014. 69-90, 2014.
- Bakker, D. C. E., Pfeil, B., Smith, K., Harasawa, S., Landa, C., Nakaoka, S., Nojiri, Y., Metzl, N., O'Brien, K. M., Olsen, A., Schuster, U., T., ilbrook, B., Wanninkhof, R., Alin, S. R., Barbero, L., Bates, N. R., Bianchi, A. A., Bonou, F., Boutin, J., Bozec, Y., Burger, E., Cai, W.-J., Castle, R. D., Chen, L., Chierici, M., Cosca, C., Currie, K., Evans, W., Featherstone, C., Feely, R. A., Fransson, A., Greenwood, N., Gregor, L., Hankin, S., Hardman-Mountford, N. J., Harlay, J., Hauck, J., Hoppema, M., Humphreys, M., Hunt, C. W., Ibáñez, J. S. P., Johannessen, T., Jones, S. D., Keeling, R., Kitidis, V., Körtzinger, A., Kozyr, A., Krasakopoulou, E., Kuwata, A., Landschützer, P., Lauvset, S. K., Lefèvre, N., Lo Monaco, C., Manke, A. B., Mathis, J. T., Merlivat, L., Monteiro, P., Munro, D., Murata, A., Newberger, T., Omar, A. M., Ono, T., Paterson, K., Pierrot, D., Robbins, L. L., Sabine, C. L., Saito, S., Salisbury, J., Schneider, B., Schlitzer, R., Sieger, R., Skjelvan, I., Steinhoff, T., Sullivan, K. F., Sutherland, S. C., Sutton, A. J., Sweeney, C., Tadokoro, K., Takahashi, T., Telszewski, M., van Heuven, S. M. A. C., Vandemark, D., Wada, C.,



- Ward, B., and Watson, A. J.: A 58-year record of high quality data in version 3 of the Surface Ocean CO<sub>2</sub> Atlas (SOCAT), *Earth Syst. Sci. Data*, in prep. in prep.
- Ballantyne, A. P., Alden, C. B., Miller, J. B., Tans, P. P., and White, J. W. C.: Increase in observed net carbon dioxide uptake by land and oceans during the last 50 years, *Nature*, 488, 70-72, 2012.
- Ballantyne, A. P., Andres, R., Houghton, R., Stocker, B. D., Wanninkhof, R., Anderegg, W., Cooper, L. A., DeGrandpre, M., Tans, P. P., Miller, J. B., Alden, C., and White, J. W. C.: Audit of the global carbon budget: estimate errors and their impact on uptake uncertainty, *Biogeosciences*, 12, 2565-2584, 2015.
- Bauer, J. E., Cai, W.-J., Raymond, P. A., Bianchi, T. S., Hopkinson, C. S., and Regnier, P. A. G.: The changing carbon cycle of the coastal ocean, *Nature*, 504, 61-70, 2013.
- Best, M. J., Pryor, M., Clark, D. B., Rooney, G. G., Essery, R. L. H., Ménard, C. B., Edwards, J. M., Hendry, M. A., Porson, A., Gedney, N., Mercado, L. M., Sitch, S., Blyth, E., Boucher, O., Cox, P. M., Grimmond, C. S. B., and Harding, R. J.: The Joint UK Land Environment Simulator (JULES), model description - Part 1: Energy and water fluxes, *Geoscientific Model Development*, doi: 10.5194/gmd-4-677-2011, 2011. 677-699, 2011.
- Biemans, H., Haddeland, I., Kabat, P., Ludwig, F., Hutjes, R. W. A., Heinke, J., von Bloh, W., and Gerten, D.: Impact of reservoirs on river discharge and irrigation water supply during the 20th century, *Water Resources Research*, 47, 2011.
- Boden, T. A., Marland, G., and Andres, R. J.: Global, Regional, and National Fossil-Fuel CO<sub>2</sub> Emissions, Oak Ridge National Laboratory, U.S. Department of Energy, Oak Ridge, Tenn., U.S.A., 2013.
- Boden, T. A., Marland, G., and Andres, R. J.: Global, Regional, and National Fossil-Fuel CO<sub>2</sub> Emissions, Oak Ridge National Laboratory, U.S. Department of Energy, Oak Ridge, Tenn., U.S.A., 2015.
- Bondeau, A., Smith, P., Zaehle, S., Schaphoff, S., Lucht, W., Cramer, W., Gerten, D., Lotze-Campen, H., Müller, C., Reichstein, M., and Smith, B.: Modelling the role of agriculture for the 20th century global terrestrial carbon balance, *Global Change Biology*, 13, 1-28, 2007.
- BP: Statistical Review of World Energy 2015, <http://www.bp.com/en/global/corporate/about-bp/energy-economics/statistical-review-of-world-energy.html>, last access: 5 October 2015.
- Bruno, M. and Joos, F.: Terrestrial carbon storage during the past 200 years: A monte carlo analysis of CO<sub>2</sub> data from ice core and atmospheric measurements, *Global Biogeochemical Cycles*, 11, 111-124, 1997.
- Buitenhuis, E. T., Rivkin, R. B., Salliey, S., and Le Quéré, C.: Biogeochemical fluxes through microzooplankton, *Global Biogeochemical Cycles*, 24, 2010.
- Canadell, J. G., Ciais, P., Sabine, C., and Joos, F.: REgional Carbon Cycle Assessment and Processes (RECCAP), [http://www.biogeosciences.net/special\\_issue107.html](http://www.biogeosciences.net/special_issue107.html), 2012-2013.
- Canadell, J. G., Le Quéré, C., Raupach, M. R., Field, C. B., Buitenhuis, E. T., Ciais, P., Conway, T. J., Gillett, N. P., Houghton, R. A., and Marland, G.: Contributions to accelerating atmospheric CO<sub>2</sub> growth from economic activity, carbon intensity, and efficiency of natural sinks, *Proceedings of the National Academy of Sciences of the United States of America*, 104, 18866-18870, 2007.
- Chevallier, F., M. Fisher, P. Peylin, S. Serrar, P. Bousquet, F.-M. Bréon, A. Chédin, and Ciais, P.: Inferring CO<sub>2</sub> sources and sinks from satellite observations: Method and application to TOVS data, *J. Geophys. Res.*, D24309, 2005.
- China Coal Industry Association: Economic performance of coal in the first half of 2015 (in Chinese original title: 2015年上半年煤炭经济运行情况), <http://www.coalchina.org.cn/detail/15/07/30/00000027/content.html>, last access: July 2015.
- China Coal Resource: Economic performance of China's coal industry in the first 8 months of the year (in Chinese original title: 前8月全国煤炭行业经济运行情况), <http://www.sxcoal.com/coal/4237319/articlenew.html>, 2015.
- Ciais, P., Sabine, C., Govindasamy, B., Bopp, L., Brovkin, V., Canadell, J., Chhabra, A., DeFries, R., Galloway, J., Heimann, M., Jones, C., Le Quéré, C., Myneni, R., Piao, S., and Thornton, P.: Chapter 6: Carbon and Other Biogeochemical Cycles. In: *Climate Change 2013 The Physical Science Basis*, Stocker, T., Qin, D., and Plattner, G.-K. (Eds.), Cambridge University Press, Cambridge, 2013.
- Clarke, D. B., Mercado, L. M., Sitch, S., Jones, C. D., Gedney, N., Best, M. J., Pryor, M., Rooney, G. G., Essery, R. L. H., Blyth, E., Boucher, O., Cox, P. M., and Harding, R. J.: The Joint UK Land Environment Simulator (JULES), model description - Part 2: Carbon fluxes and vegetation dynamics. , *Geoscientific Model Development*, 4, 701-772, 2011.
- Danabasoglu, G., S.G. Yeager, D. Bailey, E. Behrens, M. Bentsen, D. Bi, A. Biastoch, C. Böning, A. Bozec, V.M. Canuto, C. Cassou, E. Chassignet, A.C. Coward, S. Danilov, N. Diansky, H. Drange, R. Farneti, E. Fernandez, P.G. Fogli, G. Forget, Y. Fujii, S.M. Griffies, A. Gusev, P. Heimbach, A. Howard, T. Jung, M. Kelley, W.G. Large, A. Leboissetier, J. Lu, G. Madec, S.J. Marsland, S. Masina, A. Navarra, A.J.G. Nurser, A. Pirani, D. Salas y Mélia, B.L. Samuels, M. Scheinert, D. Sidorenko, A.-M. Treguier, H. Tsujino, P. Uotila, S. Valcke, A. Voldoire, and Q.



- Wangi: North Atlantic simulations in Coordinated Ocean-ice Reference Experiments phase II (CORE-II). Part I: Mean states, *Ocean Model.*, 73, 2014.
- Davis, S. J. and Caldeira, K.: Consumption-based accounting of CO<sub>2</sub> emissions, *Proceedings of the National Academy of Sciences*, 107, 5687-5692, 2010.
- Davis, S. J., Peters, G. P., and Caldeira, K.: The supply chain of CO<sub>2</sub> emissions, *Proceedings of the National Academy of Science*, 108, 18554-18559, 2011.
- Denman, K. L., Brasseur, G., Chidthaisong, A., Ciais, P., Cox, P. M., Dickinson, R. E., Hauglustaine, D., Heinze, C., Holland, E., Jacob, D., Lohmann, U., Ramachandran, S., Leite da Silva Dias, P., Wofsy, S. C., and Zhang, X.: Couplings Between Changes in the Climate System and Biogeochemistry, *Intergovernmental Panel on Climate Change* 978-0-521-70596-7, 499-587 pp., 2007.
- Dlugokencky, E. and Tans, P.: Trends in atmospheric carbon dioxide, National Oceanic & Atmospheric Administration, Earth System Research Laboratory (NOAA/ESRL), <http://www.esrl.noaa.gov/gmd/ccgg/trends> last access: 8 August 2014.
- Dlugokencky, E. and Tans, P.: Trends in atmospheric carbon dioxide, National Oceanic & Atmospheric Administration, Earth System Research Laboratory (NOAA/ESRL), <http://www.esrl.noaa.gov/gmd/ccgg/trends> last access: 7 October 2015.
- Doney, S. C., Lima, I., Feely, R. A., Glover, D. M., Lindsay, K., Mahowald, N., Moore, J. K., and Wanninkhof, R.: Mechanisms governing interannual variability in upper-ocean inorganic carbon system and air-sea CO<sub>2</sub> fluxes: Physical climate and atmospheric dust, *Deep-Sea Research Part II-Topical Studies in Oceanography*, 56, 640-655, 2009.
- Durant, A. J., Le Quéré, C., Hope, C., and Friend, A. D.: Economic value of improved quantification in global sources and sinks of carbon dioxide, *Phil. Trans. A*, 269, 1967-1979, 2010.
- Earles, J. M., Yeh, S., and Skog, K. E.: Timing of carbon emissions from global forest clearance, *Nature Climate Change*, 2, 682-685, 2012.
- El-Masri, B., Barman, R., Meiyappan, P., Song, Y., Liang, M., and Jain, A. K.: Carbon dynamics in the Amazonian Basin: Integration of eddy covariance and ecophysiological data with a land surface model, *Agricultural and Forest Meteorology*, 182-183, 156-167, 2013.
- Erb, K.-H., Kastner, T., Luyssaert, S., Houghton, R. A., Kuemmerle, T., Olofsson, P., and Haberl, H.: Bias in the attribution of forest carbon sinks, *Nature Climate Change*, 3, 854-856, 2013.
- Etheridge, D. M., Steele, L. P., Langenfelds, R. L., and Francey, R. J.: Natural and anthropogenic changes in atmospheric CO<sub>2</sub> over the last 1000 years from air in Antarctic ice and firn, *Journal of Geophysical Research*, 101, 4115-4128, 1996.
- Fader, M., Rost, S., Müller, C., Bondeau, A., and Gerten, D.: Virtual water content of temperate cereals and maize: Present and potential future patterns, *J. Hydrol.*, 384, 218-231, 2010.
- FAO: Global Forest Resource Assessment 2010, 378 pp., 2010.
- FAOSTAT: Food and Agriculture Organization Statistics Division, <http://faostat.fao.org/2010>.
- Federici, S., Tubiello, F. N., Salvatore, M., Jacobs, H., and Schmidhuber, J.: New estimates of CO<sub>2</sub> forest emissions and removals: 1990-2015, *Forest Ecology and Management*, 352, 89-98, 2015.
- Francey, R. J., Trudinger, C. M., van der Schoot, M., Law, R. M., Krummel, P. B., Langenfelds, R. L., Steele, L. P., Allison, C. E., Stavert, A. R., Andres, R. J., and Rodenbeck, C.: Reply to 'Anthropogenic CO<sub>2</sub> emissions', *Nature Clim. Change*, 3, 604-604, 2013.
- Friedlingstein, P., Andrew, R. M., Rogelj, J., Peters, G. P., Canadell, J. G., Knutti, R., Luderer, G., Raupach, M. R., Schaeffer, M., van Vuuren, D. P., and Le Quéré, C.: Persistent growth of CO<sub>2</sub> emissions and implications for reaching climate targets, *Nature Geoscience*, 2014. 2014.
- Friedlingstein, P., Houghton, R. A., Marland, G., Hackler, J., Boden, T. A., Conway, T. J., Canadell, J. G., Raupach, M. R., Ciais, P., and Le Quéré, C.: Update on CO<sub>2</sub> emissions, *Nature Geoscience*, 3, 811-812, 2010.
- Friend, A. D.: Terrestrial Plant Production and Climate Change, *Journal of Experimental Botany*, 61, 1293-1309, 2010.
- Gasser, T. and Ciais, P.: A theoretical framework for the net land-to-atmosphere CO<sub>2</sub> flux and its implications in the definition of 'emissions from land-use change', *Earth System Dynamics Discussions*, 4, 179-217, 2013.
- GCP: The Global Carbon Budget 2007, [http://lmacweb.env.uea.ac.uk/lequere/co2/2007/carbon\\_budget\\_2007.htm](http://lmacweb.env.uea.ac.uk/lequere/co2/2007/carbon_budget_2007.htm), last access: November 2013.
- General Administration of Customs of the People's Republic of China a: China's major exports by quantity and RMB value, August 2015 (in Chinese original title: 2015年8月全国出口重点商品量值表 (人民币值)), <http://www.customs.gov.cn/publish/portal0/tab49666/info772246.htm>, last access: October 2015.
- General Administration of Customs of the People's Republic of China b: China's major imports by quantity and RMB value, August 2015 (in Chinese original title: 2015年8月全国进口重点商品量值表 (人民币值)), <http://www.customs.gov.cn/publish/portal0/tab49666/info772245.htm>, last access: October 2015.

- 1 Giglio, L., Randerson, J., and van der Werf, G.: Analysis of daily, monthly, and annual burned area using the fourth-  
2 generation global fire emissions database (GFED4), *JOURNAL OF GEOPHYSICAL RESEARCH-BIOGEOSCIENCES*,  
3 118, 2013.
- 4 Gitz, V. and Ciais, P.: Amplifying effects of land-use change on future atmospheric CO<sub>2</sub> levels, *Global Biogeochemical*  
5 *Cycles*, 17, 1024, 2003.
- 6 Goll, D. S., V. Brovkin, J. Liski, T. Raddatz, T. Thum, and Todd-Brown, K. E. O.: Strong dependence of CO<sub>2</sub> emissions  
7 from anthropogenic land cover change on initial land cover and soil carbon parametrization, *Global*  
8 *Biogeochem. Cycles*, 29, 2015.
- 9 Gregg, J. S., Andres, R. J., and Marland, G.: China: Emissions pattern of the world leader in CO<sub>2</sub> emissions from fossil  
10 fuel consumption and cement production, *Geophysical Research Letters*, 35, L08806, 2008.
- 11 Hansen, M., Potapov, P., and Moore, R.: High-resolution global maps of 21st century forest cover change, *Science*,  
12 342, 850–853, 2013.
- 13 Hansis, E., S. J. Davis, and Pongratz, J.: Relevance of methodological choices for accounting of land use change carbon  
14 fluxes, *Global Biogeochem. Cycles*, 29, 1230–1246, 2015.
- 15 Harris, I., Jones, P. D., Osborn, T. J., and Lister, D. H.: Updated high-resolution grids of monthly climatic observations –  
16 the CRU TS3.10 Dataset, *International Journal of Climatology*, 34, 623–642, 2015.
- 17 Harris, N., Brown S, Hagen SC: Baseline map of carbon emissions from deforestation in tropical regions, *Science*, 336,  
18 1573–1576, 2012.
- 19 Hauck, J., C. Völker, T. Wang, M. Hoppema, M. Losch, and Wolf-Gladrow, D. A.: Seasonally different carbon flux  
20 changes in the Southern Ocean in response to the southern annular mode, *Global Biogeochem. Cycles*, 27,  
21 1236–1245, 2013.
- 22 Hertwich, E. G. and Peters, G. P.: Carbon Footprint of Nations: A Global, Trade-Linked Analysis, *Environmental Science*  
23 *and Technology*, 2009. 6414–6420, 2009.
- 24 Houghton, R. A.: Revised estimates of the annual net flux of carbon to the atmosphere from changes in land use and  
25 land management 1850–2000, *Tellus Series B-Chemical and Physical Meteorology*, 55, 378–390, 2003.
- 26 Houghton, R. A., House, J. I., Pongratz, J., van der Werf, G. R., DeFries, R. S., Hansen, M. C., Le Quéré, C., and  
27 Ramankutty, N.: Carbon emissions from land use and land-cover change, *Biogeosciences*, 9, 5125–5142, 2012.
- 28 Hourdin, F., Musat, I., Bony, S., Braconnot, P., Codron, F., Dufresne, J.-I., Fairhead, L., Filiberti, M.-A., Freidlingstein, P.,  
29 Grandpeix, J.-Y., Krinner, G., LeVan, P., Li, Z.-X., and Lott, F.: The LMDZ4 general circulation model: climate  
30 performance and sensitivity to parametrized physics with emphasis on tropical convection, *Climate*  
31 *Dynamics*, 27, 2006.
- 32 Hurtt, G. C., Chini, L. P., Frolking, S., Betts, R. A., Feddema, J., Fischer, G., Fisk, J. P., Hibbard, K., Houghton, R. A.,  
33 Janetos, A., Jones, C. D., Kindermann, G., Kinoshita, T., Klein Goldewijk, K., Riahi, K., Shevliakova, E., Smith, S.,  
34 Stehfest, E., Thomson, A., Thornton, P., van Vuuren, D. P., and Wang, Y. P.: Harmonization of land-use  
35 scenarios for the period 1500–2100: 600 years of global gridded annual land-use transitions, wood harvest,  
36 and resulting secondary lands, *Climatic Change*, 109, 117–161, 2011.
- 37 IEA/OECD: CO<sub>2</sub> emissions from fuel combustion highlights, Paris, 2014.
- 38 Ilyina, T., Six, K., Segschneider, J., Maier-Reimer, E., Li, H., and Núñez-Riboni, I.: The global ocean biogeochemistry  
39 model HAMOCC: Model architecture and performance as component of the MPI-Earth System Model in  
40 different CMIP5 experimental realizations, *Journal of Advances in Modeling Earth Systems*, 5, 287–315, 2013.
- 41 IMF: World Economic Outlook of the International Monetary Fund, <http://www.imf.org/external/ns/cs.aspx?id=29>,  
42 last access: 09 October 2015 2015.
- 43 Ito, A. and Inatomi, M.: Use of a process-based model for assessing the methane budgets of global terrestrial  
44 ecosystems and evaluation of uncertainty, *Biogeosciences*, 9, 759–773, 2012.
- 45 Jackson, R. B., Canadell, J. G., Le Quéré, C., Andrew, R. M., Korsbakken, J. I., Peters, G. P., and Nakicenovic, N.:  
46 Reaching Peak Emissions, *Nature Climate Change*, submitted. submitted.
- 47 Jacobson, A. R., Mikaloff Fletcher, S. E., Gruber, N., Sarmiento, J. L., and Gloor, M.: A joint atmosphere-ocean  
48 inversion for surface fluxes of carbon dioxide: 1. Methods and global-scale fluxes, *Global Biogeochemical*  
49 *Cycles*, 21, GB1019, 2007.
- 50 Jain, A. K., Meiyappan, P., Song, Y., and House, J. I.: CO<sub>2</sub> Emissions from Land-Use Change Affected More by Nitrogen  
51 Cycle, than by the Choice of Land Cover Data, *Global Change Biology*, 9, 2893–2906, 2013.
- 52 Jain, A. K., T. West, X. Yang, and Post, W.: Assessing the Impact of Changes in Climate and CO<sub>2</sub> on Potential Carbon  
53 Sequestration in Agricultural Soils, *Geophys. Res. Lett.*, 32 L19711, 2005.
- 54 Joos, F. and Spahni, R.: Rates of change in natural and anthropogenic radiative forcing over the past 20,000 years,  
55 *Proceedings of the National Academy of Science*, 105, 1425–1430, 2008.

- Kato, E., Kinoshita, T., Ito, A., Kawamiya, M., and Yamagata, Y.: Evaluation of spatially explicit emission scenario of land-use change and biomass burning using a process-based biogeochemical model, *Journal of Land Use Science*, 8, 104-122, 2013.
- Keeling, C. D., Bacastow, R. B., Bainbridge, A. E., Ekdhal, C. A., Guenther, P. R., and Waterman, L. S.: Atmospheric carbon dioxide variations at Mauna Loa Observatory, Hawaii, *Tellus*, 28, 538-551, 1976.
- Keeling, R. F., Manning, A. C., and Dubey, M. K.: The atmospheric signature of carbon capture and storage, *Philosophical Transactions of the Royal Society a-Mathematical Physical and Engineering Sciences*, 369, 2113-2132, 2011.
- Khatiwala, S., Primeau, F., and Hall, T.: Reconstruction of the history of anthropogenic CO<sub>2</sub> concentrations in the ocean, *Nature*, 462, 346-350, 2009.
- Khatiwala, S., Tanhua, T., Mikaloff Fletcher, S. E., Gerber, M., Doney, S. C., Graven, H. D., Gruber, N., McKinley, G. A., Murata, A., Rios, A. F., and Sabine, C. L.: Global ocean storage of anthropogenic carbon, *Biogeosciences*, 10, 2169-2191, 2013.
- Kirschke, S., Bousquet, P., Ciais, P., Saunois, M., Canadell, J. G., Dlugokencky, E. J., Bergamaschi, P., Bergmann, D., Blake, D. R., Bruhwiler, L., Cameron Smith, P., Castaldi, S., Chevallier, F., Feng, L., Fraser, A., Heimann, M., Hodson, E. L., Houweling, S., Josse, B., Fraser, P. J., Krummel, P. B., Lamarque, J., Langenfelds, R. L., Le Quéré, C., Naik, V., O'Doherty, S., Palmer, P. I., Pison, I., Plummer, D., Poulter, B., Prinn, R. G., Rigby, M., Ringeval, B., Santini, M., Schmidt, M., Shindell, D. T., Simpson, I. J., Spahni, R., Steele, L. P., Strode, S. A., Sudo, K., Szopa, S., van der Werf, G. R., Voulgarakis, A., van Weele, M., Weiss, R. F., Williams, J. E., and Zeng, G.: Three decades of global methane sources and sinks, *Nature Geoscience*, 6, 813-823, 2013.
- Klein Goldewijk, K., Beusen, A., van Drecht, G., and de Vos, M.: The HYDE 3.1 spatially explicit database of human-induced global land-use change over the past 12,000 years, *Global Ecology and Biogeography*, 20, 73-86, 2011.
- Krinner, G., Viovy, N., de Noblet, N., Ogée, J., Friedlingstein, P., Ciais, P., Sitch, S., Polcher, J., and Prentice, I. C.: A dynamic global vegetation model for studies of the coupled atmosphere-biosphere system, *Global Biogeochemical Cycles*, 19, 1-33, 2005.
- Lamarque, J., Bond, T., Eyring, V., Granier, C., Heil, A., Klimont, Z., Lee, D., Liousse, C., Mieville, A., Owen, B., Schultz, M. G., Shindell, D., Smith, S. J., Stehfest, E., Van Aardenne, J., Cooper, O. R., Kainuma, M., Mahowald, N., McConnell, J. R., Naik, V., Riahi, K., and van Vuuren, D. P.: Historical (1850-2000) gridded anthropogenic and biomass burning emissions of reactive gases and aerosols: methodology and application, *Atmos. Chem. Phys.*, 10, 7017-7039, 2010.
- Landschützer, P., Gruber, N., Bakker, D. C. E., and Schuster, U.: Recent variability of the global ocean carbon sink, *Global Biogeochemical Cycles*, doi: 10.1002/2014GB004853, 2014. 2014.
- Landschützer, P., Gruber, N., Haumann, F. A., Rödenbeck, C., Bakker, D. C. E., van Heuven, S., Hoppema, M., Metzl, N., Sweeney, C., Takahashi, T., Tilbrook, B., and Wanninkhof, R.: The reinvigoration of the Southern Ocean carbon sink, *Science*, 349, 1221-1224, 2015.
- Le Quéré, C., Andres, R. J., Boden, T., Conway, T., Houghton, R. A., House, J. I., Marland, G., Peters, G. P., van der Werf, G. R., Ahlström, A., Andrew, R. M., Bopp, L., Canadell, J. G., Ciais, P., Doney, S. C., Enright, C., Friedlingstein, P., Huntingford, C., Jain, A. K., Jourdain, C., Kato, E., Keeling, R. F., Klein Goldewijk, K., Levis, S., Levy, P., Lomas, M., Poulter, B., Raupach, M. R., Schwinger, J., Sitch, S., Stocker, B. D., Viovy, N., Zaehle, S., and Zeng, N.: The global carbon budget 1959–2011, *Earth System Science Data*, doi: 10.5194/essd-5-165-2013, 2013. 165-186, 2013.
- Le Quéré, C., Moriarty, R., Andrew, R. M., Peters, G. P., Ciais, P., Friedlingstein, P., Jones, S. D., Sitch, S., Tans, P., Arneeth, A., Boden, T. A., Bopp, L., Bozec, Y., Canadell, J. G., Chini, L. P., Chevallier, F., Cosca, C. E., Harris, I., Hoppema, M., Houghton, R. A., House, J. I., Jain, A. K., Johannessen, T., Kato, E., Keeling, R. F., Kitidis, V., Klein Goldewijk, K., Koven, C., Landa, C. S., Landschützer, P., Lenton, A., Lima, I. D., Marland, G., Mathis, J. T., Metzl, N., Nojiri, Y., Olsen, A., Ono, T., Peng, S., Peters, W., Pfeil, B., Poulter, B., Raupach, M. R., Regnier, P., Rödenbeck, C., Saito, S., Salisbury, J. E., Schuster, U., Schwinger, J., Séférian, R., Segschneider, J., Steinhoff, T., Stocker, B. D., Sutton, A. J., Takahashi, T., Tilbrook, B., van der Werf, G. R., Viovy, N., Wang, Y. P., Wanninkhof, R., Wiltshire, A., and Zeng, N.: Global carbon budget 2014, *Earth Syst. Sci. Data*, 7, 47-85, 2015.
- Le Quéré, C., Peters, G. P., Andres, R. J., Andrew, R. M., Boden, T. A., Ciais, P., Friedlingstein, P., Houghton, R. A., Marland, G., Moriarty, R., Sitch, S., Tans, P., Arneeth, A., Arvanitis, A., Bakker, D. C. E., Bopp, L., Canadell, J. G., Chini, L. P., Doney, S. C., Harper, A., Harris, I., House, J. I., Jain, A. K., Jones, S. D., Kato, E., Keeling, R. F., Klein Goldewijk, K., Körtzinger, A., Koven, C., Lefèvre, N., Maignan, F., Omar, A., Ono, T., Park, G. H., Pfeil, B., Poulter, B., Raupach, M. R., Regnier, P., Rödenbeck, C., Saito, S., Schwinger, J., Segschneider, J., Stocker, B. D., Takahashi, T., Tilbrook, B., van Heuven, S., Viovy, N., Wanninkhof, R., Wiltshire, A., and Zaehle, S.: Global carbon budget 2013, *Earth Syst. Sci. Data*, 6, 235-263, 2014.

- Le Quéré, C., Raupach, M. R., Canadell, J. G., Marland, G., Bopp, L., Ciais, P., Conway, T. J., Doney, S. C., Feely, R. A., Foster, P., Friedlingstein, P., Gurney, K., Houghton, R. A., House, J. I., Huntingford, C., Levy, P. E., Lomas, M. R., Majkut, J., Metzl, N., Ometto, J. P., Peters, G. P., Prentice, I. C., Randerson, J. T., Running, S. W., Sarmiento, J. L., Schuster, U., Sitch, S., Takahashi, T., Viovy, N., van der Werf, G. R., and Woodward, F. I.: Trends in the sources and sinks of carbon dioxide, *Nature Geoscience*, 2, 831-836, 2009.
- Liu, Z., Guan, D., Wei, W., Davis, S. J., Ciais, P., Bai, J., Peng, S., Zhang, Q., Hubacek, K., Marland, G., Andres, R. J., Crawford-Brown, D., Lin, J., Zhao, H., Hong, C., Boden, T. A., Feng, K., Peters, G. P., Xi, F., Liu, J., Li, Y., Zhao, Y., Zeng, N., and He, K.: Reduced carbon emission estimates from fossil fuel combustion and cement production in China, *Nature*, 524, 335-338, 2015.
- MacDicken, K. G.: Global Forest Resources Assessment 2015: What, why and how?, *Forest Ecology and Management*, 352, 3-8, 2015.
- Manning, A. C. and Keeling, R. F.: Global oceanic and land biotic carbon sinks from the Scripps atmospheric oxygen flask sampling network, *Tellus Series B-Chemical and Physical Meteorology*, 58, 95-116, 2006.
- Marland, G.: Uncertainties in accounting for CO<sub>2</sub> from fossil fuels, *Journal of Industrial Ecology*, 12, 136-139, 2008.
- Marland, G., Andres, R. J., Blasing, T. J., Boden, T. A., Broniak, C. T., Gregg, J. S., Losey, L. M., and Treanton, K.: Energy, industry and waste management activities: An introduction to CO<sub>2</sub> emissions from fossil fuels. In: A report by the US Climate Change Science Program and the Subcommittee on Global Change Research, in *The First State of the Carbon Cycle Report (SOCCR): The North American Carbon Budget and Implications for the Global Carbon Cycle*, King, A. W., Dilling, L., Zimmerman, G. P., Fairman, D. M., Houghton, R. A., Marland, G., Rose, A. Z., and Wilbanks, T. J. (Eds.), Asheville, NC, 2007.
- Marland, G., Hamal, K., and Jonas, M.: How Uncertain Are Estimates of CO<sub>2</sub> Emissions?, *Journal of Industrial Ecology*, 13, 4-7, 2009.
- Masarie, K. A. and Tans, P. P.: Extension and integratio of atmospheric carbon dioxide data into a globally consistent measurement record, *J. Geophys. Res.-Atmos.*, 100, 11593-11610, 1995.
- McNeil, B. I., Matear, R. J., Key, R. M., Bullister, J. L., and Sarmiento, J. L.: Anthropogenic CO<sub>2</sub> uptake by the ocean based on the global chlorofluorocarbon data set, *Science*, 299, 235-239, 2003.
- Mikaloff Fletcher, S. E., Gruber, N., Jacobson, A. R., Doney, S. C., Dutkiewicz, S., Gerber, M., Follows, M., Joos, F., Lindsay, K., Menemenlis, D., Mouchet, A., Müller, S. A., and Sarmiento, J. L.: Inverse estimates of anthropogenic CO<sub>2</sub> uptake, transport, and storage by the oceans, *Global Biogeochemical Cycles*, 20, GB2002, 2006.
- Myhre, G., Alterskjær, K., and Lowe, D.: A fast method for updating global fossil fuel carbon dioxide emissions, *Environmental Research Letters*, 4, 034012, 2009.
- Narayanan, B., Aguiar, A., and McDougall, R.: Global Trade, Assistance, and Production: The GTAP 9 Data Base, <https://http://www.gtap.agecon.purdue.edu/databases/v9/default.asp>, last access: September 2015.
- National Bureau of Statistics of China: Industrial Production Operation in August 2015, [http://www.stats.gov.cn/english/PressRelease/201509/t20150915\\_1245026.html](http://www.stats.gov.cn/english/PressRelease/201509/t20150915_1245026.html), last access: September 2015.
- National Energy Administration: Conference on energy trends for the first half of 2015, [http://www.nea.gov.cn/2015-07/27/c\\_134450600.htm](http://www.nea.gov.cn/2015-07/27/c_134450600.htm), last access: July 2015.
- NOAA/ESRL: NOAA/ESRL calculation of global means, [http://www.esrl.noaa.gov/gmd/ccgg/about/global\\_means.html](http://www.esrl.noaa.gov/gmd/ccgg/about/global_means.html), last access: 7 October 2015.
- NOAA/ESRL, G. M. D.: Multi-laboratory compilation of atmospheric carbon dioxide data for the period 1968-2014, *obspack\_co2\_1\_GLOBALVIEWplus\_v1.0\_2015-07-30*. Project, C. G. A. D. I. (Ed.), 2015b.
- Oke, P. R., Griffin, D. A., Schiller, A., Matear, R. J., Fiedler, R., Mansbridge, J., Lenton, A., Cahill, M., Chamberlain, M. A., and Ridgway, K.: Evaluation of a near-global eddy-resolving ocean model, *Geosci. Model Dev.*, 6, 591-615, 2013.
- Oleson, K., Lawrence, D., Bonan, G., Drewniak, B., Huang, M., Koven, C., Levis, S., Li, F., Riley, W., Subin, Z., Swenson, S., Thornton, P., Bozbiyik, A., Fisher, R., Heald, C., Kluzek, E., Lamarque, J., Lawrence, P., Leung, L., Lipscomb, W., Muszala, S., Ricciuto, D., Sacks, W., Tang, J., and Yang, Z.: Technical Description of version 4.5 of the Community Land Model (CLM), NCAR, 2013.
- Peters, G. P., Andrew, R., and Lennos, J.: Constructing a multi-regional input-output table using the GTAP database, *Economic Systems Research*, 23, 131-152, 2011a.
- Peters, G. P., Andrew, R. M., Boden, T., Canadell, J. G., Ciais, P., Le Quéré, C., Marland, G., Raupach, M. R., and Wilson, C.: The challenge to keep global warming below 2°C, *Nature Climate Change*, 3, 4-6, 2013.
- Peters, G. P., Davis, S. J., and Andrew, R.: A synthesis of carbon in international trade, *Biogeosciences*, 9, 3247-3276, 2012a.

- Peters, G. P. and Hertwich, E. G.: Post-Kyoto Greenhouse Gas Inventories: Production versus Consumption, *Climatic Change*, 2008. 51-66, 2008.
- Peters, G. P., Marland, G., Le Quéré, C., Boden, T. A., Canadell, J. G., and Raupach, M. R.: Correspondence: Rapid growth in CO<sub>2</sub> emissions after the 2008-2009 global financial crisis, *Nature Climate Change*, 2, 2-4, 2012b.
- Peters, G. P., Minx, J. C., Weber, C. L., and Edenhofer, O.: Growth in emission transfers via international trade from 1990 to 2008, *Proceedings of the National Academy of Sciences of the United States of America*, 108, 8903-8908, 2011b.
- Peters, W., Krol, M. C., van der Werf, G. R., Houweling, S., Jones, C. D., Hughes, J., Schaefer, K., Masarie, K. A., Jacobson, A. R., Miller, J. B., Cho, C. H., Ramonet, M., Schmidt, M., Ciattaglia, L., Apadula, F., Heltai, D., Meinhardt, F., Di Sarra, A. G., Piacentino, S., Sferlazzo, D., Aalto, T., Hatakka, J., Ström, J., Haszpra, L., Meijer, H. A. J., Van Der Laan, S., Neubert, R. E. M., Jordan, A., Rodó, X., Morguí, J.-A., Vermeulen, A. T., Popa, E., Rozanski, K., Zimnoch, M., Manning, A. C., Leuenberger, M., Uglietti, C., Dolman, A. J., Ciais, P., Heimann, M., and Tans, P. P.: Seven years of recent European net terrestrial carbon dioxide exchange constrained by atmospheric observations, *Global Change Biology*, 16, 1317-1337, 2010.
- Peylin, P., R. M. Law, K. R. Gurney, F. Chevallier, A. R. Jacobson, T. Maki, Y. Niwa, P. K. Patra, W. Peters, P. J. Rayner, C. Rödenbeck, I. T. van der Laan-Luijckx, and Zhang, X.: Global atmospheric carbon budget: results from an ensemble of atmospheric CO<sub>2</sub> inversions, *Biogeosciences*, 10, 6699-6720, 2013.
- Pfeil, B., Olsen, A., Bakker, D. C. E., Hankin, S., Koyuk, H., Kozyr, A., Malczyk, J., Manke, A., Metzl, N., Sabine, C. L., Akl, J., Alin, S. R., Bates, N., Bellerby, R. G. J., Borges, A., Boutin, J., Brown, P. J., Cai, W.-J., Chavez, F. P., Chen, A., Cosca, C., Fassbender, A. J., Feely, R. A., González-Dávila, M., Goyet, C., Hales, B., Hardman-Mountford, N., Heinze, C., Hood, M., Hoppema, M., Hunt, C. W., Hydes, D., Ishii, M., Johannessen, T., Jones, S. D., Key, R. M., Körtzinger, A., Landschützer, P., Lauvset, S. K., Lefèvre, N., Lenton, A., Laurantou, A., Merlivat, L., Midorikawa, T., Mintrop, L., Miyazaki, C., Murata, A., Nakadate, A., Nakano, Y., Nakaoka, S., Nojiri, Y., Omar, A. M., Padin, X. A., Park, G.-H., Paterson, K., Perez, F. F., Pierrot, D., Poisson, A., Ríos, A. F., Santana-Casiano, J. M., Salisbury, J., Sarma, V. V. S. S., Schlitzer, R., Schneider, B., Schuster, U., Sieger, R., Skjelvan, I., Steinhoff, T., Suzuki, T., Takahashi, T., Tedesco, K., Telszewski, M., Thomas, H., Tilbrook, B., Tjiputra, J., Vandemark, D., Veness, T., Wanninkhof, R., Watson, A. J., Weiss, R., Wong, C. S., and Yoshikawa-Inoue, H.: A uniform, quality controlled Surface Ocean CO<sub>2</sub> Atlas (SOCAT) A uniform, quality controlled Surface Ocean CO<sub>2</sub> Atlas (SOCAT), *Earth Syst. Sci. Data*, 5, 125-143, 2013.
- Pongratz, J., Reick, C. H., Houghton, and House, J. I.: Terminology as a key uncertainty in net land use and land cover change carbon flux estimates, *Earth System Dynamics*, 5, 177-195, 2014.
- Pongratz, J., Reick, C. H., Houghton, R. A., and House, J. I.: Terminology as a key uncertainty in net land use flux estimates, *Earth Syst. Sci. Data Discuss.*, 4, 677-716, 2013.
- Pongratz, J., Reick, C. H., Raddatz, T., and Claussen, M.: Effects of anthropogenic land cover change on the carbon cycle of the last millennium, *Global Biogeochemical Cycles*, 23, 2009.
- Poulter, B., Frank, D., Ciais, P., Myneni, R. B., Andela, N., Bi, J., Broquet, G., Canadell, J. G., Chevallier, F., Liu, Y. Y., Running, S. W., Sitch, S., and van der Werf, G. R.: Contribution of semi-arid ecosystems to interannual variability of the global carbon cycle, *Nature*, 509, 600-603, 2014.
- Prather, M. J., Holmes, C. D., and Hsu, J.: Reactive greenhouse gas scenarios: Systematic exploration of uncertainties and the role of atmospheric chemistry, *Geophys. Res. Lett.*, 39, L09803, 2012.
- Prentice, I. C., Farquhar, G. D., Fasham, M. J. R., Goulden, M. L., Heimann, M., Jaramillo, V. J., Khashgi, H. S., Le Quéré, C., Scholes, R. J., and Wallace, D. W. R.: The Carbon Cycle and Atmospheric Carbon Dioxide. In: *Climate Change 2001: The Scientific Basis. Contribution of Working Group I to the Third Assessment Report of the Intergovernmental Panel on Climate Change*, Houghton, J. T., Ding, Y., Griggs, D. J., Noguer, M., van der Linden, P. J., Dai, X., Maskell, K., and Johnson, C. A. (Eds.), Cambridge University Press, Cambridge, United Kingdom and New York, NY, USA., 2001.
- Randerson, J., Chen, Y., van der Werf, G. R., Rogers, B. M., Morton, D. C.: Global burned area and biomass burning emissions from small fires, *JOURNAL OF GEOPHYSICAL RESEARCH-BIOGEOSCIENCES*, 117, 2012.
- Raupach, M. R., Marland, G., Ciais, P., Le Quéré, C., Canadell, J. G., Klepper, G., and Field, C. B.: Global and regional drivers of accelerating CO<sub>2</sub> emissions, *Proceedings of the National Academy of Sciences of the United States of America*, 104, 10288-10293, 2007.
- Regnier, P., Friedlingstein, P., Ciais, P., Mackenzie, F. T., Gruber, N., Janssens, I. A., Laruelle, G. G., Lauerwald, R., Luysaert, S., Andersson, A. J., Arndt, S., Arnosti, C., Borges, A. V., Dale, A. W., Gallego-Sala, A., Goddérís, Y., Goossens, N., Hartmann, J., Heinze, C., Ilyina, T., Joos, F., La Rowe, D. E., Leifeld, J., Meysman, F. J. R., Munhoven, G., Raymond, P. A., Spahni, R., Suntharalingam, P., and Thullner, M.: Anthropogenic perturbation of the carbon fluxes from land to ocean, *Nature Geoscience*, 6, 597-607, 2013.



- Reick, C. H., T. Raddatz, V. Brovkin, and Gayler, V.: The representation of natural and anthropogenic land cover change in MPI-ESM, *Journal of Advances in Modeling Earth Systems*, 5, 459–482, 2013.
- Rhein, M., Rintoul, S. R., Aoki, S., Campos, E., Chambers, D., Feely, R. A., Gulev, S., Johnson, G. C., Josey, S. A., Kostianoy, A., Mauritzen, C., Roemmich, D., Talley, L. D., and Wang, F.: Chapter 3: Observations: Ocean. In: *Climate Change 2013 The Physical Science Basis*, Cambridge University Press, 2013.
- Rödenbeck, C.: Estimating CO<sub>2</sub> sources and sinks from atmospheric mixing ratio measurements using a global inversion of atmospheric transport, Max Plank Institute, MPI-BGC, 2005.
- Rödenbeck, C., Bakker, D. C. E., Gruber, N., Iida, Y., Jacobson, A. R., Jones, S., Landschützer, P., Metzl, N., Nakaoka, S., Olsen, A., Park, G. H., Peylin, P., Rodgers, K. B., Sasse, T. P., Schuster, U., Shutler, J. D., Valsala, V., Wanninkhof, R., and Zeng, J.: Data-based estimates of the ocean carbon sink variability – first results of the Surface Ocean pCO<sub>2</sub> Mapping intercomparison (SOCOM), *Biogeosciences Discuss.*, 12, 14049–14104, 2015.
- Rödenbeck, C., Bakker, D. C. E., Metzl, N., Olsen, A., Sabine, C., Cassar, N., Reum, F., Keeling, R. F., and Heimann, M.: Interannual sea-air CO<sub>2</sub> flux variability from an observation-driven ocean mixed-layer scheme, *Biogeosciences*, doi: 10.5194/bg-11-4599-2014, 2014. 4599–4613, 2014.
- Rödenbeck, C., Keeling, R. F., Bakker, D. C. E., Metzl, N., Olsen, A., Sabine, C., and Heimann, M.: Global surface-ocean pCO<sub>2</sub> and sea–air CO<sub>2</sub> flux variability from an observation-driven ocean mixed-layer scheme, *Ocean Science*, doi: 10.5194/os-9-193-2013, 2013. 193–216, 2013.
- Rödenbeck, C., S. Houweling, M. Gloor, and M. Heimann: CO<sub>2</sub> flux history 1982–2001 inferred from atmospheric data using a global inversion of atmospheric transport, *Atmos. Chem. Phys. Discuss.*, 3, 1919–1964, 2003.
- Rost, S., Gerten, D., Bondeau, A., Lucht, W., Rohwer, J., and Schaphoff, S.: Agricultural green and blue water consumption and its influence on the global water system, *Water Resources Research*, doi: W09405, 2008. 2008.
- Rypdal, K., Paciomik, N., Eggleston, S., Goodwin, J., Irving, W., Penman, J., and Woodfield, M.: Chapter 1 Introduction to the 2006 Guidelines. In: *2006 IPCC Guidelines for National Greenhouse Gas Inventories*, Eggleston, S., Buendia, L., Miwa, K., Ngara, T., and Tanabe, K. (Eds.), Institute for Global Environmental Strategies (IGES), Hayama, Kanagawa, Japan, 2006.
- Saatchi, S. S., Harris, N. L., Brown, S.: Benchmark map of forest carbon stocks in tropical regions across three continents, *Proceedings of the National Academy of Sciences*, 108, 9899–9904, 2011.
- Schaphoff, S., Heyder, U., Ostberg, S., Gerten, D., Heinke, J., and Lucht, W.: Contribution of permafrost soils to the global carbon budget., *Environ. Res. Lett.*, 8, 10, 2013.
- Schimel, D., Alves, D., Enting, I., Heimann, M., Joos, F., Raynaud, D., Wigley, T., Prater, M., Derwent, R., Ehhalt, D., Fraser, P., Sanhueza, E., Zhou, X., Jonas, P., Charlson, R., Rodhe, H., Sadasivan, S., Shine, K. P., Fouquart, Y., Ramaswamy, V., Solomon, S., Srinivasan, J., Albritton, D., Derwent, R., Isaksen, I., Lal, M., and Wuebbles, D.: Radiative Forcing of Climate Change. In: *Climate Change 1995 The Science of Climate Change. Contribution of Working Group I to the Second Assessment Report of the Intergovernmental Panel on Climate Change*, Houghton, J. T., Meira Filho, L. G., Callander, B. A., Harris, N., Kattenberg, A., and Maskell, K. (Eds.), Cambridge University Press, Cambridge, United Kingdom and New York, NY, USA., 1995.
- Scripps: The Keeling Curve, <http://keelingcurve.ucsd.edu/>, last access: 7 November 2013 2013.
- Séférian, R., Bopp, L., Gehlen, M., Orr, J., Ethé, C., Cadule, P., Aumont, O., Salas y Méliá, D., Voldoire, A. and Madec, G.: Skill assessment of three earth system models with common marine biogeochemistry, *Climate Dynamics*, 40, 2549–2573, 2013.
- Shevliakova, E., Pacala, S., Malyshev, S., Hurtt, G., Milly, P., Caspersen, J., Sentman, L., Fisk, J., Wirth, C., and Crevoisier, C.: Carbon cycling under 300 years of land use change: Importance of the secondary vegetation sink, *Global Biogeochemical Cycles*, 23, -, 2009.
- Sitch, S., Friedlingstein, P., Gruber, N., Jones, S. D., Murray-Tortarolo, G., Ahlstrom, A., Doney, S. C., Graven, H., Heinze, C., Huntingford, C., Levis, S., Levy, P. E., Lomas, M., Poulter, B., Viovy, N., Zaehle, S., Zeng, N., Arneth, A., Bonan, G., Bopp, L., Canadell, J. G., Chevallier, F., Ciais, P., Ellis, R., Gloor, M., Peylin, P., Piao, S. L., Le Quere, C., Smith, B., Zhu, Z., and Myneni, R.: Recent trends and drivers of regional sources and sinks of carbon dioxide, *Biogeosciences*, 12, 653–679, 2015.
- Sitch, S., Smith, B., Prentice, I. C., Arneth, A., Bondeau, A., Cramer, W., Kaplan, J. O., Levis, S., Lucht, W., Sykes, M. T., Thonicke, K., and Venevsky, S.: Evaluation of ecosystem dynamics, plant geography and terrestrial carbon cycling in the LPJ dynamic global vegetation model *Global Change Biology*, 9, 161–185, 2003.
- Smith, B., Wårlind, D., Arneth, A., Hickler, T., Leadley, P., Siltberg, J., and Zaehle, S.: Implications of incorporating N cycling and N limitations on primary production in an individual-based dynamic vegetation model, *Biogeosciences*, 11, 2027–2054, 2014a.
- Smith, P., M. Bustamante, Clark, H., Dong, H., Elsiddig, E. A., Haberl, H., Harper, R., House, J. I., Jafari, M., Masera, O., Mbaw, C., Ravindranath, N. H., Rice, C. W., Robledo Abad, C., Romanovskaya, A., Sperling, F., and Tubiello, F.

- N.: Agriculture, Forestry and Other Land Use (AFOLU). In: Chapter 11 in Climate Change 2014: Mitigation of Climate Change. Contribution of Working Group III to the Fifth Assessment Report of the Intergovernmental Panel on Climate Change Edenhofer, O., R. Pichs-Madruga, Y. Sokona, E. Farahani, S. Kadner, K. Seyboth, A. Adler, I. Baum, S. Brunner, P. Eickemeier, B. Kriemann, J. Savolainen, S. Schlömer, C. von Stechow, T. Zwickel and J.C. Minx (Ed.), Cambridge University Press, Cambridge, United Kingdom and New York, NY, USA., 2014b.
- Stephens, B. B., Gurney, K. R., Tans, P. P., Sweeney, C., Peters, W., Bruhwiler, L., Ciais, P., Ramonet, M., Bousquet, P., Nakazawa, T., Aoki, S., Machida, T., Inoue, G., Vinnichenko, N., Lloyd, J., Jordan, A., Heimann, M., Shibistova, O., Langenfelds, R. L., Steele, L. P., Francey, R. J., and Denning, A. S.: Weak Northern and Strong Tropical Land Carbon Uptake from Vertical Profiles of Atmospheric CO<sub>2</sub>, *Science*, 316, 1732-1735, 2007.
- Stocker, T., Qin, D., and Plattner, G.-K.: Climate Change 2013 The Physical Science Basis, Cambridge University Press, 2013.
- Sweeney, C., Gloor, E., Jacobson, A. R., Key, R. M., McKinley, G., Sarmiento, J. L., and Wanninkhof, R.: Constraining global air-sea gas exchange for CO<sub>2</sub> with recent bomb 14C measurements, *Glob. Biogeochem. Cycles*, 21, GB2015, 2007.
- Tans, P. and Keeling, R. F.: Trends in atmospheric carbon dioxide, National Oceanic & Atmospheric Administration, Earth System Research Laboratory (NOAA/ESRL) & Scripps Institution of Oceanography, <http://www.esrl.noaa.gov/gmd/ccgg/trends/> & <http://scrippsco2.ucsd.edu/>, last access: 8 August 2014.
- Tjiputra, J. F., Roelandt, C., Bentsen, M., Lawrence, D. M., Lorentzen, T., Schwinger, J., Seland, Ø., and Heinze, C.: Evaluation of the carbon cycle components in the Norwegian Earth System Model (NorESM), *Geosci. Model Dev.*, 6, 301-325, 2013.
- Tubiello, F. N., Salvatore, M., Ferrara, A.F., House, J., Federici, S., Rossi, S., Biancalani, R., C. G., R.D., Jacobs, H., Flammini, A., Prosperi, P., Cardenas-Galindo, P., and Schmidhuber, J., Sanz Sanchez, M.J., Srivastava, N., Smith, P., : The contribution of agriculture, forestry and other land use activities to global warming 1990–2012, *Glob. Change Biol.*, doi: 10.1111/gcb.12865., 2015. 2015.
- Tyukavina, A., Baccini, A., Hansen, M. C., Potapov, P. V., Stehman, S. V., Houghton, R. A., Krylov, A. M., Turubanova, S., and Goetz, S. J.: Aboveground carbon loss in natural and managed tropical forests from 2000 to 2012, *Environmental Research Letters*, 10, 074002, 2015.
- UN a: United Nations Statistics Division: Energy Statistics, *United Nations Statistics Division: Energy Statistics* <http://unstats.un.org/unsd/energy/>, last access: October 2015.
- UN b: United Nations Statistics Division: Industry Statistics, *United Nations Statistics Division: Industry Statistics* <http://unstats.un.org/unsd/industry/default.asp>, last access: October 2015.
- UN c: United Nations Statistics Division: National Accounts Main Aggregates Database, *United Nations Statistics Division: National Accounts Main Aggregates Database* <http://unstats.un.org/unsd/snaama/Introduction.asp>, last access: 8 August 2014.
- USGS: Mineral Commodities Summaries: Cement, USGS, 2015.
- van der Werf, G. R., Dempewolf, J., Trigg, S. N., Randerson, J. T., Kasibhatla, P., Giglio, L., Murdiyarso, D., Peters, W., Morton, D. C., Collatz, G. J., Dolman, A. J., and DeFries, R. S.: Climate regulation of fire emissions and deforestation in equatorial Asia, *Proceedings of the National Academy of Science*, 15, 20350-20355, 2008.
- van der Werf, G. R., Randerson, J. T., Giglio, L., Collatz, G. J., Mu, M., Kasibhatla, P., Morton, D. C., DeFries, R. S., Jin, Y., and van Leeuwen, T. T.: Global fire emissions and the contribution of deforestation, savanna, forest, agricultural, and peat fires (1997–2009), *Atmospheric Chemistry and Physics*, 10, 11707-11735, 2010.
- van Minnen, J. G., Goldewijk, K. K., Stehfest, E., Eickhout, B., van Drecht, G., and Leemans, R.: The importance of three centuries of land-use change for the global and regional terrestrial carbon cycle, *Climatic Change*, 97, 123-144, 2009.
- van Oss, H. G.: Cement, US Geological Survey, June, 2013.
- van Oss, H. G.: Cement, US Geological Survey, 2015.
- Waha, K., van Bussel, L. G. J., Müller, C., and Bondeau, A.: Climate-driven simulation of global crop sowing dates, *Global Ecology and Biogeography*, 12, 247-259, 2012.
- Wanninkhof, R., Park, G.-H., Takahashi, T., Sweeney, C., Feely, R. A., Nojiri, Y., Gruber, N., Doney, S. C., McKinley, G. A., Lenton, A., Le Quéré, C., Heinze, C., Schwinger, J., Graven, H. D., and Khatiwala, S.: Global ocean uptake: magnitude, variability and trends, *Biogeosciences*, 2013. 1983-2000, 2013.
- Watson, R. T., Rodhe, H., Oeschger, H., and Siegenthaler, U.: Greenhouse Gases and Aerosols. In: Climate Change: The IPCC Scientific Assessment. Intergovernmental Panel on Climate Change (IPCC), Houghton, J. T., Jenkins, G. J., and Ephraums, J. J. (Eds.), Cambridge University Press, Cambridge, 1990.
- Zaehle, S., Ciais, P., Friend, A. D., and Prieur, V.: Carbon benefits of anthropogenic reactive nitrogen offset by nitrous oxide emissions, *Nature Geosci*, 4, 601-605, 2011.

- 1 Zaehle, S., P. Friedlingstein, and Friend, A. D.: Terrestrial nitrogen feedbacks may accelerate future climate change,
- 2 Geophys. Res. Lett., 37, 2010.
- 3 Zeng, N., Mariotti, A., and Wetzel, P.: Terrestrial mechanisms of interannual CO<sub>2</sub> variability, Global Biogeochemical
- 4 Cycles, 19, GB1016, 2005.

5

6

Submitted



1 **Tables**2 **Table 1.** Factors used to convert carbon in various units (by convention, Unit 1 = Unit 2 '  
3 conversion).

Unit 1	Unit 2	Conversion	Source
GtC (gigatonnes of carbon)	ppm (parts per million) <sup>a</sup>	2.12 <sup>b</sup>	Ballantyne et al. (2012)
GtC (gigatonnes of carbon)	PgC (petagrammes of carbon)	1	SI unit conversion
GtCO <sub>2</sub> (gigatonnes of carbon dioxide)	GtC (gigatonnes of carbon)	3.664	44.01/12.011 in mass equivalent
GtC (gigatonnes of carbon)	MtC (megatonnes of carbon)	1000	SI unit conversion

<sup>a</sup> Measurements of atmospheric CO<sub>2</sub> concentration have units of dry-air mole fraction. 'ppm' is an abbreviation for micromole/mol, dry air.

<sup>b</sup> the use of a factor of 2.12 assumes that all the atmosphere is well mixed within one year. In reality, only the troposphere is well mixed and the growth rate of CO<sub>2</sub> in the less well-mixed stratosphere is not measured by sites from the NOAA network. Using a factor of 2.12 makes the approximation that the growth rate of CO<sub>2</sub> in the stratosphere equals that of the troposphere on a yearly basis.

1 **Table 2.** How to cite the individual components of the global carbon budget presented here.

Component	Primary reference
Global fossil fuel and cement emissions ( $E_{FF}$ ), total and by fuel type	Boden et al. (2015; CDIAC: <a href="http://cdiac.ornl.gov/trends/emis/meth_reg.html">cdiac.ornl.gov/trends/emis/meth_reg.html</a> )
Territorial fossil fuel and cement emissions ( $E_{FF}$ ) by country	CDIAC source: Boden et al. (2015; CDIAC: <a href="http://cdiac.ornl.gov/trends/emis/meth_reg.html">cdiac.ornl.gov/trends/emis/meth_reg.html</a> )  UNFCCC (2015; <a href="http://unfccc.int/national_reports/annex_i_ghg_inventories/national_inventories_submissions/items/8108.php">http://unfccc.int/national_reports/annex_i_ghg_inventories/national_inventories_submissions/items/8108.php</a> ; accessed May 2015)
Consumption-based fossil fuel and cement emissions ( $E_{FF}$ ) by country (consumption)	Peters et al. (2011b) updated as described in this paper
Land-use change emissions ( $E_{LUC}$ )	Houghton et al. (2012) combined with Giglio et al. (2013)
Atmospheric CO <sub>2</sub> growth rate ( $G_{ATM}$ )	Dlugokencky and Tans (2015; NOAA/ESRL: <a href="http://www.esrl.noaa.gov/gmd/ccgg/trends/global">www.esrl.noaa.gov/gmd/ccgg/trends/global</a> ; accessed October 12 2015)
Ocean and land CO <sub>2</sub> sinks ( $S_{OCEAN}$ and $S_{LAND}$ )	This paper for $S_{OCEAN}$ and $S_{LAND}$ and references in Table 6 for individual models.

Publication year <sup>a</sup>	Global	Fossil fuel emissions Country (territorial)	Country (consumption)	LUC emissions	Atmosphere	Reservoirs Ocean	Land	Uncertainty & other changes
2006		Split in regions						
2007	Raupach et al. (2007)			$E_{LUC}$ based on FAO-FRA 2005; constant $E_{LUC}$ for 2006	1959-1979 data from Mauna Loa; data after 1980 from global average	Based on one ocean model tuned to reproduced observed 1990s sink		$\pm 1\sigma$ provided for all components
2008 (online)		Split between Annex B and non-Annex B		Constant $E_{LUC}$ for 2007				
2009				Fire-based emission anomalies used for 2006-2008		Based on four ocean models normalised to observations with constant delta	First use of five DGVMs to compare with budget residual	
Le Quéré et al. (2009)			Results from an independent study discussed					
2010								
Friedlingstein et al. (2010)	Projection for current year based on GDP	Emissions for top emitters		$E_{LUC}$ updated with FAO-FRA 2010				
2011								
Peters et al. (2012b)			Split between Annex B and non-Annex B					
2012		129 countries from 1959	129 countries and regions from 1990-2010 based on GTAP8.0	$E_{LUC}$ for 1997-2011 includes interannual anomalies from fire-based emissions	All years from global average	Based on 5 ocean models normalised to observations with ratio	Ten DGVMs available for $S_{Land}$ ; First use of four models to compare with $E_{LUC}$	
Le Quéré et al. (2013)								
Peters et al. (2013)								
2013		250 countries <sup>b</sup>	134 countries and regions 1990-2011 based on GTAP8.1, with detailed estimates for years 1997, 2001, 2004, and 2007	$E_{LUC}$ for 2012 estimated from 2001-2010 average		Based on six models compared with two data-products to year 2011	Coordinated DGVM experiments for $S_{Land}$ and $E_{LUC}$	Confidence levels; cumulative emissions; budget from 1750
Le Quéré et al. (2014)								
2014	Three years of BP data	Three years of BP data	Extended to 2012 with updated GDP data	$E_{LUC}$ for 1997-2013 includes interannual anomalies from fire-based emissions		Based on seven models compared with three data-products to year 2013	Based on 10 models	Inclusion of breakdown of the sinks in three latitude bands and comparison with three atmospheric inversions
Le Quéré et al. (2015)								
2015								
(this study)			National emissions from UNEFCC extended to 2014 also provided (along with CDIAC)	Detailed estimates introduced for 2011 based on GTAP9		Based on eight models compared with two data-products to year 2014	Based on ten models	The decadal uncertainty for the DGVM ensemble mean now uses $\pm 1\sigma$ of the decadal spread across models

The naming convention of the budgets has changed. Up to and including 2010, the budget year (Carbon Budget 2010) represented the latest year of the data. From 2012, the budget year (Carbon Budget 2012) refers to the initial publication year.

The CDIAC database has about 250 countries, but we show data for about 216 countries since we aggregate and disaggregate some countries to be consistent with current country definitions (see Sect. 2.1.1 for more details).

<sup>b</sup>The CDIAC database has about 250 countries, but we show data for about 216 countries since we aggregate and disaggregate some countries to be consistent with current country definitions (see Sect. 2.1.1 for more details).

<sup>b</sup>The CDIAC database has about 250 countries, but we show data for about 216 countries since we aggregate and disaggregate some countries to be consistent with current country definitions (see Sect. 2.1.1 for more details).

1 **Table 4.** Data sources used to compute each component of the global carbon budget.

Component	Process	Data source	Data reference
$E_{FF}$	Fossil fuel combustion and gas flaring	UN Statistics Division to 2011 BP for 2012-2014	UN (2014a, b) BP (2015)
	Cement production	US Geological Survey	van Oss (2015) US Geological Survey (2015)
$E_{LUC}$	Land cover change (deforestation, afforestation, and forest regrowth)	Forest Resource Assessment (FRA) of the Food and Agriculture Organisation (FAO)	FAO (2010)
	Wood harvest	FAO Statistics Division	FAOSTAT (2010)
	Shifting agriculture	FAO FRA and Statistics Division	FAO (2010) FAOSTAT (2010)
	Interannual variability from peat fires and climate – land management interactions (1997-2013)	Global Fire Emissions Database (GFED4)	Giglio et al., (2013)
$G_{ATM}$	Change in atmospheric CO <sub>2</sub> concentration	1959-1980: CO <sub>2</sub> Program at Scripps Institution of Oceanography and other research groups	Keeling et al. (1976)
		1980-2014: US National Oceanic and Atmospheric Administration Earth System Research Laboratory	Dlugokencky and Tans (2015) Ballantyne et al. (2012)
$S_{OCEAN}$	Uptake of anthropogenic CO <sub>2</sub>	1990-1999 average: indirect estimates based on CFCs, atmospheric O <sub>2</sub> , and other tracer observations	Manning and Keeling (2006) Keeling et al. (2011) McNeil et al. (2003) Mikaloff Fletcher et al. (2006) as assessed by the IPCC in Denman et al. (2007)
	Impact of increasing atmospheric CO <sub>2</sub> , climate and variability	Ocean models	Table 6
$S_{LAND}$	Response of land vegetation to:  Increasing atmospheric CO <sub>2</sub> concentration  Climate and variability  Other environmental changes	Budget residual	

2

**Table 5.** Comparison of the processes included in the E<sub>LUC</sub> of the global carbon budget and the DGVMs. See Table 6 for model references. All models include deforestation and forest regrowth after abandonment of agriculture (or from afforestation activities on agricultural land).

	Bookkeeping	CLIM4.5BGC	ISAM	JSBACH	JULES	LPJ-GUESS	LPJ	LPJmL	OCNv1.r240	ORCHIDEE	VISIT
Wood harvest and forest degradation <sup>a</sup>	yes	yes	yes	yes	no	no	no	no	yes	no	yes <sup>b</sup>
Shifting cultivation	yes	yes	no	yes	no	no	no	no	no	no	yes
Cropland harvest	yes	yes	yes	yes <sup>c</sup>	no	yes	no	yes	yes	yes	yes
Peat fires	no	yes	no	no	no	no	no	no	no	no	no
Fire simulation and/or suppression	for US only	yes	no	yes	no	yes	yes	yes	no	no	yes
Climate and variability	no	yes	yes	yes	yes	yes	yes	yes	yes	yes	yes
CO <sub>2</sub> fertilisation	no	yes	yes	yes	yes	yes	yes	yes	yes	yes	yes
Carbon-nitrogen interactions, including N deposition	no	yes	yes	no	no	no	no	no	yes	no	no

<sup>a</sup>Refers to the routine harvest of established managed forests rather than pools of harvested products. <sup>b</sup>Wood stems are harvested according to the land-use data. <sup>c</sup>Carbon from crop harvest is entirely transferred into the litter pools.

1 **Table 6.** References for the process models and data products included in Figs. 6-8.

Model/data name	Reference	Change from Le Quéré et al. (2015)
<i>Dynamic global vegetation models</i>		
CLM4.5BGC <sup>a</sup>	Oleson et al. (2013)	No change
ISAM	Jain et al. (2013) <sup>b</sup>	We accounted for crop harvest for C3 and C4 crops based on Arora and Boer (2005) and agricultural soil carbon loss due to tillage (Jain et al., 2005)
JSBACH	Reick et al. (2013) <sup>c</sup>	Not applicable
JULES <sup>e</sup>	Clarke et al. (2011) <sup>e</sup>	Updated JULES version 4.3 compared to v3.2 for last years budget. A number of small code changes but no change in major science sections with the exception to an update in the way litter flux is calculated.
LPJ-GUESS	Smith et al. (2014a)	Implementation of C/N interactions in soil and vegetation, including a complete update of the soil organic matter scheme
LPJ <sup>f</sup>	Sitch et al. (2003)	No change
LPJmL	Bondeau et al. (2007) <sup>g</sup>	Not applicable
OCNv1.r240	Zaehle et al. (2011) <sup>h</sup>	Revised photosynthesis parameterisation allowing for temperature acclimation as well as cold and heat effects on canopy processes. Revised grassland phenology. Included wood harvest as a driver to simulate harvest and post-harvest regrowth. Using Hurtt land-use data set
ORCHIDEE	Krinner et al. (2005)	Revised parameters values for photosynthetic capacity for boreal forests (following assimilation of FLUXNET data), updated parameters values for stem allocation, maintenance respiration and biomass export for tropical forests (based on literature) and, CO2 down-regulation process added to photosynthesis.
VISIT	Kato et al. (2013) <sup>i</sup>	Not applicable
<i>Data products for land-use change emissions</i>		
Bookkeeping	Houghton et al. (2012)	No change
Fire-based emissions	van der Werf et al. (2010)	No change
<i>Ocean biogeochemistry models</i>		
NEMO-PlankTOM5	Buitenhuis et al. (2010) <sup>j</sup>	No change
NEMO-PISCES (IPSL) <sup>k</sup>	Aumont and Bopp (2006)	No change
CCSM-BEC	Doney et al. (2009)	No change; small difference in the mean flux are caused by a change in how global and annual means were computed
MICOM-HAMOCC (NorESM-OC)	Assmann et al. (2010) <sup>l,m</sup>	Revised light penetration formulation and parameters for ecosystem module, revised salinity restoring scheme enforcing salt conservation, new scheme enforcing global freshwater balance, and model grid changed from displaced pole to tripolar
MPIOM-HAMOCC	Ilyina et al. (2013)	No change
NEMO-PISCES (CNRM)	Séférian et al. (2013) <sup>n</sup>	No change
CSIRO	Oke et al. (2013)	No change

MITgcm-REcoM2	Hauck et al. (2013) <sup>o</sup>	Not applicable
---------------	----------------------------------	----------------

---

*Data products for ocean CO<sub>2</sub> flux*


---

Landschützer <sup>p</sup>	Landschützer et al. (2015)	No change
Jena CarboScope <sup>p</sup>	Rödenbeck et al. (2014) <sup>q</sup>	No change

---

*Atmospheric inversions for total CO<sub>2</sub> fluxes (land-use-change + land + ocean CO<sub>2</sub> fluxes)*


---

CarbonTracker <sup>r</sup>	Peters et al. (2010)	No change
Jena CarboScope	Rödenbeck et al. (2003) <sup>s</sup>	No change
MACC <sup>t</sup>	Chevallier et al. (2005)	No change

---

<sup>a</sup>Community Land Model 4.5<sup>b</sup>See also El-Masri et al. (2013)<sup>c</sup>See also Goll et al (2015)<sup>d</sup>Joint UK Land Environment Simulator<sup>e</sup>See also Best et al. (2011)<sup>f</sup>Lund-Potsdam-Jena<sup>g</sup>The LPJmL (Lund-Potsdam-Jena managed Land) version used includes also developments described in Rost et al. (2008; river routing and irrigation), Fader et al. (2010; agricultural management), Biemans et al. (2011; reservoir management), Shapfhoof et al. (2013; permafrost and 5 layer hydrology), and Waha et al. (2012; sowing data) (sowing dates)<sup>h</sup>See also Zaehle et al. (2010) and Friend et al. (2010)<sup>i</sup>see also Ito and Inatomi (2012)<sup>j</sup>With no nutrient restoring below the mixed layer depth<sup>k</sup>Referred to as LSCE in previous carbon budgets<sup>l</sup>With updates to the physical model as described in Tjiputra et al. (2013)<sup>m</sup>Further information (e.g., physical evaluation) for these models can be found in Danabasoglu et al. (2014)<sup>n</sup>using winds from Atlas et al. (2011)<sup>o</sup>A few changes have been applied to the ecosystem model: (1) The constant Fe:C ratio was substituted by a constant Fe:N ratio. (2) A sedimentary iron source was implemented. (3) the following parameters were changed:<sup>p</sup>*CHL\_N\_max*=3.78, *Fe2N* = 0.033, *deg\_CHL\_d* = 0.1, *Fe2N\_d* = 0.033, *ligandStabConst*=200, *constantIronSolubility* = 0.02<sup>p</sup>updates using SOCATv3 plus new 2012-2014 data<sup>q</sup>Updated version oc\_1.2gcp2015<sup>r</sup>Version CTE2015, updates include using CO<sub>2</sub> observations from obspack\_co2\_1\_GLOBALVIEWplus\_v1.0\_2015-07-30 (NOAA/ESRL, 2015b), prior SiBCASA biosphere and fire fluxes on 3 hourly resolution and fossil fuel emissions for 2010-2014 scaled to updated global totals.<sup>s</sup>Updated version s81\_v3.7<sup>t</sup>The MACCv14.2 CO<sub>2</sub> inversion system, initially described by Chevallier et al. (2005), relies on the global tracer transport model LMDZ (Hourdin et al., 2006; see also Supplementary Material Peylin et al., 2013).

**Table 7.** Comparison of results from the bookkeeping method and budget residuals with results from the DGVMs and inverse estimates for the periods 1960-1969, 1970-1979, 1980-1989, 1990-1999, 2000-2009, last decade and last year available. All values are in  $\text{GtC yr}^{-1}$ . The DGM uncertainties represents  $\pm 1\sigma$  of the decadal or annual (for 2014 only) estimates from the ten individual models, for the inverse models all three results are given where available.

	Mean (GtC yr <sup>-1</sup> )						
	1960-1969	1970-1979	1980-1989	1990-1999	2000-2009	2005-2014	2014
	Land-use change emissions ( <i>E<sub>LUC</sub></i> )						
Bookkeeping method	1.5 ± 0.5	1.3 ± 0.5	1.4 ± 0.5	1.6 ± 0.5	1.0 ± 0.5	0.9 ± 0.5	1.1 ± 0.5
DGVMS <sup>a</sup>	1.2 ± 0.4	1.2 ± 0.4	1.3 ± 0.4	1.2 ± 0.4	1.2 ± 0.4	1.4 ± 0.4	1.4 ± 0.5
	Residual terrestrial sink ( <i>S<sub>LAND</sub></i> )						
Budget residual	1.7 ± 0.7	1.7 ± 0.8	1.6 ± 0.8	2.6 ± 0.8	2.4 ± 0.8	3.0 ± 0.8	4.1 ± 0.9
DGVMS <sup>a</sup>	1.1 ± 0.6	2.1 ± 0.3	1.7 ± 0.4	2.3 ± 0.3	2.7 ± 0.4	3.0 ± 0.5	3.6 ± 0.9
	Total land fluxes ( <i>S<sub>LAND</sub></i> − <i>E<sub>LUC</sub></i> )						
Budget ( <i>E<sub>FF</sub></i> − <i>G<sub>ATM</sub></i> − <i>S<sub>OCEAN</sub></i> )	0.2 ± 0.5	0.4 ± 0.6	0.2 ± 0.6	1.0 ± 0.6	1.5 ± 0.6	2.1 ± 0.7	3.0 ± 0.7
DGVMS <sup>a</sup>	−0.1 ± 0.6	0.9 ± 0.4	0.5 ± 0.5	1.1 ± 0.5	1.5 ± 0.4	1.6 ± 0.4	2.3 ± 0.9
Inversions (CTE2015/Jena CarboScope/MACC)*	−/−/−	−/−/−	−/0.3*/0.8*	−/1.1*/1.8*	−/1.6*/2.4*	2.0*/2.0*/3.3*	2.8*/2.6*/4.2*

<sup>a</sup>Note that the decadal uncertainty calculation for the DGVMS is smaller here compared to previous Global Carbon Budgets because it uses  $\pm 1\sigma$  of the decadal estimates for the DGVMS, compared to the average of the annual  $\pm 1\sigma$  estimates in previous years. It thus represents the true model range for their decadal estimates. This change was introduced to be consistent with the decadal uncertainty calculations in Table 8

\* Estimate are not corrected for the influence of river fluxes, which would reduce the fluxes by  $0.45 \text{ GtC yr}^{-1}$  when neglecting the anthropogenic influence on land (Section 7.2.2). CTE2015 refers to Peters et al. (2010), Jena CarboScope to Rödenbeck et al. (2014) and MACC to Chevallier et al. (2005); see Table 6.



**Table 8.** Decadal mean in the five components of the anthropogenic CO<sub>2</sub> budget for the periods 1960-1969, 1970-1979, 1980-1989, 1990-1999, 2000-2009, last decade and last year available. All values are in GtC yr<sup>-1</sup>. All uncertainties are reported as ±1σ. A data set containing data for each year during 1959-2014 is available on <http://cdiac.ornl.gov/GCP/carbonbudget/2015/>. Please follow the terms of use and cite the original data sources as specified on the data set.

	Mean (GtC yr <sup>-1</sup> )						
	1960-1969	1970-1979	1980-1989	1990-1999	2000-2009	2005-2014	2014
<i>Emissions</i>							
Fossil fuel combustion and cement production (E <sub>FF</sub> )	3.1 ± 0.2	4.7 ± 0.2	5.5 ± 0.3	6.4 ± 0.3	7.8 ± 0.4	9.0 ± 0.5	9.8 ± 0.5
Land-use change emissions (E <sub>LUC</sub> )	1.5 ± 0.5	1.3 ± 0.5	1.4 ± 0.5	1.6 ± 0.5	1.0 ± 0.5	0.9 ± 0.5	1.1 ± 0.5
<i>Partitioning</i>							
Atmospheric growth rate (G <sub>ATM</sub> )	1.7 ± 0.1	2.8 ± 0.1	3.4 ± 0.1	3.1 ± 0.1	4.0 ± 0.1	4.4 ± 0.1	3.9 ± 0.2
Ocean sink (S <sub>OCEAN</sub> )*	1.1 ± 0.5	1.5 ± 0.5	2.0 ± 0.5	2.2 ± 0.5	2.3 ± 0.5	2.6 ± 0.5	2.9 ± 0.5
Residual terrestrial sink (S <sub>LAND</sub> )	1.7 ± 0.7	1.7 ± 0.8	1.6 ± 0.8	2.6 ± 0.8	2.4 ± 0.8	3.0 ± 0.8	4.1 ± 0.9

\*The uncertainty in S<sub>OCEAN</sub> for the 1990s is directly based on observations, while that for other decades combines the uncertainty from observations with the model spread (Sect. 2.4.3).

**Table 9.** Actual CO<sub>2</sub> emissions from fossil fuel combustion and cement production ( $E_{FF}$ ) compared to projections made the previous year based on world GDP (IMF October 2015) and the fossil fuel intensity of GDP ( $I_{FF}$ ) based on subtracting the CO<sub>2</sub> and GDP growth rates. The 'Actual' values are the latest estimate available and the 'Projected' value for 2015 refers to those presented in this paper. A correction for leap years is applied (Section 2.1.3).

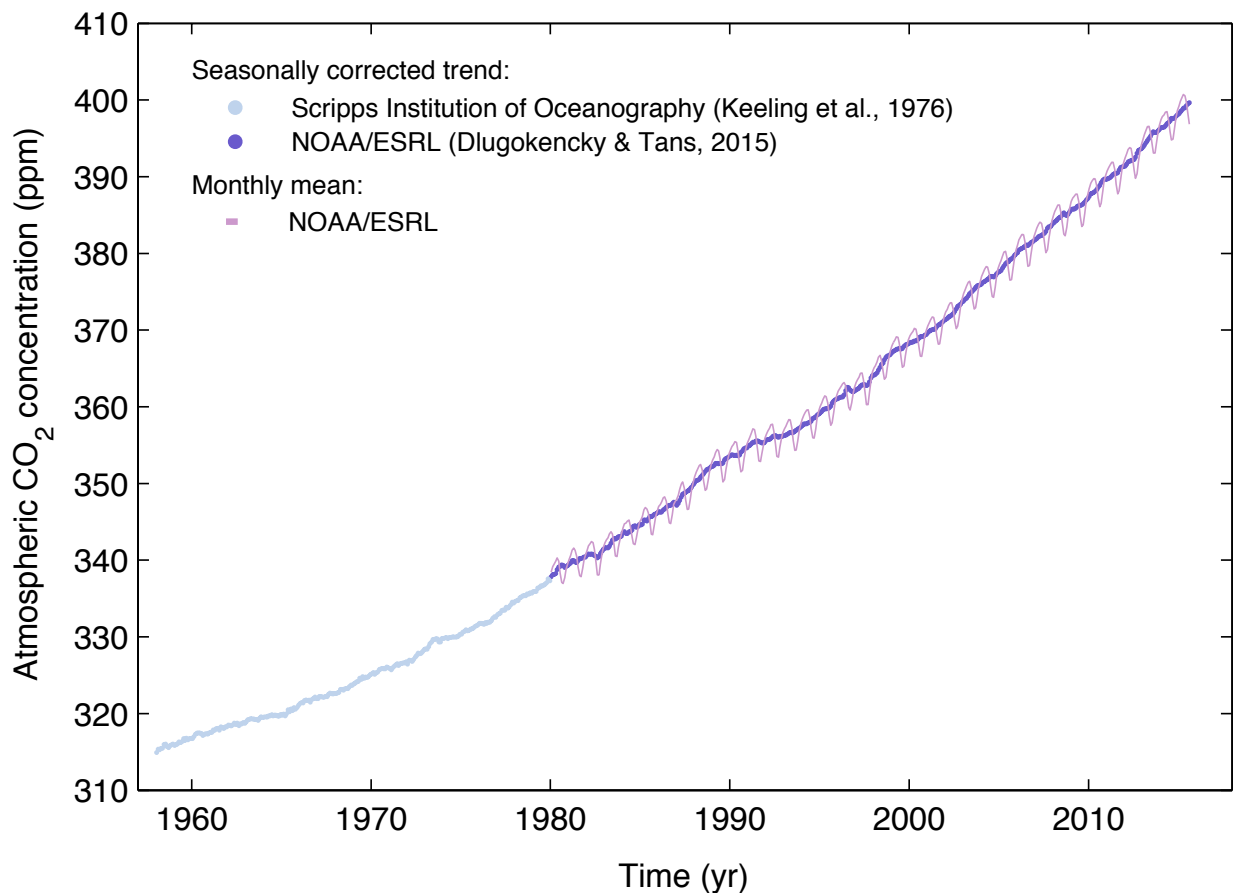
	$E_{FF}$		GDP		$I_{FF}$	
	Projected	Actual	Projected	Actual	Projected	Actual
2009 <sup>a</sup>	-2.8%	-0.5%	-1.1%	-0.4%	-1.7%	-0.9%
2010 <sup>b</sup>	>3%	4.9%	4.8%	5.2%	>-1.7%	-0.3%
2011 <sup>c</sup>	3.1±1.5%	3.2%	4.0%	3.9%	-0.9±1.5%	-0.7%
2012 <sup>d</sup>	2.6% (1.9 to 3.5)	2.2%	3.3%	3.2%	-0.7%	-1.0%
2013 <sup>e</sup>	2.1% (1.1 to 3.1)	2.3%	2.9%	3.2%	-0.8%	-0.9%
2014 <sup>f</sup>	2.5% (1.3 to 3.5)	0.6%	3.3%	3.4%	-0.7%	-2.8%
2015 <sup>g</sup>	-0.6% (-1.6 to 0.5)	--	3.1%	--	-3.7%	--

<sup>a</sup>Le Quéré et al. (2009). <sup>b</sup>Friedlingstein et al. (2010). <sup>c</sup>Peters et al. (2013). <sup>d</sup>Le Quéré et al. (2013). <sup>e</sup>Le Quéré et al. (2014). <sup>f</sup>Friedlingstein et al. (2014) and (Le Quéré et al., 2015). <sup>g</sup>This study.

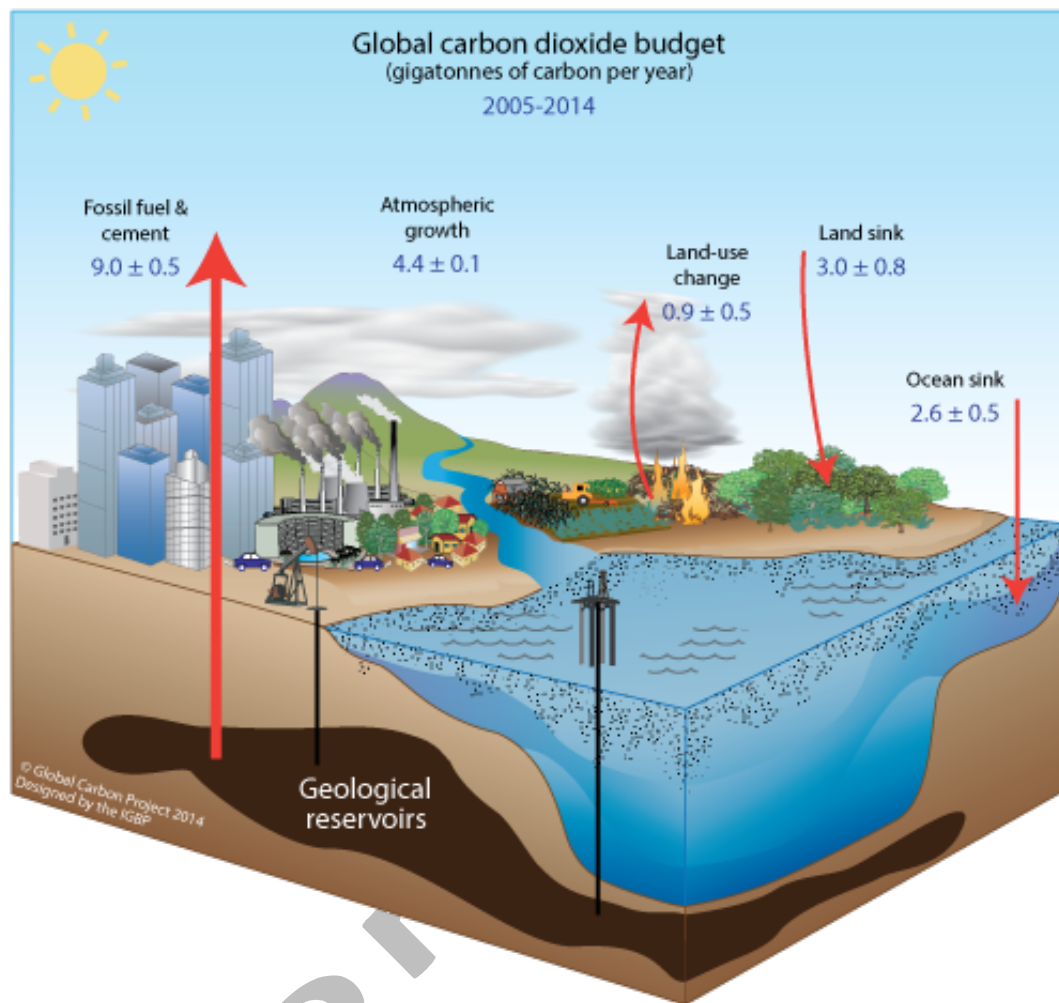
**Table 10.** Cumulative CO<sub>2</sub> emissions for the periods 1750-2014, 1870-2014 and 1870-2015 in gigatonnes of carbon (GtC). We also provide the 1850-2005 time-period used in a number of model evaluation publications. All uncertainties are reported as  $\pm 1\sigma$ . All values are rounded to nearest 5 GtC as in Stocker et al. (2013), reflecting the limits of our capacity to constrain cumulative estimates. Thus some columns will not exactly balance because of rounding errors.

Units of GtC	1750-2014	1850-2005	1870-2014	1870-2015
<i>Emissions</i>				
Fossil fuel combustion and cement production ( $E_{FF}$ )	405 $\pm$ 20	320 $\pm$ 15	400 $\pm$ 20	410 $\pm$ 20*
Land-use change emissions ( $E_{LUC}$ )	190 $\pm$ 65	150 $\pm$ 55	145 $\pm$ 50	145 $\pm$ 50*
Total emissions	590 $\pm$ 70	470 $\pm$ 55	545 $\pm$ 55	555 $\pm$ 55*
<i>Partitioning</i>				
Atmospheric growth rate ( $G_{ATM}$ )	255 $\pm$ 5	195 $\pm$ 5	230 $\pm$ 5	
Ocean sink ( $S_{OCEAN}$ )	170 $\pm$ 20	160 $\pm$ 20	155 $\pm$ 20	
Residual terrestrial sink ( $S_{LAND}$ )	165 $\pm$ 70	115 $\pm$ 60	160 $\pm$ 60	

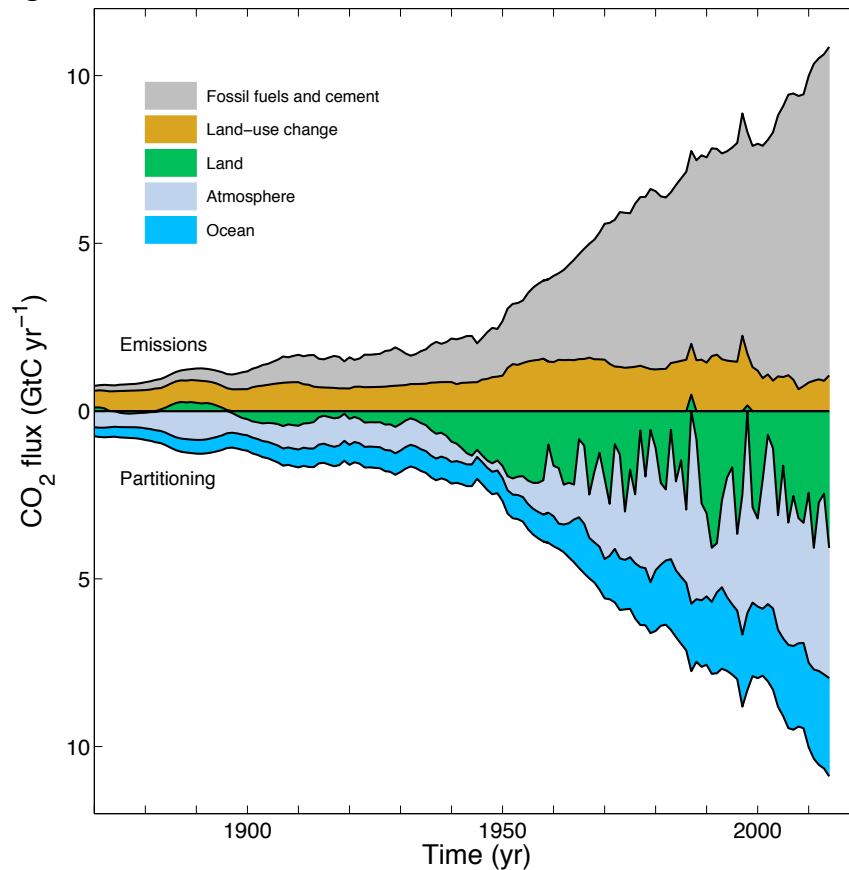
\* The extension to year 2015 uses the emissions projections for fossil fuel combustion and cement production for 2015 of 9.7 GtC (Sect. 3.2) and assumes a constant  $E_{LUC}$  flux (Sect. 2.2).

**Fig. 1**

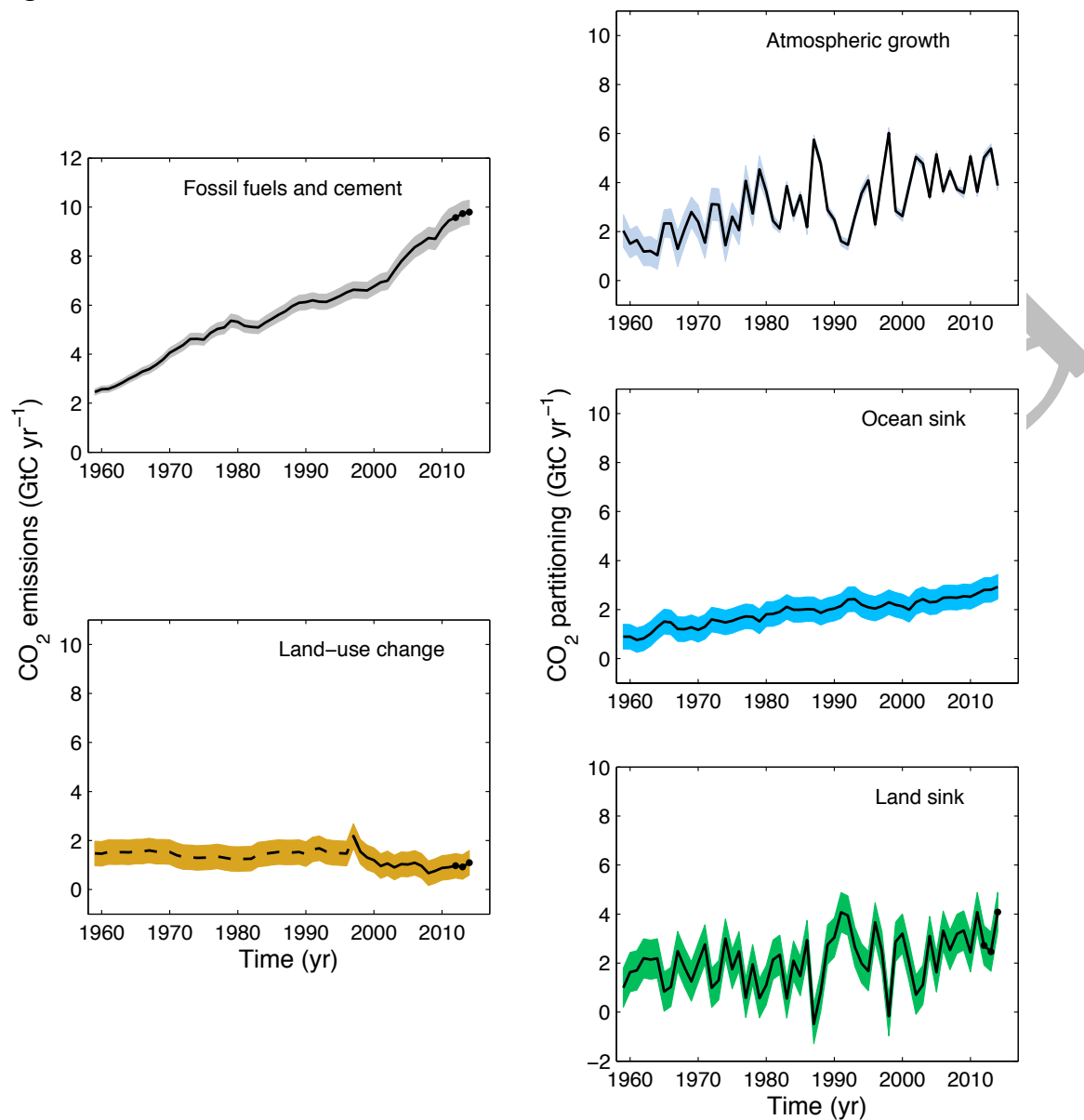
**Figure 1.** Surface average atmospheric CO<sub>2</sub> concentration, deseasonalised (ppm). The 1980-2015 monthly data are from NOAA/ESRL (Dlugokencky and Tans, 2015) and is based on an average of direct atmospheric CO<sub>2</sub> measurements from multiple stations in the marine boundary layer (Masarie and Tans, 1995). The 1958-1979 monthly data are from the Scripps Institution of Oceanography, based on an average of direct atmospheric CO<sub>2</sub> measurements from the Mauna Loa and South Pole stations (Keeling et al., 1976). To take into account the difference of mean CO<sub>2</sub> between the NOAA/ESRL and the Scripps station networks used here, the Scripps surface average (from two stations) was harmonised to match the NOAA/ESRL surface average (from multiple stations) by adding the mean difference of 0.542 ppm, calculated here from overlapping data during 1980-2012. The mean seasonal cycle is also shown from 1980.

1 **Fig. 2**

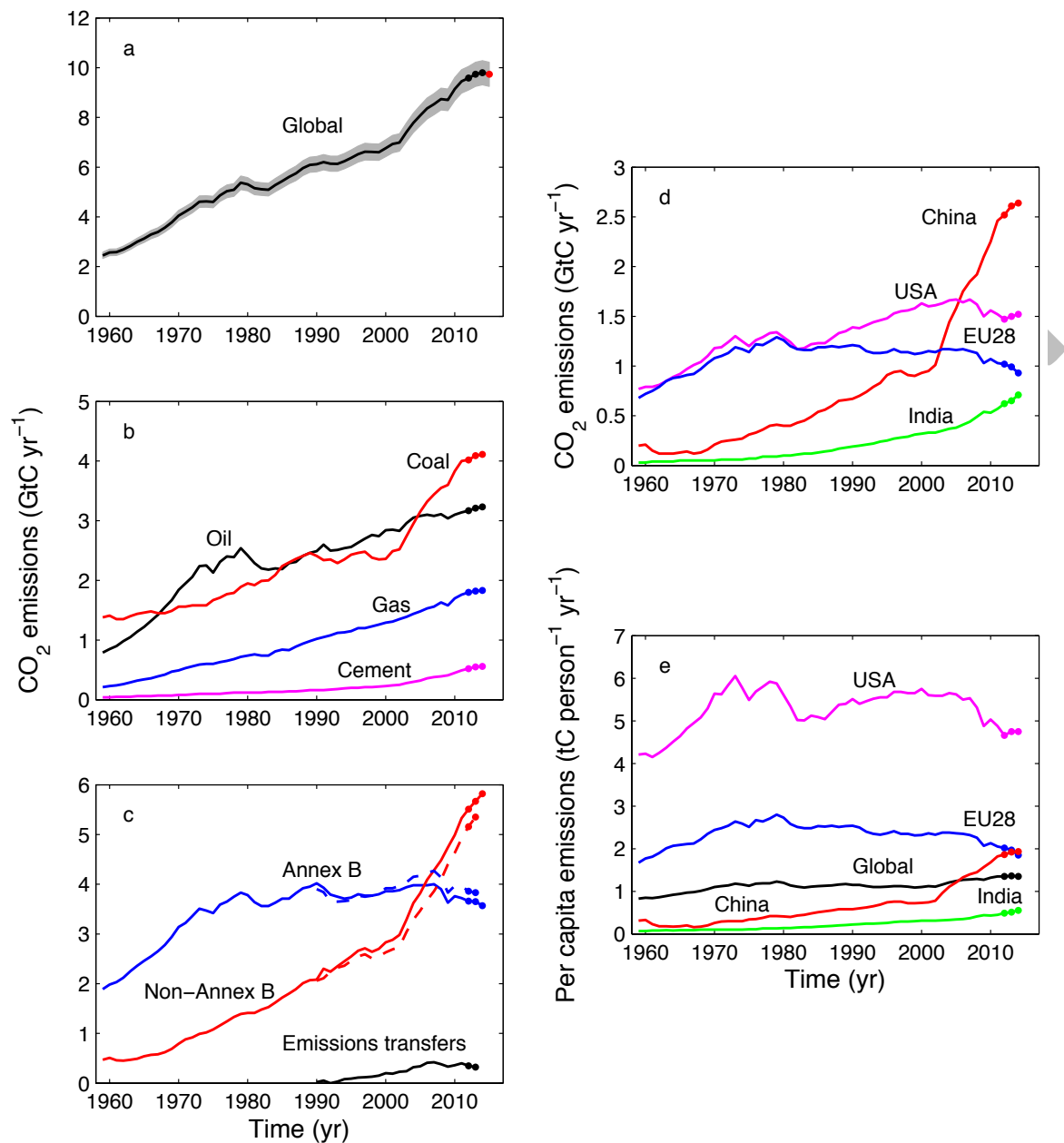
**Figure 2.** Schematic representation of the overall perturbation of the global carbon cycle caused by anthropogenic activities, averaged globally for the decade 2005-2014. The arrows represent emission from fossil fuel burning and cement production ( $E_{FF}$ ); emissions from deforestation and other land-use change ( $E_{LUC}$ ); the growth of carbon in the atmosphere ( $G_{ATM}$ ) and the uptake of carbon by the 'sinks' in the ocean ( $S_{OCEAN}$ ) and land ( $S_{LAND}$ ) reservoirs. All fluxes are in units of  $GtC\ yr^{-1}$ , with uncertainties reported as  $\pm 1\sigma$  (68% confidence that the real value lies within the given interval) as described in the text. This figure is an update of one prepared by the International Geosphere Biosphere Programme for the GCP, first presented in Le Quéré (2009).

1 **Fig. 3**

**Figure 3.** Combined components of the global carbon budget illustrated in Fig. 2 as a function of time, for emissions from fossil fuel combustion and cement production ( $E_{FF}$ ; grey) and emissions from land-use change ( $E_{LUC}$ ; brown), as well as their partitioning among the atmosphere ( $G_{ATM}$ ; light blue), land ( $S_{LAND}$ ; green) and oceans ( $S_{OCEAN}$ ; dark blue). All time-series are in  $\text{GtC yr}^{-1}$ .  $G_{ATM}$  and  $S_{OCEAN}$  (and by construction also  $S_{LAND}$ ) prior to 1959 are based on different methods. The primary data sources for fossil fuel and cement emissions are from Boden et al. (2013), with uncertainty of about  $\pm 5\%$  ( $\pm 1\sigma$ ); land-use change emissions are from Houghton et al. (2012) with uncertainties of about  $\pm 30\%$ ; atmospheric growth rate prior to 1959 is from Joos and Spahni (2008) with uncertainties of about  $\pm 1\text{--}1.5 \text{ GtC decade}^{-1}$  or  $\pm 0.1\text{--}0.15 \text{ GtC yr}^{-1}$  (Bruno and Joos, 1997), and from Dlugokencky and Tans (2015) from 1959 with uncertainties of about  $\pm 0.2 \text{ GtC yr}^{-1}$ ; the ocean sink prior to 1959 is from Khatiwala et al. (2013) with uncertainty of about  $\pm 30\%$ , and from this study from 1959 with uncertainties of about  $\pm 0.5 \text{ GtC yr}^{-1}$ ; and the residual land sink is obtained by difference (Eq. 8), resulting in uncertainties of about  $\pm 50\%$  prior to 1959 and  $\pm 0.8 \text{ GtC yr}^{-1}$  after that. See the text for more details of each component and their uncertainties.

1 **Fig. 4**

**Figure 4.** Components of the global carbon budget and their uncertainties as a function of time, presented individually for (a) emissions from fossil fuel combustion and cement production ( $E_{\text{FF}}$ ), (b) emissions from land-use change ( $E_{\text{LUC}}$ ), (c) atmospheric  $\text{CO}_2$  growth rate ( $G_{\text{ATM}}$ ), (d) the ocean  $\text{CO}_2$  sink ( $S_{\text{OCEAN}}$ , positive indicates a flux from the atmosphere to the ocean), and (e) the land  $\text{CO}_2$  sink ( $S_{\text{LAND}}$ , positive indicates a flux from the atmosphere to the land). All time-series are in  $\text{GtC yr}^{-1}$  with the uncertainty bounds representing  $\pm 1\sigma$  in shaded colour. Data sources are as in Fig. 3. The black dots in panels (a), (b) and (e) show values for 2012, 2013 and 2014, that originate from a different data set to the remainder of the data, as explained in the text.

1 **Fig. 5**

**Figure 5.** CO<sub>2</sub> emissions from fossil fuel combustion and cement production for (a) the globe, including an uncertainty of  $\pm 5\%$  (grey shading), the emissions extrapolated using BP energy statistics (black dots) and the emissions projection for year 2014 based on GDP projection (red dot), (b) global emissions by fuel type, including coal (red), oil (black), gas (blue), and cement (purple), and excluding gas flaring which is small (0.6% in 2013), (c) territorial (full line) and consumption (dashed line) emissions for the countries listed in the Annex B of the Kyoto Protocol (blue lines; mostly advanced economies with emissions limitations) versus non-Annex B countries (red lines), also shown are the emissions transfer from non-Annex B to Annex B countries (black line) (d) territorial CO<sub>2</sub> emissions for the top three country emitters (USA - purple; China - red;

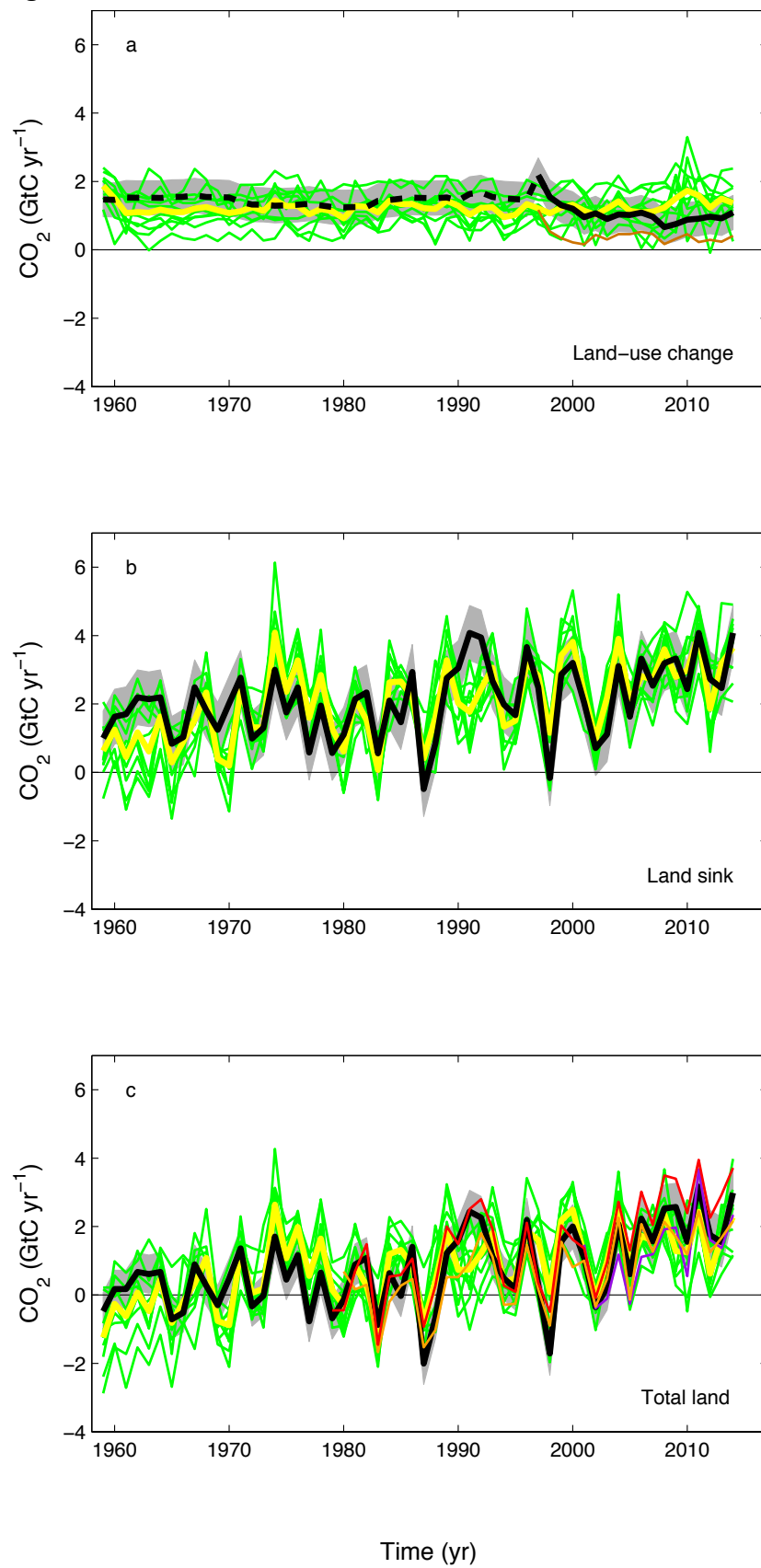


1 India - green) and for the European Union (EU; blue for the 28 member states of the EU in 2012),  
2 and (e) per-capita emissions for the top three country emitters and the EU (all colours as in panel  
3 (d)) and the world (black). In panels (b) to (e), the dots show the data that were extrapolated from  
4 BP energy statistics for 2012, 2013 and 2014. All time-series are in  $\text{GtC yr}^{-1}$  except the per-capita  
5 emissions (panel (e)), which are in tonnes of carbon per person per year ( $\text{tC person}^{-1} \text{ yr}^{-1}$ ). All  
6 territorial emissions are primarily from Boden et al. (2013) except national data for the USA and  
7 EU28 for 1990-2011, which are reported by the countries to the UNFCCC as detailed in the text;  
8 consumption-based emissions are updated from Peters et al. (2011a).

9  
10

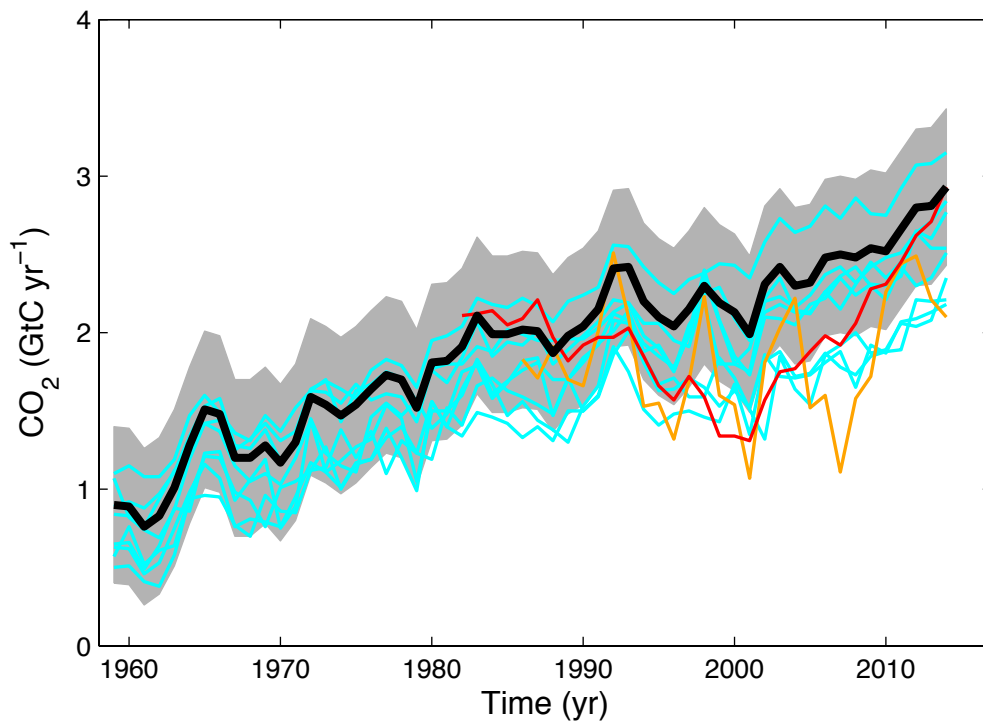
Submitted

1 **Fig. 6**



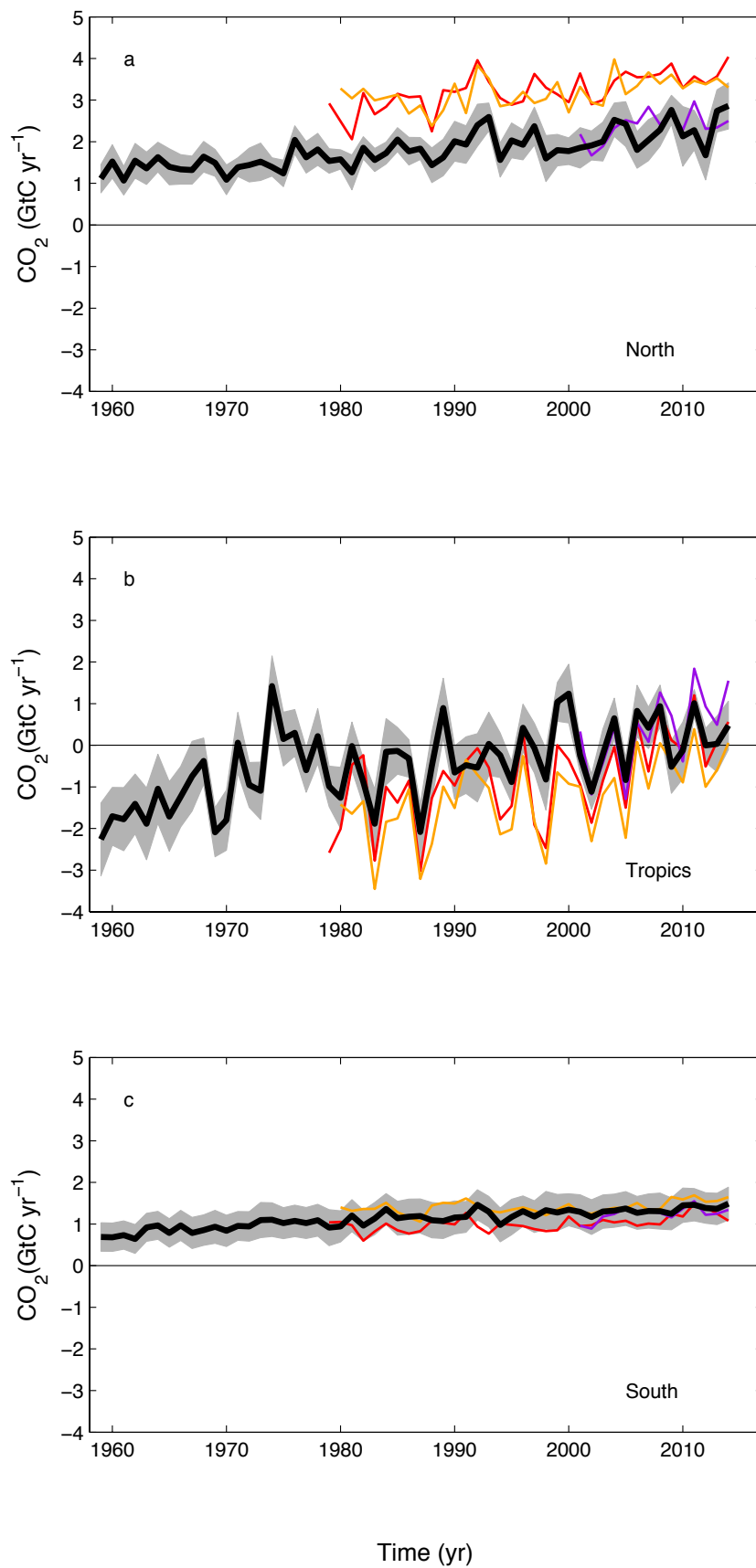
2

**Figure 6.** Comparison of the atmosphere-land CO<sub>2</sub> flux showing budget values of  $E_{LUC}$  (black). **(a)** CO<sub>2</sub> emissions from land-use change showing individual DGVM model results (green) and the multi model mean (yellow), and fire-based results (brown); land-use change data prior to 1997 (dashed black) highlights the start of satellite data from that year. **(b)** Land CO<sub>2</sub> sink ( $S_{LAND}$ ; black) showing individual DGVM model results (green) and multi model mean (yellow). **(c)** Total land CO<sub>2</sub> fluxes ( $b - a$ ) from DGVM model results (green) and the multi model mean (yellow), atmospheric inversions Chevallier et al. (2005; MACC, v14.2) in red; Rödenbeck et al. (2003; Jena CarboScope, s81\_v3.7) in orange; Peters et al. (2010; Carbon Tracker, vCTE2015) in purple; see Table 6, and the carbon balance from Eq. (1) (black). In **(c)** the inversions were corrected for the pre-industrial land sink of CO<sub>2</sub> from river input, by adding a sink of 0.45 GtC yr<sup>-1</sup> (Jacobson et al., 2007). This correction does not take into account the anthropogenic contribution to river fluxes (see Sect. 2.7.2).

**Fig. 7**

**Figure 7.** Comparison of the atmosphere-ocean  $\text{CO}_2$  flux shows the budget values of  $S_{\text{OCEAN}}$  (black), individual ocean models before normalisation (blue), and the two ocean data-based products (Rödenbeck et al. (2014) in orange and Landschützer et al. (2015) in red; see Table 6). Both data-based products were corrected for the pre-industrial ocean source of  $\text{CO}_2$  from river input to the ocean, which is not present in the models, by adding a sink of  $0.45 \text{ GtC yr}^{-1}$  (Jacobson et al., 2007), to make them comparable to  $S_{\text{OCEAN}}$ . This correction does not take into account the anthropogenic contribution to river fluxes (see Section 2.7.2).

1 **Fig. 8**



2  
3 **Figure 8.** Surface CO<sub>2</sub> flux ( $S_{\text{OCEAN}} + S_{\text{LAND}} + E_{\text{LUC}}$ ) by latitude bands for the (a) North (north of 30°N),  
4 (b) Tropics (30°S-30°N), and (c) South (south of 30°S). Estimates from the combination of the

1 multi-model means for the land and oceans are shown (black) with  $\pm 1\sigma$  of the model ensemble (in  
2 grey). Results from the three atmospheric inversions are shown Chevallier et al. (2005; MACC,  
3 v14.2) in red; Rödenbeck et al. (2003; Jena CarboScope, s81\_v3.7) in orange; Peters et al. (2010;  
4 Carbon Tracker, vCTE2015) in purple; see Table 6.

5

Submitted

Fig. 9

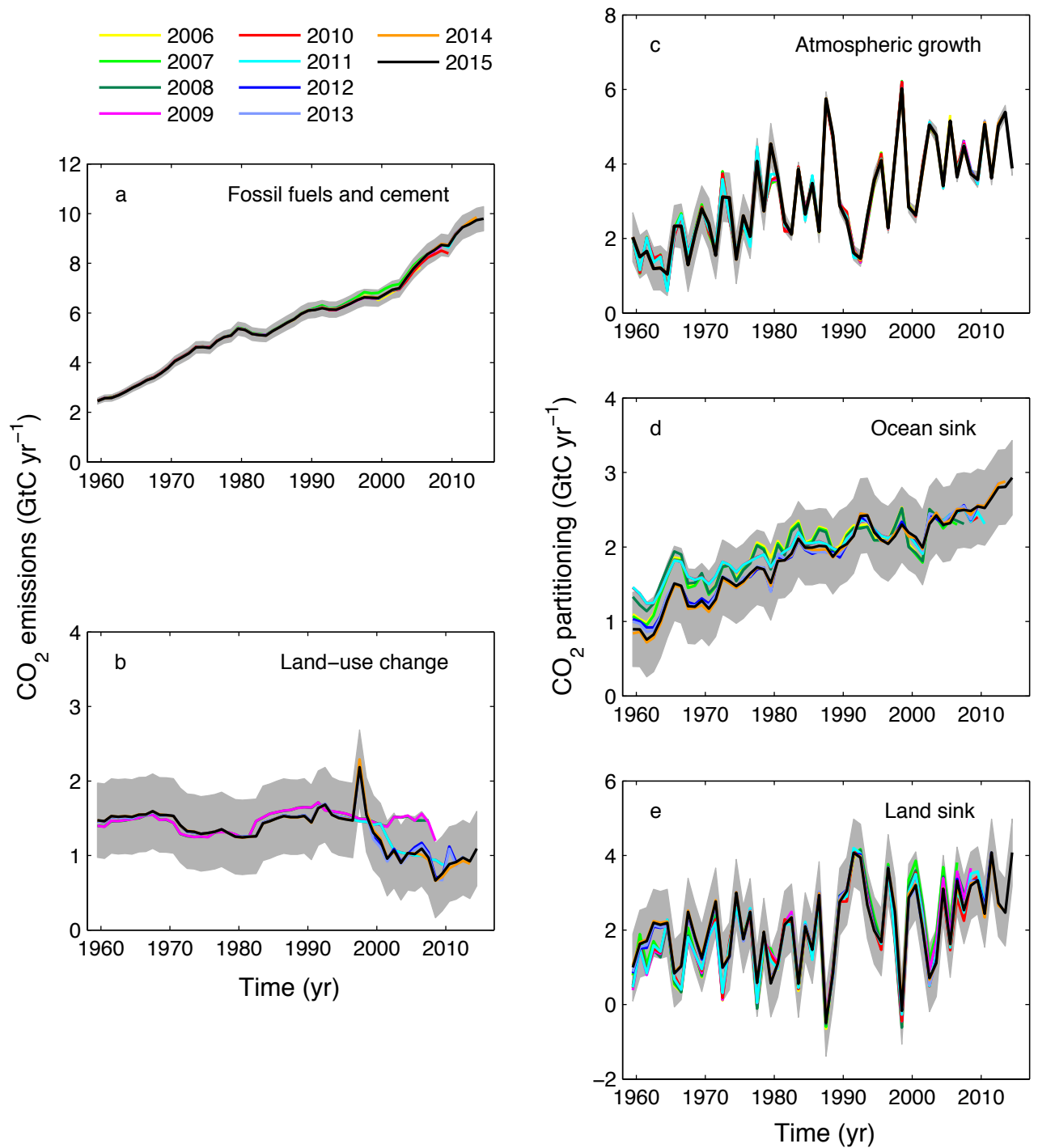


**Figure 9.** Comparison of global carbon budget components released annually by GCP since 2006. CO<sub>2</sub> emissions from both (a) fossil fuel combustion and cement production ( $E_{FF}$ ), and (b) land-use change ( $E_{LUC}$ ), and their partitioning among (c) the atmosphere ( $G_{ATM}$ ), (d) the ocean ( $S_{OCEAN}$ ), and (e) the land ( $S_{LAND}$ ). See legend for the corresponding years, with the 2006 carbon budget from Raupach et al.(2007); 2007 from Canadell et al. (2007); 2008 released online only; 2009 from Le

- 1 Quéré et al. (2009); 2010 from Friedlingstein et al. (2010); 2011 from Peters et al. (2012b); 2012
- 2 from Le Quéré et al. (2013); 2013 from Le Quéré et al. (2014), 2014 from Le Quéré et al. (2015)
- 3 and this year's budget (2015; this study). The budget year generally corresponds to the year when
- 4 the budget was first release. All values are in GtC yr<sup>-1</sup>.

Submitted



1 **Appendix Attribution of fCO<sub>2</sub> measurements for years 2013-2014 used in addition to SOCAT v3 (Bakker et al., 2014; Bakker et al., in prep.) to**  
2 **inform ocean data products.**

Vessel	Start date	End date	Regions	No. of samples	Principal Investigators	DOI (if available)/comment
Atlantic Companion	2014-02-21	2014-02-26	North Atlantic	2462	<u>Steinhoff, T., M. Becker and A. Körtzinger</u>	
Atlantic Companion	2014-04-26	2014-05-02	North Atlantic	3036	<u>Steinhoff, T., M. Becker and A. Körtzinger</u>	
Atlantic Companion	2014-05-31	2014-06-04	North Atlantic	2365	<u>Steinhoff, T., M. Becker and A. Körtzinger</u>	
Atlantic Companion	2014-06-16	2014-06-22	North Atlantic	6124	<u>Steinhoff, T., M. Becker and A. Körtzinger</u>	
Atlantic Companion	2014-08-27	2014-08-30	North Atlantic	3963	<u>Steinhoff, T., M. Becker and A. Körtzinger</u>	
Atlantic Companion	2014-09-28	2014-10-04	North Atlantic	7239	<u>Steinhoff, T., M. Becker and A. Körtzinger</u>	
Benguela Stream	2014-07-15	2014-07-20	North Atlantic	4523	<u>Schuster, U.</u>	
Benguela Stream	2013-12-28	2014-01-05	North Atlantic, Tropical Atlantic	6241	<u>Schuster, U.</u>	
Benguela Stream	2014-01-08	2014-01-13	North Atlantic, Tropical Atlantic	4400	<u>Schuster, U.</u>	
Benguela Stream	2014-02-23	2014-03-02	North Atlantic, Tropical Atlantic	6014	<u>Schuster, U.</u>	
Benguela Stream	2014-02-23	2014-03-02	North Atlantic, Tropical Atlantic	5612	<u>Schuster, U.</u>	
Benguela Stream	2014-04-18	2014-04-27	North Atlantic, Tropical Atlantic	7376	<u>Schuster, U.</u>	
Benguela Stream	2014-04-30	2014-05-08	North Atlantic, Tropical Atlantic	6819	<u>Schuster, U.</u>	
Benguela Stream	2014-05-17	2014-05-25	North Atlantic, Tropical Atlantic	6390	<u>Schuster, U.</u>	
Benguela Stream	2014-06-14	2014-06-21	North Atlantic, Tropical Atlantic	3397	<u>Schuster, U.</u>	
Benguela Stream	2014-06-25	2014-07-03	North Atlantic, Tropical Atlantic	6624	<u>Schuster, U.</u>	
Benguela Stream	2014-07-23	2014-07-31	North Atlantic, Tropical Atlantic	6952	<u>Schuster, U.</u>	
Benguela Stream	2014-11-12	2014-11-20	North Atlantic, Tropical Atlantic	5043	<u>Schuster, U.</u>	
Benguela Stream	2014-12-10	2014-12-19	North Atlantic, Tropical Atlantic	7046	<u>Schuster, U.</u>	
Benguela Stream	2014-12-10	2014-12-19	North Atlantic, Tropical Atlantic	7046	<u>Schuster, U.</u>	
Cap Blanche	2014-02-01	2014-02-13	Tropical Pacific, Southern Ocean	6148	<u>Feely, R., C. Cosca, S. Alin and G. Lebon</u>	
Cap Blanche	2014-03-27	2014-04-10	Tropical Pacific, Southern Ocean	6428	<u>Feely, R., C. Cosca, S. Alin and G. Lebon</u>	
Cap Blanche	2014-05-23	2014-06-05	Tropical Pacific, Southern Ocean	6016	<u>Feely, R., C. Cosca, S. Alin and G. Lebon</u>	
Cap Blanche	2014-07-18	2014-07-30	Tropical Pacific, Southern Ocean	5394	<u>Feely, R., C. Cosca, S. Alin and G. Lebon</u>	
Cap Blanche	2014-09-12	2014-09-25	Tropical Pacific, Southern Ocean	6083	<u>Feely, R., C. Cosca, S. Alin and G. Lebon</u>	
Cap Blanche	2014-11-13	2014-11-26	Tropical Pacific, Southern Ocean	5876	<u>Feely, R., C. Cosca, S. Alin and G. Lebon</u>	
Cap Vilano	2013-02-01	2013-02-13	Tropical Pacific, Southern Ocean	4709	<u>Cosca, C., R. Feely, S. Alin and G. Lebon</u>	

Cap Vilano	2013-03-28	2013-04-11	Tropical Pacific, Southern Ocean	5390	Cosca, C., <u>Reely, S.</u> , Alin and G. Lebon	10.3334/CDIAC/OTG.VOS_EXP2014
Cap Vilano	2013-05-24	2013-06-06	Tropical Pacific, Southern Ocean	5096	Cosca, C., <u>Reely, S.</u> , Alin and G. Lebon	10.3334/CDIAC/OTG.VOS_EXP2014
Colibri	2014-07-04	2014-07-15	North Atlantic, Tropical Atlantic	4853	<u>Lefèvre, N.</u> and D. Diverres	10.3334/CDIAC/OTG.VOS_EXP2014
Colibri	2014-08-27	2014-09-03	North Atlantic, Tropical Atlantic	3881	<u>Lefèvre, N.</u> and D. Diverres	10.3334/CDIAC/OTG.VOS_EXP2014
Colibri	2014-09-12	2014-09-23	North Atlantic, Tropical Atlantic	5940	<u>Lefèvre, N.</u> and D. Diverres	10.3334/CDIAC/OTG.VOS_EXP2014
Colibri	2014-10-25	2014-11-04	North Atlantic, Tropical Atlantic	5725	<u>Lefèvre, N.</u> and D. Diverres	10.3334/CDIAC/OTG.VOS_EXP2014
Colibri	2014-07-18	2014-07-19	Tropical Atlantic	313	<u>Lefèvre, N.</u> and D. Diverres	10.3334/CDIAC/OTG.VOS_EXP2014
Explorer of the Seas	2013-06-25	2013-06-27	North Atlantic	672	Wanninkhof, R., <u>D. Pierrot</u> and <u>L. Barbero</u>	10.3334/CDIAC/OTG.VOS_EXP2014
Explorer of the Seas	2013-07-06	2013-07-11	North Atlantic	1496	Wanninkhof, R., <u>D. Pierrot</u> and <u>L. Barbero</u>	10.3334/CDIAC/OTG.VOS_EXP2014
Explorer of the Seas	2013-07-20	2013-07-25	North Atlantic	4375	Wanninkhof, R., <u>D. Pierrot</u> and <u>L. Barbero</u>	10.3334/CDIAC/OTG.VOS_EXP2014
Explorer of the Seas	2013-08-03	2013-08-08	North Atlantic	1436	Wanninkhof, R., <u>D. Pierrot</u> and <u>L. Barbero</u>	10.3334/CDIAC/OTG.VOS_EXP2014
Explorer of the Seas	2013-08-17	2013-08-22	North Atlantic	1138	Wanninkhof, R., <u>D. Pierrot</u> and <u>L. Barbero</u>	10.3334/CDIAC/OTG.VOS_EXP2014
Explorer of the Seas	2014-04-08	2014-04-09	North Atlantic	209	Wanninkhof, R., <u>D. Pierrot</u> and <u>L. Barbero</u>	10.3334/CDIAC/OTG.VOS_EXP2014
Explorer of the Seas	2014-04-19	2014-04-24	North Atlantic	1424	Wanninkhof, R., <u>D. Pierrot</u> and <u>L. Barbero</u>	10.3334/CDIAC/OTG.VOS_EXP2014
Explorer of the Seas	2014-05-03	2014-05-08	North Atlantic	1512	Wanninkhof, R., <u>D. Pierrot</u> and <u>L. Barbero</u>	10.3334/CDIAC/OTG.VOS_EXP2014
Explorer of the Seas	2014-05-17	2014-05-22	North Atlantic	1349	Wanninkhof, R., <u>D. Pierrot</u> and <u>L. Barbero</u>	10.3334/CDIAC/OTG.VOS_EXP2014
Explorer of the Seas	2014-05-31	2014-06-05	North Atlantic	1194	Wanninkhof, R., <u>D. Pierrot</u> and <u>L. Barbero</u>	10.3334/CDIAC/OTG.VOS_EXP2014
Explorer of the Seas	2014-06-14	2014-06-19	North Atlantic	1142	Wanninkhof, R., <u>D. Pierrot</u> and <u>L. Barbero</u>	10.3334/CDIAC/OTG.VOS_EXP2014
Explorer of the Seas	2014-06-28	2014-07-03	North Atlantic	1479	Wanninkhof, R., <u>D. Pierrot</u> and <u>L. Barbero</u>	10.3334/CDIAC/OTG.VOS_EXP2014
Explorer of the Seas	2014-07-12	2014-07-17	North Atlantic	1489	Wanninkhof, R., <u>D. Pierrot</u> and <u>L. Barbero</u>	10.3334/CDIAC/OTG.VOS_EXP2014
Explorer of the Seas	2014-07-26	2014-07-31	North Atlantic	1474	Wanninkhof, R., <u>D. Pierrot</u> and <u>L. Barbero</u>	10.3334/CDIAC/OTG.VOS_EXP2014
Explorer of the Seas	2014-08-09	2014-08-14	North Atlantic	1468	Wanninkhof, R., <u>D. Pierrot</u> and <u>L. Barbero</u>	10.3334/CDIAC/OTG.VOS_EXP2014
Explorer of the Seas	2014-08-23	2014-08-28	North Atlantic	1277	Wanninkhof, R., <u>D. Pierrot</u> and <u>L. Barbero</u>	10.3334/CDIAC/OTG.VOS_EXP2014
Explorer of the Seas	2014-08-29	2014-09-06	North Atlantic	2846	Wanninkhof, R., <u>D. Pierrot</u> and <u>L. Barbero</u>	10.3334/CDIAC/OTG.VOS_EXP2014
Explorer of the Seas	2014-09-06	2014-09-11	North Atlantic	1479	Wanninkhof, R., <u>D. Pierrot</u> and <u>L. Barbero</u>	10.3334/CDIAC/OTG.VOS_EXP2014
Explorer of the Seas	2014-09-11	2014-09-20	North Atlantic	2956	Wanninkhof, R., <u>D. Pierrot</u> and <u>L. Barbero</u>	10.3334/CDIAC/OTG.VOS_EXP2014
Explorer of the Seas	2014-09-20	2014-09-22	North Atlantic	728	Wanninkhof, R., <u>D. Pierrot</u> and <u>L. Barbero</u>	10.3334/CDIAC/OTG.VOS_EXP2014
Explorer of the Seas	2014-10-04	2014-10-09	North Atlantic	1444	Wanninkhof, R., <u>D. Pierrot</u> and <u>L. Barbero</u>	10.3334/CDIAC/OTG.VOS_EXP2014
Explorer of the Seas	2014-10-18	2014-10-23	North Atlantic	1504	Wanninkhof, R., <u>D. Pierrot</u> and <u>L. Barbero</u>	10.3334/CDIAC/OTG.VOS_EXP2014
Explorer of the Seas	2013-04-02	2013-04-07	North Atlantic, Tropical Atlantic	1301	Wanninkhof, R., <u>D. Pierrot</u> and <u>L. Barbero</u>	10.3334/CDIAC/OTG.VOS_EXP2014
Explorer of the Seas	2013-06-27	2013-07-06	North Atlantic, Tropical Atlantic	3329	Wanninkhof, R., <u>D. Pierrot</u> and <u>L. Barbero</u>	10.3334/CDIAC/OTG.VOS_EXP2014

Explorer of the Seas	2013-07-11	2013-07-20	North Atlantic, Tropical Atlantic	3372	Wanninkhof, R., <u>D. Pierrot</u> and <u>L. Barbero</u>	10.3334/CDIAC/OTG_VOS_EXP2014
Explorer of the Seas	2013-07-25	2013-08-03	North Atlantic, Tropical Atlantic	3350	Wanninkhof, R., <u>D. Pierrot</u> and <u>L. Barbero</u>	10.3334/CDIAC/OTG_VOS_EXP2014
Explorer of the Seas	2013-08-08	2013-08-17	North Atlantic, Tropical Atlantic	3393	Wanninkhof, R., <u>D. Pierrot</u> and <u>L. Barbero</u>	10.3334/CDIAC/OTG_VOS_EXP2014
Explorer of the Seas	2014-04-01	2014-04-05	North Atlantic, Tropical Atlantic	1189	Wanninkhof, R., <u>D. Pierrot</u> and <u>L. Barbero</u>	10.3334/CDIAC/OTG_VOS_EXP2014
Explorer of the Seas	2014-04-10	2014-04-19	North Atlantic, Tropical Atlantic	3297	Wanninkhof, R., <u>D. Pierrot</u> and <u>L. Barbero</u>	10.3334/CDIAC/OTG_VOS_EXP2014
Explorer of the Seas	2014-04-24	2014-05-03	North Atlantic, Tropical Atlantic	2968	Wanninkhof, R., <u>D. Pierrot</u> and <u>L. Barbero</u>	10.3334/CDIAC/OTG_VOS_EXP2014
Explorer of the Seas	2014-05-08	2014-05-17	North Atlantic, Tropical Atlantic	3324	Wanninkhof, R., <u>D. Pierrot</u> and <u>L. Barbero</u>	10.3334/CDIAC/OTG_VOS_EXP2014
Explorer of the Seas	2014-05-22	2014-05-31	North Atlantic, Tropical Atlantic	2850	Wanninkhof, R., <u>D. Pierrot</u> and <u>L. Barbero</u>	10.3334/CDIAC/OTG_VOS_EXP2014
Explorer of the Seas	2014-06-05	2014-06-14	North Atlantic, Tropical Atlantic	3374	Wanninkhof, R., <u>D. Pierrot</u> and <u>L. Barbero</u>	10.3334/CDIAC/OTG_VOS_EXP2014
Explorer of the Seas	2014-06-19	2014-06-28	North Atlantic, Tropical Atlantic	3386	Wanninkhof, R., <u>D. Pierrot</u> and <u>L. Barbero</u>	10.3334/CDIAC/OTG_VOS_EXP2014
Explorer of the Seas	2014-07-03	2014-07-12	North Atlantic, Tropical Atlantic	3397	Wanninkhof, R., <u>D. Pierrot</u> and <u>L. Barbero</u>	10.3334/CDIAC/OTG_VOS_EXP2014
Explorer of the Seas	2014-07-17	2014-07-26	North Atlantic, Tropical Atlantic	3404	Wanninkhof, R., <u>D. Pierrot</u> and <u>L. Barbero</u>	10.3334/CDIAC/OTG_VOS_EXP2014
Explorer of the Seas	2014-07-31	2014-08-09	North Atlantic, Tropical Atlantic	3392	Wanninkhof, R., <u>D. Pierrot</u> and <u>L. Barbero</u>	10.3334/CDIAC/OTG_VOS_EXP2014
Explorer of the Seas	2014-08-14	2014-08-23	North Atlantic, Tropical Atlantic	3307	Wanninkhof, R., <u>D. Pierrot</u> and <u>L. Barbero</u>	10.3334/CDIAC/OTG_VOS_EXP2014
Explorer of the Seas	2014-09-25	2014-10-04	North Atlantic, Tropical Atlantic	2967	Wanninkhof, R., <u>D. Pierrot</u> and <u>L. Barbero</u>	10.3334/CDIAC/OTG_VOS_EXP2014
Explorer of the Seas	2014-10-09	2014-10-18	North Atlantic, Tropical Atlantic	3069	Wanninkhof, R., <u>D. Pierrot</u> and <u>L. Barbero</u>	10.3334/CDIAC/OTG_VOS_EXP2014
Explorer of the Seas	2014-10-23	2014-11-01	North Atlantic, Tropical Atlantic	3074	Wanninkhof, R., <u>D. Pierrot</u> and <u>L. Barbero</u>	10.3334/CDIAC/OTG_VOS_EXP2014
Explorer of the Seas	2014-11-01	2014-11-11	North Atlantic, Tropical Atlantic	1809	Wanninkhof, R., <u>D. Pierrot</u> and <u>L. Barbero</u>	10.3334/CDIAC/OTG_VOS_EXP2014
Explorer of the Seas	2014-11-21	2014-11-24	North Atlantic, Tropical Atlantic	567	Wanninkhof, R., <u>D. Pierrot</u> and <u>L. Barbero</u>	10.3334/CDIAC/OTG_VOS_EXP2014
Explorer of the Seas	2014-12-04	2014-12-13	North Atlantic, Tropical Atlantic	3773	Wanninkhof, R., <u>D. Pierrot</u> and <u>L. Barbero</u>	10.3334/CDIAC/OTG_VOS_EXP2014
Explorer of the Seas	2014-12-23	2014-12-27	North Atlantic, Tropical Atlantic	1516	Wanninkhof, R., <u>D. Pierrot</u> and <u>L. Barbero</u>	10.3334/CDIAC/OTG_VOS_EXP2014
Explorer of the Seas	2014-12-27	2015-01-04	North Atlantic, Tropical Atlantic	1315	Wanninkhof, R., <u>D. Pierrot</u> and <u>L. Barbero</u>	10.3334/CDIAC/OTG_VOS_EXP2014
Explorer of the Seas	2014-11-25	2014-11-29	Tropical Atlantic	1653	Wanninkhof, R., <u>D. Pierrot</u> and <u>L. Barbero</u>	10.3334/CDIAC/OTG_VOS_EXP2014
Explorer of the Seas	2014-11-29	2014-12-04	Tropical Atlantic	1680	Wanninkhof, R., <u>D. Pierrot</u> and <u>L. Barbero</u>	10.3334/CDIAC/OTG_VOS_EXP2014
Explorer of the Seas	2014-12-14	2014-12-18	Tropical Atlantic	899	Wanninkhof, R., <u>D. Pierrot</u> and <u>L. Barbero</u>	10.3334/CDIAC/OTG_VOS_EXP2014
Explorer of the Seas	2014-12-18	2014-12-23	Tropical Atlantic	1787	Wanninkhof, R., <u>D. Pierrot</u> and <u>L. Barbero</u>	10.3334/CDIAC/OTG_VOS_EXP2014
Finnaid	2012-01-13	2014-12-31	North Atlantic	22000	<u>Glockzin, M.</u>	
G.O. Sais	2014-07-08	2014-11-16	Arctic, North Atlantic	24405	<u>Lausset, S.K.</u> and <u>I. Skjelan</u>	
Gordon Gunter	2014-02-20	2014-02-26	North Atlantic	22000	Wanninkhof, R., <u>D. Pierrot</u> and <u>L. Barbero</u>	10.3334/CDIAC/OTG_AOML_BIGELOW_ECOAST_2014
Gordon Gunter	2014-03-01	2014-03-09	North Atlantic	3742	Wanninkhof, R., <u>D. Pierrot</u> and <u>L. Barbero</u>	10.3334/CDIAC/OTG_AOML_BIGELOW_ECOAST_2014
Gordon Gunter	2014-03-11	2014-04-03	North Atlantic	8189	Wanninkhof, R., <u>D. Pierrot</u> and <u>L. Barbero</u>	10.3334/CDIAC/OTG_AOML_BIGELOW_ECOAST_2014

Gordon Gunter	2014-04-08	2014-04-28	North Atlantic	7753	Wanninkhof, R., D. Pierrot and L. Barbero	10.3334/CDIAC/OTG.AOML_BIGELOW_ECOAST_2014
Gordon Gunter	2014-06-06	2014-06-13	North Atlantic, Tropical Atlantic	3338	Wanninkhof, R., D. Pierrot and L. Barbero	10.3334/CDIAC/OTG.AOML_BIGELOW_ECOAST_2014
Gordon Gunter	2014-07-04	2014-07-16	Tropical Atlantic	5399	Wanninkhof, R., D. Pierrot and L. Barbero	10.3334/CDIAC/OTG.AOML_BIGELOW_ECOAST_2014
Gordon Gunter	2014-07-21	2014-07-30	Tropical Atlantic	4074	Wanninkhof, R., D. Pierrot and L. Barbero	10.3334/CDIAC/OTG.AOML_BIGELOW_ECOAST_2014
Henry B. Bigelow	2014-03-29	2014-04-04	North Atlantic	2196	Wanninkhof, R., D. Pierrot and L. Barbero	10.3334/CDIAC/OTG.AOML_BIGELOW_ECOAST_2014
Henry B. Bigelow	2014-04-11	2014-04-25	North Atlantic	6651	Wanninkhof, R., D. Pierrot and L. Barbero	10.3334/CDIAC/OTG.AOML_BIGELOW_ECOAST_2014
Henry B. Bigelow	2014-05-06	2014-05-16	North Atlantic	4302	Wanninkhof, R., D. Pierrot and L. Barbero	10.3334/CDIAC/OTG.AOML_BIGELOW_ECOAST_2014
Henry B. Bigelow	2014-05-16	2014-05-23	North Atlantic	3233	Wanninkhof, R., D. Pierrot and L. Barbero	10.3334/CDIAC/OTG.AOML_BIGELOW_ECOAST_2014
Henry B. Bigelow	2014-05-27	2014-06-01	North Atlantic	2085	Wanninkhof, R., D. Pierrot and L. Barbero	10.3334/CDIAC/OTG.AOML_BIGELOW_ECOAST_2014
Henry B. Bigelow	2014-06-18	2014-07-01	North Atlantic	5458	Wanninkhof, R., D. Pierrot and L. Barbero	10.3334/CDIAC/OTG.AOML_BIGELOW_ECOAST_2014
Henry B. Bigelow	2014-07-25	2014-07-30	North Atlantic	2226	Wanninkhof, R., D. Pierrot and L. Barbero	10.3334/CDIAC/OTG.AOML_BIGELOW_ECOAST_2014
Henry B. Bigelow	2014-08-05	2014-08-16	North Atlantic	5231	Wanninkhof, R., D. Pierrot and L. Barbero	10.3334/CDIAC/OTG.AOML_BIGELOW_ECOAST_2014
Henry B. Bigelow	2014-09-08	2014-09-19	North Atlantic	4847	Wanninkhof, R., D. Pierrot and L. Barbero	10.3334/CDIAC/OTG.AOML_BIGELOW_ECOAST_2014
Henry B. Bigelow	2014-09-23	2014-10-03	North Atlantic	4620	Wanninkhof, R., D. Pierrot and L. Barbero	10.3334/CDIAC/OTG.AOML_BIGELOW_ECOAST_2014
Henry B. Bigelow	2014-10-07	2014-10-23	North Atlantic	7736	Wanninkhof, R., D. Pierrot and L. Barbero	10.3334/CDIAC/OTG.AOML_BIGELOW_ECOAST_2014
Henry B. Bigelow	2014-10-28	2014-11-13	North Atlantic	6615	Wanninkhof, R., D. Pierrot and L. Barbero	10.3334/CDIAC/OTG.AOML_BIGELOW_ECOAST_2014
James Clark Ross	2014-03-20	2014-04-12	North Atlantic	2113	Kittidis, V. and I. Brown	
Laurence M. Gould	2012-12-31	2013-02-06	Southern Ocean	10816	Sweeney, C., T. Takahashi, T. Newberger and D.R. Munro	accessed from CDIAC on 08/06/2015
Laurence M. Gould	2013-02-13	2013-02-24	Southern Ocean	2030	Sweeney, C., T. Takahashi, T. Newberger and D.R. Munro	accessed from CDIAC on 08/06/2015
Laurence M. Gould	2013-03-11	2013-04-07	Southern Ocean	4110	Sweeney, C., T. Takahashi, T. Newberger and D.R. Munro	accessed from CDIAC on 08/06/2015
Laurence M. Gould	2013-04-13	2013-05-05	Southern Ocean	4099	Sweeney, C., T. Takahashi, T. Newberger and D.R. Munro	accessed from CDIAC on 08/06/2015
Laurence M. Gould	2013-05-12	2013-05-24	Southern Ocean	3171	Sweeney, C., T. Takahashi, T. Newberger and D.R. Munro	accessed from CDIAC on 08/06/2015
Laurence M. Gould	2013-06-01	2013-07-05	Southern Ocean	3808	Sweeney, C., T. Takahashi, T. Newberger and D.R. Munro	accessed from CDIAC on 08/06/2015
Laurence M. Gould	2013-09-14	2013-09-26	Southern Ocean	3410	Sweeney, C., T. Takahashi, T. Newberger and D.R. Munro	accessed from CDIAC on 08/06/2015
Laurence M. Gould	2013-10-05	2013-10-22	Southern Ocean	2284	Sweeney, C., T. Takahashi, T. Newberger and D.R. Munro	accessed from CDIAC on 08/06/2015
Laurence M. Gould	2013-10-28	2013-11-15	Southern Ocean	3788	Sweeney, C., T. Takahashi, T. Newberger and D.R. Munro	accessed from CDIAC on 08/06/2015
Laurence M. Gould	2013-11-23	2013-12-19	Southern Ocean	7535	Sweeney, C., T. Takahashi, T. Newberger and D.R. Munro	accessed from CDIAC on 08/06/2015
Laurence M. Gould	2014-01-01	2014-02-07	Southern Ocean	11783	Sweeney, C., T. Takahashi, T. Newberger and D.R. Munro	
Laurence M. Gould	2014-02-14	2014-03-16	Southern Ocean	5805	Sweeney, C., T. Takahashi, T. Newberger and D.R. Munro	
Laurence M. Gould	2014-03-22	2014-04-03	Southern Ocean	1109	Sweeney, C., T. Takahashi, T. Newberger and D.R. Munro	
Laurence M. Gould	2014-04-09	2014-05-10	Southern Ocean	3170	Sweeney, C., T. Takahashi, T. Newberger and D.R. Munro	

Laurence M. Gould	2014-06-23	2014-08-21	Southern Ocean	3615	<u>Sweeney, C., T. Takahashi, T. Newberger and D.R. Munro</u>	10.3334/CDIAC/OTG.TSM_NH_70W_43N
Laurence M. Gould	2014-09-14	2014-09-26	Southern Ocean	2058	<u>Sweeney, C., T. Takahashi, T. Newberger and D.R. Munro</u>	10.3334/CDIAC/otg.TSM_LatPac_125W_48N
Laurence M. Gould	2014-10-08	2014-10-20	Southern Ocean	1642	<u>Sweeney, C., T. Takahashi, T. Newberger and D.R. Munro</u>	
Laurence M. Gould	2014-10-28	2014-11-22	Southern Ocean	6921	<u>Sweeney, C., T. Takahashi, T. Newberger and D.R. Munro</u>	
Laurence M. Gould	2014-11-28	2014-12-20	Southern Ocean	6476	<u>Sweeney, C., T. Takahashi, T. Newberger and D.R. Munro</u>	
Marion Dufresne	2014-01-09	2014-02-16	Indian Ocean, Southern Ocean	7524	<u>Meizl, N. and C. Lo Monaco</u>	
Mitai	2012-11-28	2013-02-13	Southern Ocean	4832	<u>Murata, A.</u>	
Mooring	2012-08-22	2013-07-09	North Atlantic	1507	<u>Sutton, A.</u>	
Mooring	2013-10-04	2014-04-29	North Pacific	1651	<u>Sutton, A.</u>	
Mooring	2012-11-02	2013-06-06	Tropical Pacific	4257	<u>Sutton, A.</u>	
Mooring	2013-06-06	2013-11-28	Tropical Pacific	1415	<u>Sutton, A.</u>	
New Century 2	2014-08-11	2014-09-08	North Atlantic, Tropical Atlantic, North Pacific, Tropical Pacific	2698	<u>Nakaoka, S.</u>	
New Century 2	2014-12-12	2015-01-12	North Atlantic, Tropical Atlantic, North Pacific, Tropical Pacific	1811	<u>Nakaoka, S.</u>	
New Century 2	2014-04-11	2014-04-26	North Pacific	1608	<u>Nakaoka, S.</u>	
New Century 2	2014-04-27	2014-05-10	North Pacific	1442	<u>Nakaoka, S.</u>	
New Century 2	2014-05-13	2014-05-27	North Pacific	1408	<u>Nakaoka, S.</u>	
New Century 2	2014-05-28	2014-06-09	North Pacific	1392	<u>Nakaoka, S.</u>	
New Century 2	2014-06-12	2014-06-25	North Pacific	1220	<u>Nakaoka, S.</u>	
New Century 2	2014-06-25	2014-07-05	North Pacific	1174	<u>Nakaoka, S.</u>	
New Century 2	2014-09-10	2014-09-24	North Pacific	1108	<u>Nakaoka, S.</u>	
New Century 2	2014-09-25	2014-10-07	North Pacific	1004	<u>Nakaoka, S.</u>	
New Century 2	2014-10-11	2014-10-27	North Pacific	1001	<u>Nakaoka, S.</u>	
New Century 2	2014-10-28	2014-11-09	North Pacific	1174	<u>Nakaoka, S.</u>	
New Century 2	2014-07-14	2014-08-10	North Pacific, Tropical Pacific	2167	<u>Nakaoka, S.</u>	
New Century 2	2014-11-14	2014-12-12	North Pacific, Tropical Pacific	2391	<u>Nakaoka, S.</u>	
Nuka Arctica	2014-07-07	2014-07-15	Arctic, North Atlantic	2333	<u>Onar, A., A. Olsen and T. Johannessen</u>	
Nuka Arctica	2014-08-27	2014-09-05	Arctic, North Atlantic	2607	<u>Onar, A., A. Olsen and T. Johannessen</u>	
Nuka Arctica	2014-09-08	2014-09-18	Arctic, North Atlantic	2398	<u>Onar, A., A. Olsen and T. Johannessen</u>	
Nuka Arctica	2014-01-06	2014-01-12	Arctic, North Atlantic	2369	<u>Onar, A., A. Olsen and T. Johannessen</u>	
Nuka Arctica	2014-01-14	2014-01-24	Arctic, North Atlantic	2728	<u>Onar, A., A. Olsen and T. Johannessen</u>	
Nuka Arctica	2014-01-24	2014-02-01	Arctic, North Atlantic	1990	<u>Onar, A., A. Olsen and T. Johannessen</u>	

Nuka Arctica	2014-02-04	2014-02-14	Arctic, North Atlantic	2661	<u>Onar, A., A. Olsen and T. Johannessen</u>
Nuka Arctica	2014-02-15	2014-02-22	Arctic, North Atlantic	2030	<u>Onar, A., A. Olsen and T. Johannessen</u>
Nuka Arctica	2014-02-26	2014-03-05	Arctic, North Atlantic	2179	<u>Onar, A., A. Olsen and T. Johannessen</u>
Nuka Arctica	2014-03-07	2014-03-13	Arctic, North Atlantic	2311	<u>Onar, A., A. Olsen and T. Johannessen</u>
Nuka Arctica	2014-03-18	2014-03-27	Arctic, North Atlantic	3262	<u>Onar, A., A. Olsen and T. Johannessen</u>
Nuka Arctica	2014-03-29	2014-04-05	Arctic, North Atlantic	2799	<u>Onar, A., A. Olsen and T. Johannessen</u>
Nuka Arctica	2014-04-09	2014-04-17	Arctic, North Atlantic	3136	<u>Onar, A., A. Olsen and T. Johannessen</u>
Nuka Arctica	2014-04-18	2014-04-25	Arctic, North Atlantic	2429	<u>Onar, A., A. Olsen and T. Johannessen</u>
Nuka Arctica	2014-05-13	2014-05-18	Arctic, North Atlantic	1420	<u>Onar, A., A. Olsen and T. Johannessen</u>
Nuka Arctica	2014-05-23	2014-05-31	Arctic, North Atlantic	1191	<u>Onar, A., A. Olsen and T. Johannessen</u>
Nuka Arctica	2014-06-11	2014-06-12	Arctic, North Atlantic	274	<u>Onar, A., A. Olsen and T. Johannessen</u>
Nuka Arctica	2014-06-13	2014-06-22	Arctic, North Atlantic	3077	<u>Onar, A., A. Olsen and T. Johannessen</u>
Nuka Arctica	2014-07-26	2014-08-05	Arctic, North Atlantic	3362	<u>Onar, A., A. Olsen and T. Johannessen</u>
Nuka Arctica	2014-08-08	2014-08-14	Arctic, North Atlantic	2266	<u>Onar, A., A. Olsen and T. Johannessen</u>
Nuka Arctica	2014-08-15	2014-08-23	Arctic, North Atlantic	2483	<u>Onar, A., A. Olsen and T. Johannessen</u>
Nuka Arctica	2014-09-20	2014-09-28	Arctic, North Atlantic	1931	<u>Onar, A., A. Olsen and T. Johannessen</u>
Nuka Arctica	2014-09-28	2014-10-06	Arctic, North Atlantic	769	<u>Onar, A., A. Olsen and T. Johannessen</u>
Nuka Arctica	2014-10-08	2014-10-16	Arctic, North Atlantic	1029	<u>Onar, A., A. Olsen and T. Johannessen</u>
Nuka Arctica	2014-10-17	2014-10-24	Arctic, North Atlantic	1540	<u>Onar, A., A. Olsen and T. Johannessen</u>
Nuka Arctica	2014-10-28	2014-11-06	Arctic, North Atlantic	648	<u>Onar, A., A. Olsen and T. Johannessen</u>
Nuka Arctica	2014-11-20	2014-11-28	Arctic, North Atlantic	1451	<u>Onar, A., A. Olsen and T. Johannessen</u>
Polarstern	2014-07-07	2014-08-02	Arctic	25088	<u>van Heuven, S. and M. Hoppema</u>
Polarstern	2014-08-05	2014-10-04	Arctic	55349	<u>van Heuven, S. and M. Hoppema</u>
Polarstern	2014-06-08	2014-06-30	Arctic, North Atlantic	20871	<u>van Heuven, S. and M. Hoppema</u>
Polarstern	2014-03-09	2014-04-12	North Atlantic, Tropical Atlantic, Southern Ocean	32939	<u>van Heuven, S. and M. Hoppema</u>
Polarstern	2014-10-26	2014-11-28	North Atlantic, Tropical Atlantic, Southern Ocean	30655	<u>van Heuven, S. and M. Hoppema</u>
Polarstern	2013-12-21	2014-03-04	Southern Ocean	69740	<u>van Heuven, S. and M. Hoppema</u>
Polarstern	2014-12-03	2015-01-31	Southern Ocean	28299	<u>van Heuven, S. and M. Hoppema</u>
Pouiquoi Pas?	2014-05-17	2014-06-28	North Atlantic	2835	<u>Padin, X.A. and F.F. Pérez</u>
Reykjafoss	2013-09-06	2013-09-17	North Atlantic	3481	<u>Wanninkhof, R., D. Pierrot and L. Barbero</u>
Reykjafoss	2013-09-19	2013-09-30	North Atlantic	3991	<u>Wanninkhof, R., D. Pierrot and L. Barbero</u>

Reykjafoss	2013-10-17	2013-10-25	North Atlantic	2291	<u>Wanninkhof, R., D. Pierrot and L. Barbero</u>	
Reykjafoss	2013-10-31	2013-11-08	North Atlantic	2715	<u>Wanninkhof, R., D. Pierrot and L. Barbero</u>	
Ronald H. Brown	2013-10-20	2013-10-30	Tropical Atlantic	4608	<u>Wanninkhof, R., D. Pierrot and L. Barbero</u>	10.3334/CDIAC/OTG.VOS_RB_2013
Ronald H. Brown	2014-02-28	2014-03-13	Tropical Pacific	6052	<u>Wanninkhof, R., D. Pierrot and L. Barbero</u>	10.3334/CDIAC/OTG.VOS_RB_2014
Santa Cruz	2014-01-17	2014-01-30	North Atlantic, Tropical Atlantic	5258	<u>Lefèvre, N. and D. Diverres</u>	
Santa Cruz	2014-02-19	2014-02-28	North Atlantic, Tropical Atlantic	3251	<u>Lefèvre, N. and D. Diverres</u>	
Simon Stevin	2014-08-20	2014-08-20	North Atlantic	31827	<u>Gkirtzalis, T.</u>	
Simon Stevin	2014-08-21	2014-08-21	North Atlantic	30640	<u>Gkirtzalis, T.</u>	
Simon Stevin	2014-08-22	2014-08-22	North Atlantic	5382	<u>Gkirtzalis, T.</u>	
Simon Stevin	2014-08-25	2014-08-25	North Atlantic	508	<u>Gkirtzalis, T.</u>	
Simon Stevin	2014-08-27	2014-08-27	North Atlantic	28904	<u>Gkirtzalis, T.</u>	
Simon Stevin	2014-08-28	2014-08-28	North Atlantic	15148	<u>Gkirtzalis, T.</u>	
Simon Stevin	2014-08-29	2014-08-29	North Atlantic	12492	<u>Gkirtzalis, T.</u>	
Simon Stevin	2014-09-01	2014-09-01	North Atlantic	21372	<u>Gkirtzalis, T.</u>	
Simon Stevin	2014-09-03	2014-09-03	North Atlantic	23069	<u>Gkirtzalis, T.</u>	
Simon Stevin	2014-09-08	2014-09-08	North Atlantic	24445	<u>Gkirtzalis, T.</u>	
Simon Stevin	2014-10-22	2014-10-23	North Atlantic	28397	<u>Gkirtzalis, T.</u>	
Simon Stevin	2014-10-24	2014-10-24	North Atlantic	11920	<u>Gkirtzalis, T.</u>	
Skogafoss	2014-03-17	2014-04-11	North Atlantic	10168	<u>Wanninkhof, R., D. Pierrot and L. Barbero</u>	10.3334/CDIAC/OTG.VOS_SKO2014
Skogafoss	2014-05-10	2014-06-05	North Atlantic	11010	<u>Wanninkhof, R., D. Pierrot and L. Barbero</u>	10.3334/CDIAC/OTG.VOS_SKO2014
Skogafoss	2014-06-07	2014-06-28	North Atlantic	6702	<u>Wanninkhof, R., D. Pierrot and L. Barbero</u>	10.3334/CDIAC/OTG.VOS_SKO2014
Skogafoss	2014-06-29	2014-07-26	North Atlantic	7280	<u>Wanninkhof, R., D. Pierrot and L. Barbero</u>	10.3334/CDIAC/OTG.VOS_SKO2014
Skogafoss	2014-07-27	2014-08-21	North Atlantic	5528	<u>Wanninkhof, R., D. Pierrot and L. Barbero</u>	10.3334/CDIAC/OTG.VOS_SKO2014
Skogafoss	2014-08-22	2014-09-01	North Atlantic	3601	<u>Wanninkhof, R., D. Pierrot and L. Barbero</u>	10.3334/CDIAC/OTG.VOS_SKO2014
Soyo-maru	2013-12-08	2013-12-19	North Pacific	10583	<u>Ichikawa, T. and I. Ono</u>	
Soyo-maru	2014-02-10	2014-02-24	North Pacific	15841	<u>Ichikawa, T. and I. Ono</u>	
Soyo-maru	2014-03-02	2014-03-09	North Pacific	9589	<u>Ichikawa, T. and I. Ono</u>	
Soyo-maru	2014-05-10	2014-05-18	North Pacific	9608	<u>Ichikawa, T. and I. Ono</u>	
Soyo-maru	2014-05-24	2014-06-19	North Pacific	29872	<u>Ichikawa, T. and I. Ono</u>	
Soyo-maru	2014-08-22	2014-08-26	North Pacific	4162	<u>Ichikawa, T. and I. Ono</u>	
Soyo-maru	2014-01-24	2014-01-30	North Pacific, Tropical Pacific	8784	<u>Ichikawa, T. and I. Ono</u>	

Trans Future 5	2013-08-26	2013-08-27	North Pacific	58	<u>Nakaoaka, S. and Y. Nojiri</u>
Trans Future 5	2013-09-27	2013-09-27	North Pacific	63	<u>Nakaoaka, S. and Y. Nojiri</u>
Trans Future 5	2013-11-04	2013-11-05	North Pacific	58	<u>Nakaoaka, S. and Y. Nojiri</u>
Trans Future 5	2013-11-08	2013-11-09	North Pacific	52	<u>Nakaoaka, S. and Y. Nojiri</u>
Trans Future 5	2013-12-16	2013-12-16	North Pacific	56	<u>Nakaoaka, S. and Y. Nojiri</u>
Trans Future 5	2013-12-20	2013-12-20	North Pacific	56	<u>Nakaoaka, S. and Y. Nojiri</u>
Trans Future 5	2014-02-10	2014-02-10	North Pacific	77	<u>Nakaoaka, S. and Y. Nojiri</u>
Trans Future 5	2014-02-14	2014-02-15	North Pacific	41	<u>Nakaoaka, S. and Y. Nojiri</u>
Trans Future 5	2014-03-24	2014-03-25	North Pacific	63	<u>Nakaoaka, S. and Y. Nojiri</u>
Trans Future 5	2014-03-28	2014-03-29	North Pacific	61	<u>Nakaoaka, S. and Y. Nojiri</u>
Trans Future 5	2014-05-06	2014-05-07	North Pacific	73	<u>Nakaoaka, S. and Y. Nojiri</u>
Trans Future 5	2014-05-09	2014-05-09	North Pacific	59	<u>Nakaoaka, S. and Y. Nojiri</u>
Trans Future 5	2014-06-16	2014-06-17	North Pacific	70	<u>Nakaoaka, S. and Y. Nojiri</u>
Trans Future 5	2014-06-20	2014-06-20	North Pacific	61	<u>Nakaoaka, S. and Y. Nojiri</u>
Trans Future 5	2014-07-28	2014-07-29	North Pacific	71	<u>Nakaoaka, S. and Y. Nojiri</u>
Trans Future 5	2014-08-01	2014-08-01	North Pacific	50	<u>Nakaoaka, S. and Y. Nojiri</u>
Trans Future 5	2014-09-08	2014-09-08	North Pacific	55	<u>Nakaoaka, S. and Y. Nojiri</u>
Trans Future 5	2014-09-12	2014-09-12	North Pacific	54	<u>Nakaoaka, S. and Y. Nojiri</u>
Trans Future 5	2014-10-20	2014-10-21	North Pacific	53	<u>Nakaoaka, S. and Y. Nojiri</u>
Trans Future 5	2014-10-24	2014-10-24	North Pacific	55	<u>Nakaoaka, S. and Y. Nojiri</u>
Trans Future 5	2014-12-01	2014-12-01	North Pacific	52	<u>Nakaoaka, S. and Y. Nojiri</u>
Trans Future 5	2014-12-05	2014-12-05	North Pacific	53	<u>Nakaoaka, S. and Y. Nojiri</u>
Trans Future 5	2013-09-28	2013-10-09	North Pacific, Tropical Pacific	11 18	<u>Nakaoaka, S. and Y. Nojiri</u>
Trans Future 5	2013-11-09	2013-11-18	North Pacific, Tropical Pacific	11 04	<u>Nakaoaka, S. and Y. Nojiri</u>
Trans Future 5	2013-12-21	2014-01-02	North Pacific, Tropical Pacific	11 68	<u>Nakaoaka, S. and Y. Nojiri</u>
Trans Future 5	2014-02-16	2014-02-25	North Pacific, Tropical Pacific	11 22	<u>Nakaoaka, S. and Y. Nojiri</u>
Trans Future 5	2014-03-30	2014-04-09	North Pacific, Tropical Pacific	11 21	<u>Nakaoaka, S. and Y. Nojiri</u>
Trans Future 5	2014-05-10	2014-05-19	North Pacific, Tropical Pacific	11 59	<u>Nakaoaka, S. and Y. Nojiri</u>
Trans Future 5	2014-06-21	2014-07-02	North Pacific, Tropical Pacific	11 24	<u>Nakaoaka, S. and Y. Nojiri</u>
Trans Future 5	2014-08-02	2014-08-11	North Pacific, Tropical Pacific	11 42	<u>Nakaoaka, S. and Y. Nojiri</u>
Trans Future 5	2014-10-25	2014-11-04	North Pacific, Tropical Pacific	10 86	<u>Nakaoaka, S. and Y. Nojiri</u>



Trans Future 5	2014-12-06	2014-12-15	North Pacific, Tropical Pacific	1104	<u>Nakaoke, S. and Y. Nojiri</u>
Trans Future 5	2013-10-23	2013-11-03	North Pacific, Tropical Pacific, Southern Ocean	1432	<u>Nakaoke, S. and Y. Nojiri</u>
Trans Future 5	2013-12-03	2013-12-15	North Pacific, Tropical Pacific, Southern Ocean	1434	<u>Nakaoke, S. and Y. Nojiri</u>
Trans Future 5	2014-01-25	2014-02-07	North Pacific, Tropical Pacific, Southern Ocean	1558	<u>Nakaoke, S. and Y. Nojiri</u>
Trans Future 5	2014-03-12	2014-03-23	North Pacific, Tropical Pacific, Southern Ocean	1451	<u>Nakaoke, S. and Y. Nojiri</u>
Trans Future 5	2014-04-24	2014-05-05	North Pacific, Tropical Pacific, Southern Ocean	1381	<u>Nakaoke, S. and Y. Nojiri</u>
Trans Future 5	2014-06-03	2014-06-15	North Pacific, Tropical Pacific, Southern Ocean	1456	<u>Nakaoke, S. and Y. Nojiri</u>
Trans Future 5	2014-07-16	2014-07-27	North Pacific, Tropical Pacific, Southern Ocean	1415	<u>Nakaoke, S. and Y. Nojiri</u>
Trans Future 5	2014-08-27	2014-09-07	North Pacific, Tropical Pacific, Southern Ocean	1405	<u>Nakaoke, S. and Y. Nojiri</u>
Trans Future 5	2014-10-06	2014-10-19	North Pacific, Tropical Pacific, Southern Ocean	1422	<u>Nakaoke, S. and Y. Nojiri</u>
Trans Future 5	2014-11-18	2014-11-29	North Pacific, Tropical Pacific, Southern Ocean	809	<u>Nakaoke, S. and Y. Nojiri</u>
Trans Future 5	2014-09-23	2014-10-05	Southern Ocean	196	<u>Nakaoke, S. and Y. Nojiri</u>
Trans Future 5	2013-10-09	2013-10-21	Tropical Pacific, Southern Ocean	880	<u>Nakaoke, S. and Y. Nojiri</u>
Trans Future 5	2013-11-19	2013-12-01	Tropical Pacific, Southern Ocean	921	<u>Nakaoke, S. and Y. Nojiri</u>
Trans Future 5	2014-01-02	2014-01-17	Tropical Pacific, Southern Ocean	1000	<u>Nakaoke, S. and Y. Nojiri</u>
Trans Future 5	2014-02-25	2014-03-10	Tropical Pacific, Southern Ocean	909	<u>Nakaoke, S. and Y. Nojiri</u>
Trans Future 5	2014-04-10	2014-04-23	Tropical Pacific, Southern Ocean	941	<u>Nakaoke, S. and Y. Nojiri</u>
Trans Future 5	2014-05-20	2014-06-01	Tropical Pacific, Southern Ocean	910	<u>Nakaoke, S. and Y. Nojiri</u>
Trans Future 5	2014-07-02	2014-07-15	Tropical Pacific, Southern Ocean	1027	<u>Nakaoke, S. and Y. Nojiri</u>
Trans Future 5	2014-08-12	2014-08-25	Tropical Pacific, Southern Ocean	1040	<u>Nakaoke, S. and Y. Nojiri</u>
Trans Future 5	2014-11-05	2014-11-17	Tropical Pacific, Southern Ocean	853	<u>Nakaoke, S. and Y. Nojiri</u>
Trans Future 5	2014-12-16	2014-12-30	Tropical Pacific, Southern Ocean	939	<u>Nakaoke, S. and Y. Nojiri</u>
Wakataka-maru	2014-05-10	2014-05-20	North Pacific	9360	<u>Kuwata, A. and K. Tadokoro</u>
Wakataka-maru	2014-06-05	2014-06-11	North Pacific	9025	<u>Kuwata, A. and K. Tadokoro</u>
Walton Smith	2013-03-31	2013-04-18	North Atlantic, Tropical Atlantic	8392	<u>Millero, F.</u>
Walton Smith	2013-04-19	2013-04-28	North Atlantic, Tropical Atlantic	4890	<u>Millero, F.</u>
Walton Smith	2014-04-28	2014-05-25	North Atlantic, Tropical Atlantic	12666	<u>Millero, F.</u>
Walton Smith	2013-05-25	2013-05-27	Tropical Atlantic	898	<u>Millero, F.</u>
Walton Smith	2013-06-13	2013-06-15	Tropical Atlantic	1214	<u>Millero, F.</u>
Walton Smith	2013-06-20	2013-06-27	Tropical Atlantic	2883	<u>Millero, F.</u>
Walton Smith	2013-07-06	2013-07-18	Tropical Atlantic	5529	<u>Millero, F.</u>

Walton Smith	2013-08-13	2013-08-28	Tropical Atlantic	7900	<u>Millero, F.</u>
Walton Smith	2013-10-08	2013-10-09	Tropical Atlantic	509	<u>Millero, F.</u>
Walton Smith	2013-10-17	2013-10-18	Tropical Atlantic	707	<u>Millero, F.</u>
Walton Smith	2013-12-20	2013-12-21	Tropical Atlantic	748	<u>Millero, F.</u>
Walton Smith	2014-04-22	2014-04-22	Tropical Atlantic	214	<u>Millero, F.</u>
Walton Smith	2014-04-23	2014-04-24	Tropical Atlantic	657	<u>Millero, F.</u>
Walton Smith	2014-04-26	2014-04-26	Tropical Atlantic	155	<u>Millero, F.</u>